INNOVATIONS IN LIFE SCIENCES

IN TODAY'S WORLD

Dr. Jyothi Hiremath
Dr. Shivaveerakumar S.

INNOVATIONS IN LIFE SCIENCES IN TODAY'S WORLD

EMPYREAL
PUBLISHING HOUSE

India | UAE | Nigeria | Uzbekistan | Montenegro

www.empyrealpublishinghouse.com

INNOVATIONS IN LIFE SCIENCES IN TODAY'S WORLD

By:

Dr. Jyothi Hiremath
Assistant Professor, Department of Food Science and Nutrition, Khaja Bandanawaz University, Kalaburagi

Dr. Shivaveerakumar S.
Assistant Professor, Department of Studies in Microbiology, Davangere University, Davanagere, Karnataka

First Impression: January 2023

INNOVATIONS IN LIFE SCIENCES IN TODAY'S WORLD

ISBN: 978-93-93810-11-3

Rs. 650/- ($18)

DISCLAIMER

Information contained in this book has been published by Empyreal Publishing House and has been obtained by the editors from sources believed to be reliable and are correct to the best of her knowledge. The author is solely responsible for the contents of the articles compiled in this book. Responsibility of authenticity of the work or the concepts/views presented by the author through this book shall lie with the author and the publisher has no role or claim or any responsibility in this regards. Errors, if any, are purely unintentional and readers are requested to communicate such error to the author to avoid discrepancies in future.

Published by:
Empyreal Publishing House

PREFACE

The life sciences comprise fields of science involving the study of living organisms such as plants, animals and humans. While biology remains the centerpiece of the life sciences, technological advances in molecular biology and biotechnology have led to a burgeoning of specializations and new interdisciplinary fields.

The innovations in life sciences includes many disciplines, however, such as anthropology, ecology, entomology, botany, zoology, microbiology, physiology, biotechnology, evolutionary biology, genetics, human anatomy, marine biology, molecular and cell biology, neuroscience, palaeontology, plant biology, and biochemistry. There are various levels of investigation involved, ranging from the study of interactions between organic molecules to those between animals and plants and their surroundings. In order to give you an overview of the abilities you will need to acquire as a life scientist, we set out to compile in this book a thorough collection of papers spanning all fundamental areas of life sciences.

ACKNOWLEDGEMENT

We would like to express our gratitude to God, the Almighty, and the numerous people who helped us complete this book, including those who offered support, discussed ideas, read what we wrote, supplied feedback, and helped with the editing, proofreading, and design. We want to express our gratitude to all the authors who contributed chapters to this book. We would like to thank our parent organisations. We are grateful to our family members and special thanks to our Daughter and Son, Ms. Nimisha S. Chandrikimath and Mr. Sohan S. Chandrikimath for their constant cooperation. Without the constant direction and assistance provided by our publisher, Empyreal Publishing House, this book would not have reached readers throughout the globe, including students, research scholars, and faculty members.

Dr. Jyothi Hiremath

Dr. Shivaveerakumar S.

Table of Contents

 ISBN: 978-93-93810-19-9

TRANSITION METAL (II) COMPLEXES WITH SCHIFF BASES: DESIGN, SPECTRUM CHARACTERISATION, AND BIOLOGICAL STUDIES

Rehab K. Al-Shemary

ABSTRACT

The equimolar reaction of 3-Amino-1-(4-chlorobenzyl)-2-pyrrolidinone with N-Methyl-2-pyrrolecarboxaldehyde, 5-Chloro-2-thiophene carboxaldehyde, and 2-hydroxy-5-(methyl sulfanyl) benzaldehyde yielded a new set of three physiologically active Schiff base ligands, L1–L3. The produced Schiff bases were later employed. Complex formation reaction using several metal elements such as Co(II), Ni(II), Cu(II), and Zn(II) as chlorides utilising a ligand: metal molar ratio of 2:1. Physical, spectroscopic, and analytical data were used to determine each chemical's structure and bonding type. Except for the Cu(II) complexes, which had a deformed geometry, all-metal(II) complexes had an octahedral geometry. All of the compounds created were tested in vitro for antibacterial and antifungal activity against four Gram-negative bacteria (Shigella sonnei, Escherichia coli, Salmonella typhi, and Pseudomonas aeruginosa) by using the method of agar well diffusion, and two Gram-positive (Bacillus subtilis and Staphylococcus aureus) bacterial strains, as well as six fungal strains (Fusarium solani, Trichophyton longifusus, Microsporum canis, Aspergillus flavus Candida glabrata, and Candida albicans). The synthesised compounds demonstrated moderate to considerable bactericidal capability between one or more bacterial species. The cytotoxic effects of these compounds were also investigated using an in vitro Brine, Shrimp bioassay. Due to chelation/coordination, the results also revealed that metal complexes had higher activity than ligands.

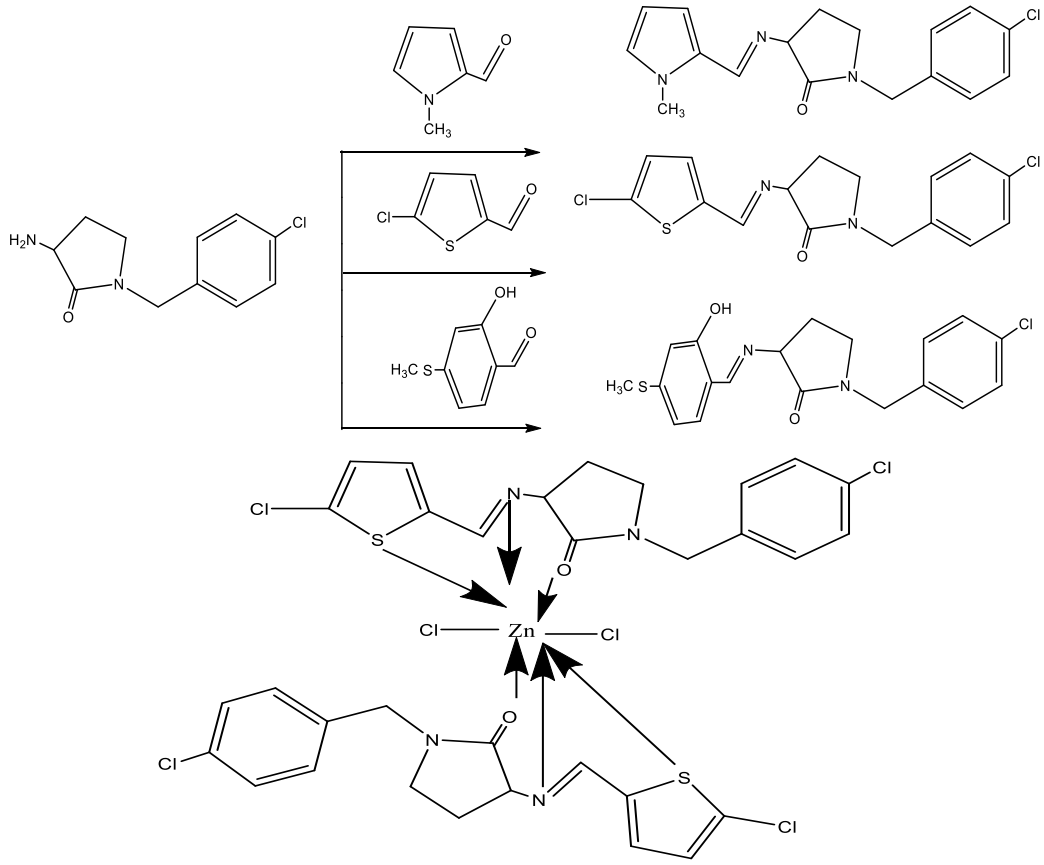

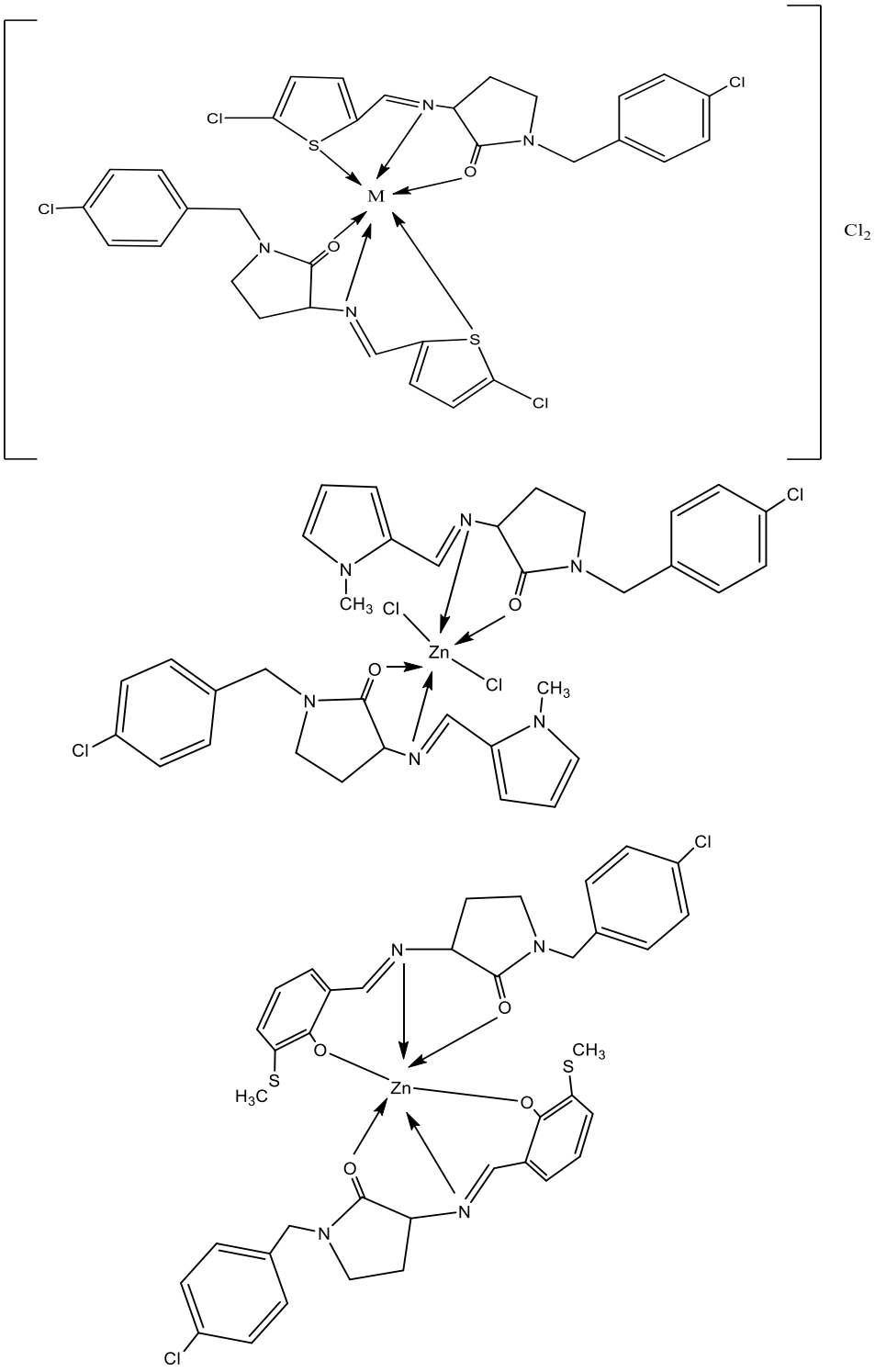

INTRODUCTION

Pyrroles and their derivatives play a crucial role in current heterocyclic chemistry because of their biological activity[1]. Furthermore, these molecules form heterocyclic rings, frequently found in pharmaceutically exciting compounds. [2]. Trazodone is letrozole, anastrozole, antidepressant, and Vorozole are anticancer drugs [3]. The azomethine bond (C=N) is necessary for biological activity. Numerous compounds have azomethine with antifungal and antibacterial

activities have been found [4]. The azomethine linkage (C=N) has been shown to have antibacterial properties in various Schiff bases[5]. Many Schiff bases have been shown to have antitumor, antibacterial,plant growth regulating and antifungal [6]. Cytotoxic properties N and S atoms are also known to play a role in metal coordination in the active sites of various biomolecules. Metal-based antibacterial and antifungal chemicals are in high demand, hence metallo-organic chemistry is developing as a new field of study [7]. Several studies have shown that attaching a medicine to a metal element boosts the drug's activity [8]. In some instances, the complex has even more healing properties than the parent drug Metal elements such as zinc, copper, cobalt, and nickel have received particular attention in recent research have found that due of their lower size and higher nuclear charge. As a result, it has a strong preference for forming coordination compounds [9]. A large body of research shows that when biologically inactive compounds are coordinated with these metal elements, they become active, and less bioactive components become more active[10]. We present the prepation of a new type of Schiff bases, L^1–L^3, derived from condensation reactions of 3-Amino-1-(4-chlorobenzyl)-2-pyrrolidinone with N-Methyl-2-pyrrolecarboxaldehyde,5-Chloro-2-thiophene carboxaldehyde,and2-hydroxy-5-(methylsulfanyl)benzaldehyde and their cobalt(II), nickel(II) (Scheme1). Antibacterial activity against two Gram-positive (B.subtilis, S.aureus,) and four Gram-negative (S. sonnei, E.coli, , S. typhi and Pseudomonas aeruginosa) bacterial strains, as well as antifungal activity against six fungus strains, was investigated in vitro (T. longifusus, C. albicans, F. solani, C.glabrata M.canis,and A. flavus, in vitro Brine Shrimp bioassay, was used, to investigate the cytotoxic properties of these compounds.

EXPERIMENTAL

MATERIALS AND METHODS

All of the chemicals used were of the annular variety. As chloride, all-metal salts were used. Melting points were recorded using the Fisher Johns melting point equipment. The SHIMADZU FT-IR spectrometer was used to record infrared spectra. A Perkin Elmer, the USA model, was used for the C, H, and N analyses. In DMSO-d6 using TMS as an internal standard, ^{1}H and ^{13}C NMR spectra were captured on a Bruker Spectrospin Avance DPX-500 spectrometer. Electron impact mass spectra (EIMS) on a JEOL MS Route instrument were captured. At the International Centre for Chemical Sciences, University of Baghdad in Iraq, the antibacterial, antifungal, and cytotoxic characteristics of the compounds were examined in vitro.

Synthesis of Schiff Bases Ligands:

A general procedure (L^1–L^3) N-Methyl-2-pyrrolecarboxaldehyde,5-Chloro-2-thiophene carboxaldehyde, or 2-hydroxy-5-(methyl sulfanyl)benzaldehyde (10 mmol) in (20 ml) methanol solution was added to a magnetically stirred (20 ml) methanol solution of(10 mmol) 3-Amino-1-(4-chlorobenzyl)-2-pyrrolidinone and refluxed for 6 hours under TLC monitoring. After the reaction was completed, the resultant mixture was cooled to room temperature, filtered, and rotary evaporated to almost half its initial volume. A light-brown solid was produced after three hours of resting at ambient temperature. After the reaction was completed, using a rotary evaporator, the resultant mixture was cooled to ambient temperature, filtered, and reduced to approximately half its original volume. After 3 hours at room temperature, a light-brown solid product was formed. The ligands were synthesized using the same method. However, before recrystallising ethanol, the ligand L3 was precipitated, filtered, and washed with hot methanol during reflux: (1:1) methanol mixture. TLC was used to determine the purity of the product of compounds.

Empirical formula	Formula	Mwt	Color	Dec.°C	Yield %	Elemental Analysis %Found(calculated)				
						C	**H**	**N**	**M**	**Cl**

L1	$C_{17}H_{18}ClN_3O$	315.80	brown	210	70	64.41 (64.66)	5.07 (5.75)	13.26 (13.31)	-	11.27 (11.23)
$[Co(L^1)_2Cl_2]$	C34H36Cl4CoN6O2	761.44	Dark brown	350	68	54.27 (53.63)	4.27 (4.77)	11.27 (11.04)	7.87 (7.74)	18.11 (18.62)
$[Ni(L^2)_2Cl_2]$	C34H36Cl4NiN6O2	761.20	Light Brown	340	74	53.38 (53.65)	4.49 (4.77)	11.89 (11.04)	7.51 (7.71)	18.50 (18.63)
$[Cu(L^2)_2Cl_2]$	$C_{34}H_{36}Cl_4CuN_6O_2$	766.05	green	320	76	54.78 (53.31)	4.83 (4.74)	10.56 (10.97)	8.54 (8.30)	18.39 (18.51)
$[Zn(L^2)_2Cl_2]$	$C_{34}H_{36}Cl_4ZnN_6O_2$	767.88	Brown	330	72	53.56 (53.18)	4.86 (4.73)	10.76 (10.94)	8.62 (8.51)	18.22 (18.47)
L2	$C16H_{14}Cl_2N2OS$	353.26	brown	282	68	54.54 (54.40)	3.30 (3.99)	7.76 (7.93)	-	20.30 (20.07)
$[Co(L^2)_2]Cl_2$	$C_{32}H_{28}cl_6CoO_2N_4S_2$	836.76	Reddish green	282	69	45.56 (45.96)	3.93 (3.37)	6.83 (6.70)	7.41 (7.05)	25.65 (25.43)
$[Ni(L^2)_2]Cl_2$	$C32H28Cl_6N4NiO2S2$	836.12	green	282	72	45.56 (45.97)	3.76 (3.38)	6.85 (6.70)	7.87 (7.02)	25.20 (25.44)
$[Cu(L^2)_2]Cl_2$	$C32H28N4CuO_2Cl_6S_2$	871.10	purple	265	70	45.87 (45.70)	3.45 (3.36)	6.54 (6.66)	7.56 (7.56)	25.65 (25.29)
$[Zn(L^2)_2]Cl_2$	$C_{32}H_{28}N_4ZnO_2Cl_6S_2$	842.80	Dark green	282	67	45.23 (45.60)	3.22 (3.35)	6.33 (6.65)	7.56 (7.56)	25.43 (25.24)
L3	C19H19ClN2O2S	374.88	Dark brown	271	76	60.45 (60.87)	5.21 (5.11)	8.83 (8.47)	-	9.33 (9.46)
$[Co(L^3)_2]$	$C_{38}H_{36}Cl_2N_4S_2O_4Co$	806.68	green	282	73	56.30 (56.58)	4.21 (4.50)	6.78 (6.95)	7.54 (7.31)	8.80 (8.79)
$[Ni(L^3)_2]$	$C_{38}H_{36}Cl_2N_4S_2O_4Ni$	806.44	Light green	282	72	56.76 (56.60)	4.64 (4.50)	6.85 (6.95)	7.90 (7.82)	8.85 (8.79)
$[Cu(L^3)_2]$	$C_{38}H_{36}Cl_2N_4S_2O_4Cu$	874.75	Dark brown	282	71	56.30 (4.47)	4.30 (4.85)	6.40 (6.91)	7.54 (7.83)	8.57 (8.74)
$[Zn(L^3)_2]$	$C_{38}H_{36}Cl_2N_4S_2O_4Zn$	813.13	green	282	70	56.65 (56.13)	4.45 (4.89)	6.87 (6.91)	8.32 (8.08)	8.53 (8.72)

Synthesis of complexes: general complexes make(0.952 g, 4 mmol) a cobalt (II) complex Co(II) Cl2.6H2O was added dropwise to a magnetically stirred solution of ligands L1-L3 in (20 mL) a hot ethanol solution. The mixture was then refluxed for1 hours. A solid product created during the refluxing process, which was filtered, washed with ethanol, and dried with diethyl ether. Recrystallisation of TLC pure product from (1:2) hot aqueous ethanol. Other complexes were prepared using the same method (Scheme 1). Tables 1 and 2 contain physical, analytical, and spectral data.

Compounds	**Chemical shifts δ (ppm)Assignments in d^6-DMSO**
L^1	2.5 (dd, 2H, pyrrolidinone CH2-N),2.7 (dd, 2H, pyrrolidinone CH_2) ,4.5(d, 2H, methylene CH_2), 6.18 (dd, 2H, J = 4.6, 4.2 Hz, pyrrole C-H), 6.85 (d, 2H, J = 4.0 Hz, pyrrole, C-H), 7.12 (d, 2H, J = 4.6 Hz, pyrrole, C-H), 7.22-8.82 (m, 2H, aromatic ,C-H), 8.78 (s, 2H, C-H azomethine).^{13}CNMR of L^1(DMSO-d_6,d,ppm):28.7 (CH_2,pyrrole), 45.3(CH_2-N),49.7(CH_2,methylene),38.5 (CH_3), 76.8 (N-C), 157.78(C=O), 121.56-130.54 (C=C ,aromatic), 133.70 (C-Cl), 165.8 (C=N azomethine).
$[Zn(L^1)_2]Cl_2$	2.5 (dd, 2H, pyrrolidinone CH2-N),2.7 (dd, 2H, pyrrolidinone CH_2) ,4.3(d, 2H, methylene CH_2),6.18 (dd, 2H, J = 4.5, 3.9 Hz, pyrrole C-H), 6.85 (d, 2H, J = 4.0 Hz, pyrrole, C-H), 7.12 (d, 2H, J = 4.7Hz, pyrrole, C-H), 7.22-

	8.82 (m, 2H, aromatic ,C-H), 9.12 (s, 2H, C-H azomethine).^{13}C NMR of Zn(II) complex (DMSO-d6, d, ppm): 28.7(CH2,pyrrole),45.6(CH_2-N),49.7(CH_2,methylene),38.5 (CH3), 76.8 (N-C), 154.87 (C=O), 121.96-130.7 (C=C ,aromatic), 133.70 (C-Cl), 161.4 (C=N azomethine).
L^2	2.4(dd, 2H, pyrrolidinone CH_2-N),2.8 (dd, 2H, pyrrolidinone CH_2) ,4.1(d, 2H, methylene CH_2), 6.74 (d, 2H, J = 3.8 Hz, thiophene =CH),6.90 (d, 2H, J = 3.8 Hz, thiophene(=CH),8.02 (d, 2H, J = 4.6 Hz, thiophene, CH_2-N), 7.20-8.84 (m, 2H, aromatic ,C-H), 8.93(s, 2H, C-H azomethine).^{13}C NMR of L_2 (DMSO-d6, d, ppm): 26.4(CH_2 ,pyrrole), 45.3(CH_2-N),49.7 (CH_2,methylene), 76.8 (N-C), 160.23 (C=O), 121.96-138.6 (C=C ,aromatic), 133.70 (C-Cl), 164.8 (C=N azomethine).
[Zn $(L^2)_2Cl_2$]	2.4(dd, 2H, pyrrolidinone CH2-N),2.8 (dd, 2H, pyrrolidinone CH_2) ,4.1(d, 2H, methylene CH_2), 6.74 (d, 2H, J = 3.8 Hz, thiophene =CH),6.90 (d, 2H, J = 3.7 Hz, thiophene(=CH),8.56 (d, 2H, J = 4.6 Hz, thiophene, CH_2-N), 7.20-8.84 (m, 2H, aromatic ,C-H), 9.12 (s, 2H, C-H azomethine).^{13}C NMR of Zn(II) complex (DMSO-d6, d, ppm): 26.4(CH_2 ,pyrrole), 45.3(CH_2-N),49.7 (CH_2 ,methylene), 76.8 (N-C), 155.32 (C=O), 121.96-138.6 (C=C aromatic), 133.70 (C-Cl), 161.5 (C=N azomethine).
L^3	2.3 (s, 3H, thiophenol ,CH_3-S), 2.6 (dd, 2H, pyrrolidinone CH_2-N), ,4.2(d, 2H, CH_2 methylene),7.20-8.88 (m, 2H, C-H aromatic), 9.23(s,2H,C-Hazomethine), 11.87(s,2H,O-H hydroxyl). ^{13}C NMR of L3 (DMSO-d_6, d, ppm): 27.5(CH_2 ,pyrrole), 44.5(CH_2-N),48.5 (CH_2,methylene), 37.2 (CH_3), 77.2 (N-C), 153.76 (C=O), 120.23-131.43 (C=C aromatic), 134.44 (C-Cl), 164.1 (C=N azomethine), 177.11 (O-H $_{hydroxyl}$).
[Zn $(L^3)_2Cl_2$]	2.3 (s, 3H, thiophenol ,CH_3-S), 2.6 (dd, 2H, pyrrolidinone CH_2-N), 4.2(d, 2H, methylene CH_2), 7.20-8.88 (m, 2H, C-H aromatic),9.06 (s,2H,C-H azomethine).^{13}C NMR of Zn(II) complex (DMSO-d6, d, ppm): 27.5(CH_2 ,pyrrole), 44.5 (CH_2-N),48.5 (CH_2,methylene), 37.2 (CH3), 77.2 (N-C), 150.88 (C=O), 120.23-131.43 (C=C aromatic), 134.44 (C-Cl), 155.8 (C=N azomethine), 177.11 (O-H $_{hydroxyl}$).

Biological activity 154.87 -150.88 160.23 - 155.8

Antibacterial Studies

The disk diffusion method was used to evaluate the whole newly synthesized compounds against four Gram-negative (S. Typhi, P. aeruginosa, E. coli, S. sonnei,) and two bacterial strains that are gram-positive (B. subtilis and S. aureus). First, to create a 10 mg/mL solution, the test compounds (complex/ligand) were dissolved in DMSO. Then, a micropipette applied the key to the sterilised filter paper disks in a specified volume (10 µL). After drying at room temperature, the disks were placed overnight in sterile, dry containers.The negative control consisted of disks soaked in 10 µL of DMSO at 25^{o}C and dried in the air. The common antibiotic disks that were employed as a positive control were manufactured in the laboratory as described before by injecting a conventional antibiotic solution at a known concentration. As a traditional antibiotic, ampicillin was utilized. Bacterial cultures were grown over night at 37°C in a nutrient broth medium and then distributed over solidified nutrient agar medium. The medium surface was then covered with the test and control disks using sterile forceps. For 24-48 hours, the plates were incubated at 37°C. The information was gathered by measuring each chemical's inhibitory zone in millimeters. The experiments were carried out three times, and statistical analysis was done on the outcomes.

Antifungal Activity (in vitro)

Antifungal activities of all compounds were studied against six fungal strains (, C.albicans, F. solani, T.longifusus, C.glabrata, M. canis,and, A. flavus) according to literature protocol. Fungal spore suspensions of 10^5 (CFU) mL^{-1} were added to Sabouraud dextrose agar and then transferred to Petri plates. Disks soaked in 20 mL (200 g/mL in DMSO) of test chemicals were placed on the agar surface in various places. The plates were incubated at 32ºC for 7days. The results were compared to the common drugs miconazole and amphotericin B and the smallest inhibitory dose (MIC) were expressed as a percentage of inhibition. The disk diffusion method was used to select compounds for minimum inhibitory concentration (MIC) investigations that have a significant antibacterial activity (greater than 80%). The minimal inhibitory concentration was determined by producing disks containing 10, 25, 50, and 100 µg/mL using the test substances and adhering to the methodology.

In Vitro Cytotoxicity

All generated compounds exhibited cytotoxic action. Meyer et al. methodology .it's was used to evaluate in vitro. Brine shrimp (Artemia salina Leach) eggs were incubated in a shallow rectangular plastic dish (20-30 cm) filled with artificial saltwater. Then, 50 mg of eggs were sprinkled into the vast chamber in the dark.

On the other hand, the matter compartment was exposed to a conventional light. After two days, nauplii were collected using a pipette from the side under standard lighting. A test compound sample was generated by dissolving 20 mg of each chemical in 2 mL of DMSO. In 9 vials, 500, 50, and 5 µg/mL were transferred (three for each dilution were used for each test sample and Ld60 is the mean of three values). Overnight, the solvent was allowed to evaporate. After two days, when the shrimp larvae were ready, each vial was filled with salt water (1 mL) and 10 shrimps (30 shrimps per dilution). Seawater was used to adjust the volume to 5 mL for each vial. The number of survivors was counted after 24 hours. The Finney computer software evaluated the data and determined the LD50 values.

RESULTS AND DISCUSSION

Chemistry

As illustrated in Scheme 1, the Schiff base ligands L^1–L^3 were produced by condensation reactions of 3-Amino-1-(4-chlorobenzyl)-2-pyrrolidinone with N-Methyl-2-pyrrolecarboxaldehyde with 5-Chloro-2-thiophene carboxaldehyde, and 2-hydroxy-5-(methyl sulfanyl) benzaldehyde under reflux. At ambient temperature, all of these compounds were soluble in ethanol, dioxane, DMF, and DMSO, but methanol was only soluble after heating. The ligands' compositions matched their microanalytical and mass spectral data. Complexes of metals of these ligands were synthesized by reacting them with (Zn (II), Cu (II), Ni (II), and Co (II)) chlorides in molar ratio as 2: 1 (ligand : metal). At room temperature, All-metal complexes were resistant to oxygen and moisture. Except for DMF and DMSO, they were insoluble in all organic solvents.Tables 1 and 2 contain physical measurements and analytical data for the complexes. Spectra in the infrared region ,the experimental section and Table 2 contain the characteristic bands of the infrared spectra of ligands L^1–L^3 and their metal(II) complexes. All ligands contained donor sites such as carbonyl (C=O), azomethine linkage (-C=N), and thienyl (-C-S), or hydroxyl (-OH) groups that had a proclivity to interact with metal ions. The IR spectra of all ligands L^1-L^3 revealed peaks at 1720–1704, and 1635-1613cm^{-1}, respectively, attributable to the vibration of the (C=O), and (C=N) moieties. Furthermore, the ligand L^3 exhibited a broad spectral band at 3283 cm^{-1} due to intramolecular hydrogen-bonded hydroxyl (-OH) group vibrations with azomethine (-C=N) group. All of the Schiff base ligands include IR spectral bands related to azomethine-N, which have been shifted to a lower frequency in range(1614-1618)cm^{-1},confirming N-azomethine involvement in complex formation.

1. A new band appeared at 450-426 cm $^{-1}$ in all metal(II) complexes due to (M–N) vibrations, indicating the coordination of N-azomethine with metal ions. A new band appeared at 520–532 cm $^{-1}$ in all metal(II) complexes due to (M–O) vibrations, indicating the coordination of O-carbonyl with metal ions.
2. The lack of the wide (OH) band at 3283 cm^{-1} in metal complex spectra, followed by the emergence of a new band attributed to (C-O) at 1375-1386 cm^{-1}, demonstrated hydroxyl-O deprotonation and coordination to the metal atom. The development of a new band at 520-532 cm^{-1} due to M-O strengthens the case for metal-oxygen coordination.
3. The spectra of the metal(II) complexes show that the bands that arise at 957 cm^{-1} in the spectra of the ligands, L^2 due to (C-S) vibration are moved to a lower frequency at 943-938 cm^{-1}, indicating participation and coordination of the thienyl-S ring in the complexation event. This coordination is further strengthened by the emergence of a new band at 462-459 cm^{-1} as a result of M-S.
4. All other bands inside the spectra of all prepared compounds are unaltered.
6. The IR spectra of all prepared compounds indicated decisively that the azomethine-N, carbonyl-O, thiophene-S, or hydroxyl-O groups are tri-dentately coordinated to the metal atoms.

^{1}H NMR Spectra

The experimental section contains the ^{1}H NMR spectral data of the ligands L^1–L^3 and their diamagnetic Zn(II) complexes. All protons of Schiff bases ligands and Zn(II) complexes that appeared as signals due to heteroaromatic/aromatic groups were found to be in their expected region. The azomethine (-CH=N) protons appeared as a single in the spectra of all the ligands L^1– L^3 at 8.78–9.23 ppm. The Peaks in the spectrum of ligand L^1 at 6.18 ppm were assigned to pyrrolidinone protons as a doublet and at 6.85 ppm to CH_2-pyrrolidinone as the doublet's doublet. A pyrrole-CH proton peak was also visible in the spectrum of ligand L^1 at 7.12 ppm. At 6.74and 6.90ppm, the Schiff base ligand L^2 showed thiophene protons as singlets at 8.02 ppm, and the ligand L^3 showed a singlet proton of a hydroxyl group (-OH). The intense, experienced downfield shifting of hydroxyl proton indicated its participation in intramolecular hydrogen bonding with the azomethine group. At 6.65 and 6.90 ppm, the ligand L^3 displayed thiophene group protons as doublets. The downfield shifting of azomethine (-CH=N) protons signals present at 8.78-9.06 ppm in the free ligands to 9.03-9.23ppm in the spectra of their zinc(II) complexes, respectively, is used to assign the coordination of the azomethine (CH=N). A signal of hydroxyl (OH) proton that appeared at 11.87ppm in the spectra of ligand L^3, respectively, vanished in the spectra of their corresponding zinc complexes, indicating deprotonation and coordination of the N- and O-atoms with the zinc metal atom. Due to the deshielding effect, the thiophene proton of ligand L^2 was shifted downfield from 8.02 to 8.56 ppm in their Zn(II) complexes, justifying the coordination of thienyl-S. In the spectra of the Zn(II) complexes, all other protons experienced a downfield shift of 0.16–0.20 ppm due to increased conjugation.

Table 2: Conductivity, magnetic and spectral data of metal (II) complexes.

compounds	**Λ max (cm^{-1})**	**B.M (μeff)**	**ύ cm^{-1}**	**IR (cm^{-1})**
L^1	-	-	35842 31746	1617(HC=N),1720(C=O),1561,1543(C=C), 1460(C-N), 678(C-Cl)
$[Co(L^1)_2Cl_2]$	14.4	5.20	29,726 17,334 8786	1608(HC=N),1710(C=O),1563,1542(C=C),1463(C-N),678(C-Cl),548 (M-N), 426 (M-O), 432(M-Cl)
$[Ni(L^1)_2Cl_2]$	18.7	1.73	30303 25,132	1606(HC=N),1708(C=O),1564, 1541(C=C),1461(C-N), 670(C-Cl), 542

			14,454	(M-N), 423 (M-O), 429 (M-Cl)
$[Cu(L^1)_2Cl_2]$	15.8	3.24	29,871 16,125 10,123	1603 (HC=N), 1705(C=O), 1565,1543(C=C), 673(C-Cl),546 (M-N), 428 (M-O), 430 (M-Cl)
$[Zn(L^1)_2Cl_2]$	17.5	Dia	29,761 *26,737* 20,491	1610(HC=N),1703(C=O),1563,1542(C=C),544(M-N), 428 (M-O), 423(M-Cl)
L^2	-	-	35842 31746	1635(HC=N), 1704(C=O), 1570,1545 (C=C), 957(C-S),670 (C-Cl).
$[Co(L^2)_2]Cl_2$	88.4	5.07	30,234 17,864 8978	1629(HC=N), 1685 (C=O),1568,1540(C=C),943(C-S), 678 (C-Cl), 531(M-N), 432(M-O), 459 (M-S)
$[Ni(L^2)_2]Cl_2$	85.0	1.69	29,411 25,790 14,454	1625(HC=N),1678(C=O),1566,1544(C=C),947(C-S), 676 (C-Cl), 529(M-N),462 (M-S)
$[Cu(L^2)_2]Cl_2$	89.5	3.13	10,345 16,897 29,871	1622(HC=N),1698(C=O),1568,1540(C=C),940(C-S), 678 (C-Cl), 533(M-N), 440(M-O), 456 (M-S)
$[Zn(L^2)_2]Cl_2$	87.6	Dia	29,632 *26,315* 21,505	1626(HC=N),1693(C=O),1565,1541(C=C),938(C-S), 673(C-Cl), 520(M-N), 438 (M-O), 454 (M-S)
L^3	-	-	35842 31746	3283(OH),1710(C=O),1630(HC=N), 1566,1544(C=C), 1375 (C-O),660(C-Cl),
$[Co(L^3)_2]$	11.5	5.12	29,896 17,657 8854	1693 (C=O),1612 (HC=N), 1566,1544(C=C), 1386 1220 (C-O)663(C-Cl), 546(M-N),449 (M-O)
$[Ni(L^3)_2]$	13.7 1	1.67	30,303 25,654 14,896	1687 (C=O),1617 (HC=N), 1566,1544(C=C), 1382(C-O), 667(C-Cl), 542(M-N),450 (M-O)
$[Cu(L^3)_2]$	8.2	3.27	29,411 27,397 20,408	1683(C=O),1614(HC=N),1566,1544(C=C),1380 (C-O) , 669(C-Cl), 549(M-N),447 (M-O)
$[Zn(L^3)_2]$	11.6	Dia	29,761 *26,315* 20,408	1690(C=O),1620(HC=N),1566,1544(C=C),1378 (C-O), 662(C-Cl), 550(M-N),445 (M-O)

957-938

^{13}C NMR Spectra

The 13C NMR spectra of the Schiff base ligands L^1-L^3 and their Zn(II) complexes were recorded in DMSO-d_6. The azomethine carbon (-CH=N) was found at 158.7-160.4 in the 13C NMR spectra of all Schiff base ligands L1-L3. The spectra of the ligands L1 and L2 indicated pyrrole and thienyl carbons in the 114.5-131.5 and 116.7-144.6 ppm ranges, respectively. All carbons of the phenyl group in ligand L3 appeared at 120.23-131.43 ppm.The carbon of the hydroxyl (OH) group in this ligand L^3 was observed downfield at 162.5ppm.

Table3: Antibacterial bioassay of prepared compounds (1mg/mL DMSO concentration).

Compounds	% Zone of inhibition (mm)						Statistical analysis.	Average
	E. coli	S. sonnei	P.aeruginosa	S. typhi	S. aureus	B. subtilis.		
L^1	16	18	17	16	14	15	1.41	14.0
$[Co(L^1)_2Cl_2]$	19	22	21	19	16	18	2.65	18.1
$[Ni(L^1)_2Cl_2]$	21	20	22	18	18	19	1.23	19.7
$[Cu(L^1)_2Cl_2]$	19	20	20	19	15	18	1.76	17.6
$[Zn(L^1)_2Cl_2]$	19	20	21	16	16	14	2.98	19.1
L^2	15	14	16	17	15	13	1.12	14.1
$[Co(L^2)_2]Cl_2$	21	15	19	20	18	21	2.67	18.4
$[Ni(L^2)_2]Cl_2$	18	16	19	21	24	22	2.76	19.4
$[Cu(L^2)_2]Cl_2$	16	14	17	18	17	20	1.84	18.1
$[Zn(L^2)_2]Cl_2$	18	16	17	19	16	19	1.58	16.4
L^3	14	13	13	14	15	13	0.82	13.7
$[Co(L^3)_2]$	19	20	19	17	19	16	1.50	17.7
$[Ni(L^3)_2]$	16	18	17	20	17	18	1.43	18.6
$[Cu(L^3)_2]$	15	13	14	15	17	18	1.24	16.7
$[Zn(L^3)_2]$	17	16	18	17	18	11	0.89	17.0
3-amino-1H-1,2,4-triazole	7	12	15	11	12	12	1.86	11.08
standard drugs (ampicillin)	24	23	30	29	28	30	2.63	25.1

Activity < 10 = weak; >10 = moderate; > 16 = significant

Table 4: Antifungal bioassay of ligands and metal (II) complexes (concentration used 200 µg/mL).

No	Compounds	% Inhibition						SA (mm)	Average
		T. longifucus	C. albicans	A. flavus	M. canis	F.Solani	C.glab rata		
1	L^1	36	54	28	43	39	57	13.23	45.7
2	$[Co(L^1)_2Cl_2]$	48	61	30	51	44	62	14.76	45.4
3	$[Ni(L^1)_2Cl_2]$	33	50	26	53	48	70	18.26	43.9
4	$[Cu(L^1)_2Cl_2]$	45	64	28	57	43	60	14.76	50.4
5	$[Zn(L^1)_2Cl_2]$	40	47	31	68	47	60	13.79	47.2
6	L^2	30	41	62	47	31	50	13.34	44.8
7	$[Co(L^2)_2]Cl_2$	41	49	50	48	32	57	11.65	47.3
8	$[Ni(L^2)_2]Cl_2$	37	46	54	43	34	61	15.32	48.1
9	$[Cu(L^2)_2]Cl_2$	43	57	53	54	38	65	9.75	48.2
10	$[Zn(L^2)_2]Cl_2$	35	66	58	45	42	59	12.54	46.7
11	L^3	46	56	29	48	43	46	13.02	43.39
12	$[Co(L^3)_2]$	40	68	49	59	30	51	15.13	47.0
13	$[Ni(L^3)_2]$	36	69	39	61	26	46	16.18	48.6
14	$[Cu(L^3)_2]$	39	67	48	55	34	42	14.71	46.6
15	$[Zn(L^3)_2]$	47	69	47	53	24	56	15.90	49.9
16	standard drugs miconazole	(68µg/mL:1.765 x10^{-7} M/mL)	(107.4µg/mL:2.5765 x 10^{-7} M/mL	(18µg/mL:2.356 x 10^{-8} M/mL	(98.4µg/mL: 2.874x 10^{-7} M/mL	(71.34µg/mL:1453x10^{-7} M/mL)	(109.2 µg/mL :2.212 x 10^{-7} M/mL	-	-

These studies further supported the mode of bonding explained by the IR and ^{1}H NMR spectral data. Downfield shifting of azomethine carbon (-CH=N-) and carbonyl carbon (C=O) in the spectra of all Schiff base ligands to 161.2–162.59 and 154.72–158.30 ppm in the spectra of their

zinc(II) complexes, respectively, indicated the coordination of O-carbonyl and N-azomethine to the zinc metal ion. correspondingly, all carbons attached to hetero atoms like S of thienyl and N of azomethine showed downfield shifting of 1.5–0.7ppm in the spectra of Zn(II) complexes of ligands L^1 and L^2. All other carbons of the ligands in the spectra of the Zn(II) complexes suffered downfield shifting of 0.7- 0.34ppm due to enhanced conjugation and coordination with the metal atoms.

Mass Spectra

The Schiff base ligands L^1–L^3 have mass spectral data and fragmentation patterns that support forming the ligands with the proposed structures and bonding patterns. The spectra of ligand L^1 revealed a molecular ion peak of $[C_6H_8N_2]^{\cdot+}$ at m/z 108(Calcd. 108.14), which loses hydrogen (H) as a radical to produce the most stable fragment at m/z 107 of $[C_6H_7N_2]^{+}$. The ligand, L2 $[C_5H_4ClNS]^{\cdot+}$, had a molecular mass of 145 (Calcd. 145.60) and a base peak of $[C_5H_4ClNS]^{+}$ at m/z 144. The molecular ion peak of ligand L3 was found to be 151 (Calcd. 151.23) of $[C_8H_9NS]^{\cdot+}$, with the most stable fragment $[C_8H_9NS]^{+}$, at m/z 150. The C=N, C-Cl, C-O, C-C, and C-N bonds were all cleaved in the fragmentation pattern.

Magnetic Susceptibility and Conductance Measurements

All of the metal(II) complexes' molar conductance data were determined at room temperaturein DMF as a solvent .Their results in (X1 cm^2 mol^{-1}) are listed in Table 2. Higher molar conductance values indicate that the metal(II) complexes are electrolytic. In contrast, lower values indicate that they are non-electrolytic. For example, the metal complexes 5–8 have molar conductance values in the range of 85.0–89.5 X1 cm^2 mol^{-1} due to their electrolytic nature. The metal complexes L^1–$[Cu(L^1)_2Cl_2]$ and $[Cu(L^2)_2]Cl_2$–$[Co(L^2)_2]Cl_2$, on the other hand, had molar conductance values in the range 11.5–18.7 X1 cm2 mol^{-1}, indicating that they were non-electrolytic.

Table 2 shows the determined magnetic moment (B.M) values of all metal(II) complexes at room temperature. The magnetic moment values of Co(II) complexes were found in the range of 4.34–4.62 B.M suggesting the Co(II) complexes as high-spin with three unpaired electrons in an octahedral environment. The magnetic moment values of the Ni(II) complexes were in the range of 3.27–3.47 B.M, indicating that each Ni(II) ion has two unpaired electrons, implying that these complexes have octahedral geometry. The magnetic moment values obtained for Cu(II) complexes range from 1.51 to 1.67 B.M, indicating one unpaired electron per Cu(II) ion in the d9-system, implying spin-free distorted octahedral geometry. As expected, all of the Zn(II) complexes were diamagnetic.

Electronic Spectra

The electronic spectral values of all complexes are recorded in Table 2. The electronic spectra of Co(II) complexes revealed three absorption bands in the 8786-8892, 17,334-17,759, and 29,726-30,150 cm-1 ranges, which were assigned to transitions $^4T_1g \rightarrow {}^4T_2g_{(F)}$, $^4T_1g \rightarrow {}^4A_2g_{(F)}$, and $^4T_1g \rightarrow {}^4Tg_{(P)}$, indicating an octahedral geometry around the Co(II) ion. The electronic spectral data of Ni(II) complexes revealed d-d bands in the regions 10,123–10,345, 16,125–16,897, and 29,176–29,871 cm^{-1}, allowing the transitions $^3A_2g_{(F)} \rightarrow {}^3T_2g_{(F)}$, $^3A_2g_{(F)} \rightarrow {}^3T_1g_{(F)}$, and $^3A_2g_{(F)} \rightarrow {}^3T_2g_{(F)}$ to be assigned octahedral geometry. The electronic spectra of Cu(II) complexes exhibited a low-energy absorption band around 14,454-14,896 cm-1, which was attributed to the transitions 2Eg2T2g. The high-energy band at 25,132-25,790 cm-1 is caused by a prohibited ligand metal charge transfer. Based on this, a distorted octahedral geometry for Cu(II) complexes is proposed.There were no d–d transitions in the diamagnetic Zn(II) complexes. The charge transfer band's spectra were dominated only at 28,749–28,778 cm^{-1}. Table 2 Conductivity, magnetic, and spectral data of metal(II) complexes are similar.

BIOLOGICAL ACTIVITY

Antibacterial Bioassay

According to the literature protocol, the antibacterial activity of prepaed compounds was investigated two Gram-positive (B.subtilis, S. aureus,) and four Gram(-) (S.sonnei, E.coli, , S.typhi and P.aeruginosa) bacterial strains. The results were compared to those produced with the widely-used antibiotic ampicillin and the simple triazole compound 3-amino-1H-1,2,4-triazole.The growth of the several strains examined was suppressed by the Schiff base ligands in distinct ways. Their metal(II) complexes inhibited the growth of various bacterial strains in a moderate to significant way. The antibacterial efficacy of Schiff base ligand L^1 was significant (66%) with C. Albicans and moderate (38–47%) with T. longifucus, A. flavus, and C. glabrata bacterial strains. P

All of the studied bacterial strains exhibited moderate activity (35–49%) with the Schiff base ligands L^2 and L^3. Compounds$[Ni(L^1)_2Cl_2]$, $[Ni(L^1)_2Cl_2]$, $[Ni(L^2)_2Cl_2]$,$[Ni(L^3)_2Cl_2]$, $[Cu(L^3)_2Cl_2]$ $[Ni(L^3)_2Cl_2$, and $[Zn(L^3)_2]$ appeared significant activity (50–75 %) with all of the tested bacterial strains, while compounds$[Co(L^2)_2]Cl_2$ and $[Cu(L^2)_2]Cl_2$ appeared significant efficacy (52–80%) with all of the tested bacterial strains, and moderate efficacy (48–52%) with C. glabrata. Similarly, compounds $[Cu(L^1)_2Cl_2]$and L^2 appeared significant efficacy (59–87%) with all tested bacterial strains. As well as moderate efficacy (51%) with F.Solani with tested bacterial strains. Compound 8 demonstrated significant efficacy (50–79%) with all tested bacterial strains and moderate efficacy with C. Albicans (44%). Accordingly, compound 10 demonstrated significant efficacy (64–69%) with all tested bacterial strains and moderate efficacy (43 %) except with A. flavus. When metal ions are coordinated, Metal(II) complexes have higher efficacy, according to the average data of efficacy (14.2 mm) of ligands and the data of average efficacy (18.13 mm) of their complexes.

Antifungal Bioassay

The effects of the produced compounds on the fungi C. glabrata T. longifusus, A. flavus,C.albican, F. solani, and M. canis are shown in Table 4. The outcomes were contrasted with those of the common medications miconazole and amphotericin B. The ligand L^1 demonstrated high activity (45-67%) against (C. albicans) and (C.glabrata) fungal strains, moderate activity (32-43%) against (T. longifucus), (M. canis), and (F.Solani), and weak activity against (A. flavus) fungal strainsThe ligand L^1 demonstrated high activity (45-67%) against (C. albicans) and (C.glabrata) fungal strains, moderate activity (32-43%) against (T. longifucus), (M. canis), and (F.Solani), and weak activity against (A. flavus) fungal strains. The ligand L^3 also showed significant activity (70%) against (C. albicans) and moderate activity (37–59%) against (T. longifucus), (A. flavus), (M. canis) and (F.Solani) and weaker activity (22%) against (F.Solani) fungal strains. From the antifungal activity data, it was observed that the metal(II) $[Co(L^1)_2Cl_2]$ -$[Zn(L^1)_2Cl_2]$ complexes had high activity (55-73%) against (C. albicans) and (C.glabrata) fungal strains, moderate activity (38-47%) against (T. longifucus) and (F.Solani), and weaker activity (27-32%) against (A. flavus) fungal strains. Complexes $[Co(L^1)_2Cl_2]$ -$[Zn(L^1)_2Cl_2]$ also shown high efficacy (55-60%) against fungal strains(b), whereas complexes $[Ni(L^1)_2Cl_2]$ and $[Cu(L^1)_2Cl_2]$ had moderate activity (50-52%). It was also observed that $[Co(L^2)_2Cl_2]$ -$[Zn(L^2)_2Cl_2]$ complexes showed significant activity (48–68%) against (A. flavus) and (C.glabrata) and moderate activity (34–50%) against (T. longifucus), (C. albicans), and (M. canis) and (F.Solani) fungal strains. Only complex $[Zn(L^1)_2Cl_2]$ had lesser action (31%) against (T. longifucus) fungus strain, though. Similar to this, the $[Co(L^3)_2Cl_2]$ - $[Zn(L^3)_2Cl_2]$ complexes exhibited strong activity (54–69%) against the fungal strains (C. albicans) and (M. canis), moderate activity (36–53%) against the strains (C.glabrata), (A. flavus), and (T. longifucus), and weak activity (28–31%) against the strain (F.Solani). Additionally, comparative examinations of the average activity values of Schiff base ligands

(44.33 %) and their metal(II) complexes (47.06 %) revealed that coordination with metal ions increases the antifungal activity of the metal(II) complexes. Fig. 3 displays the comparative activity data of the metal(II) complexes and the ligands.

Minimum Inhibitory Concentration (MIC)

The first screening results of all produced compounds revealed that metal complexes $[Co(L^1)_2Cl_2]$ and $[Zn(L^2)_2]Cl_2$ were the most active (above 80%).Therefore, these two compounds were selected for minimum inhibitory concentration (MIC) studies (Table 5). The MIC values of these compounds L^1 and L^2 fall in the range 1.07 $x10^{-7}$ to 1.82 x 10^{-7} M. According to the MIC data, compound 6 is the most effective, with a maximum inhibitory concentration of 1.18 x 10^{-8} M against bacterial strain B. Subtilis.

Cytotoxic Bioassay

The Meyer et al. methodology was followed to test the synthesized ligands and their metal complexes for cytotoxicity (Brine Shrimp bioassay). All drugs were deemed to be nearly inactive in this assay, according to the cytotoxic data listed in Table 6. It was intriguing to observe that the metal complexes displayed stronger cytotoxicity than the ligands. The future development of certain cytotoxic drugs for use in therapeutic settings may be supported by this activity relationship.

Table 5: Minimum inhibitory concentrations (M/mL) of selected compounds against bacteria

Compounds	LD50 (M/mL)	Compounds	LD50 (M/mL)
L1	>1.48x 10^{-3}	$[Ni(L^2)_2Cl_2]$	>5.45 $x10^{-4}$
L2	>1.54 $x10^{-3}$	$[Cu(L^2)_2Cl_2]$	>5.80 $x10^{-4}$
L3	>8.24 $x10^{-4}$	$[Zn(L^2)_2Cl_2]$	>5.33x 10^{-4}
$[Co(L^1)_2]Cl_2$	>2.64 x 10^{-3}	$[Co(L^3)_2]$	>7.88 x 10^{-4}
$[Ni(L^1)_2]Cl_2$	>9.54 $x10^{-4}$	$[Ni(L^3)_2]$	>8.18 $x10^{-4}$
$[Cu(L^1)_2]Cl_2$	>9.66 x 10^{-4}	$[Cu(L^3)_2]$	>6.63 x 10^{-4}
$[Zn(L^1)_2]Cl_2$	>1.15 x 10^{-3}	$[Zn(L^3)_2]$	>8.55 x 10^{-4}
$[Co(L^2)_2Cl_2]$	>5.39 x 10^{-4}		

Anti-Inflammatory Efficacy (in vitro)

- In vitro inhibition of COX2 and COX1 by drugs was calorimetrically assessed for its anti-inflammatory effects (in vitro) at 590 nm for(COX^{-1} and COX^{-2}) utilizing COX^{-1}/COX^{-2} inhibitor of ovine testing check kit. Criterion reference was applied accordingly a drug of Celecoxib.

Anti-inflammatory efficacy and inhibition of 5-LOX (In vitro)

Inhibitor of lipoxygenase (bnova 5) testing check was utilized a standard reference was utilized as drug Meclofenamate sodium. Outcomes were considered in Table 1 accordingly IC50 as means of 3 measurements the index of selectivity was determined then as IC_{50} (COX^{-1}) /IC_{50} (COX^{-2}).

Efficacy of anti-inflammatory (In vivo)

Edema in mice containing carrageenan: 50 mice were separated into 10 sets (i.e., each set, 5 mice). The control received cellulose gum in the 1st set (CMC). The 2nd set *has obtained* a drug of standard anti-inflammatory is $C_{14}H_{10}Cl_2NNaO_2$. Sets (3-10) were administered in (10 and 5mg / kg) as 2 doses, the novelty prepared compounds Outcomes were evidenced as a percentage of rat paw edema. After 1 hour taking the tested doses with 1% solution (0.05 mL) in distilled sterile water, carrageenan was injected with a subculture into the left hind footpad of each mouse. After the carrageenan injection, a tolerance scale was utilized to determine the

edema volume of the foot (0 - 4) hrs. The volume of cerebral edema was compared with the vehicle control set, and the reduction percentage was determined as follows

Where Vc and Vt are the edema volume in the set remedied with control and drug, respectively. Results were debriefed as mean ± (SD). The variations between the means were checked for importance:

% decrease in edema = (1− Vt xVc) × 100 utilizing (ANOVA) followed by Duncan's exam (Table 2).

Testing of antioxidant a. Test peroxidation of lipid (5 and 6) was determined as IC50 and listed in Table 3. Outcomes are listed as IC 50 (µg/mL) in Table 3. Vitamin C has been utilized as a standard antioxidant. b. Free radical scavenging (DPPH) test was measured.

The novelty prepared components displayed a noticeable in vitro and in vivo efficacy of anti-inflammatory. These outcomes are consistent with those given by other investigators, as they reported that some new pyrimidine hybrids prevent the enzyme cyclooxygenase and have the efficacy of anti-inflammatory comparable to the standard drug as celecoxib. In this regard, other researchers have notified a pyrimidine analogue of 3-amino-1,2,4- triazole and investigation the activity of lipoxygenase-catalyzed and antioxidants of radical-blocking for pyridine and by lipoxygenase and cyclooxygenase. Compounds 3 and 4 demonstrated the efficacy of antioxidants examining higher scavenging activity towards DPPH radicals compared to vitamin C. Analogous outcomes have been notified for the derivatives of triazolopyridine and newer pyridine.

Table 1: shows the anti-inflammatory activity of newly synthesized compounds as IC 50 and M for COX^{-1}, COX^{-2}, and 5-LOX, respectively.

Group	**IC 50 (µM) COX^{-1}**	**IC 50 (µM) COX^{-2}**	**COX^{-1}/COX^{-2}**	**IC 50 (µM) 5 LOX**
$[Co(L^1)_2]Cl_2$	4.6	0.56	10.12	5.89
$[Ni(L^1)_2]Cl_2$	4.6	0.56	10.12	5.89
$[Cu(L^1)_2]Cl_2$	5.12	0.56	10.43	5.21
$[Zn(L^1)_2]Cl_2$	5.43	0.95	6.34	6.75
$[Co(L^2)_2Cl_2]$	5.76	0.89	6.65	8.82
$[Ni(L^2)_2Cl_2]$	5.56	0.84	6.60	8.90
$[Cu(L^2)_2Cl_2]$	5.61	0.78	6.58	8.82
$[Zn(L^2)_2Cl_2]$	5.67	0.80	6.57	8.76
$[Co(L^3)_2]$	5.58	0.79	6.57	8.79
$[Ni(L^3)_2]$	5.61	0.81	6.61	8.21
$[Cu(L^3)_2]$	5.66	0.84	6.65	8.34
$[Zn(L^3)_2]$	5.70	0.86	6.69	8.67
Celecoxib	5.54	0.90	7.91	N.D
Meclofenamate sodium	ND	ND	ND	7.34

Table 2: Rat paw edema inhibition % after administration of newly synthesized compounds

Groups mg/kg.b.wt	0 h	1 h	2 h	3 h	4 h
Diclofenac sodium	0.48±0.076 a	32.48±1.45a	35.76±1.55a	38.21±0.93a	42.34±3.23a
$[Co(L^1)_2]Cl_2$ 5	0.47±0.054ab	23.43±0.62b	24.61±1.22d	26.45±0.89c	30.14±1.56c
$[Co(L^1)_2]Cl_2$ 10	0.46±0.04ab	33.67±9.11a	30.55±1.22b	35.34±0.87b	42.56±0.570a
$[Ni(L^1)_2]Cl_2$ 5	0.47±0.03b	22.81±1.32bc	22.65±1.22e	23.96±1.98d	33.9±1.68
$[Ni(L^1)_2]Cl_2$ 10	0.48±0.039ab	23.22±0.69b	28.45±1.33e	34.13±3.71b	36.76±0.87b

$[Cu(L^{1})_2]Cl_2$ 5	0.48±0.043a	12.43±1.35de	16.73±1.33g	20.32±1.3e	20.54±0.43e
$[Cu(L^{1})_2]Cl_2$ 10	0.47±0.01ab	15.41±0.83cd	18.83±0.75ef	24.55±1.59c	27.87±1.45c
$[Zn(L^{1})_2]Cl_2$ 5	0.49±0.02a	9.61±1.12e	12.28±1.38h	17.19±1.26e	17.42±1.32e
$[Zn(L^{1})_2]Cl_2$ 10	0.49±0.01a	13.75±1.15de	17.52±1.13f	20.43±0.65d	21.56±0.34
$[Co(L^{2})_2Cl_2]$ 5	0.48±0.098ab	22.09±0.79b	21.87±1.54d	25.45±0.63c	27.53±1.50c
$[Co(L^{2})_2Cl_2]$ 10	0.49±0.61ab	32.71±9.35a	30.87±1.22b	35.55±0.42b	42.81±0.66a
$[Ni(L^{2})_2Cl_2]$ 5	0.48±0.51b	20.91±1.67bc	21.64±1.62e	22.88±1.43d	29.67±1.56
$[Ni(L^{2})_2Cl_2]$ 10	0.50±0.32ab	23.78±0.77b	28.41±1.28e	35.44±2.23b	38.85±0.92b
$[Cu(L^{2})_2Cl_2]$ 5	0.50±0.51a	13.87±1.90de	16.72±1.42g	1953±1.21e	20.76±0.41e
$[Cu(L^{2})_2Cl_2]$ 10 mg/kg.b.wt	0.49±0.54ab	17.81±0.64cd	19.73±0.84ef	26.83±1.44c	29.87±2.92c
$[Zn(L^{2})_2Cl_2]$ 5	0.76±0.31a	9.61±1.12e	14.52±1.65h	18.45±1.73e	20.34±2.34e
$[Zn(L^{2})_2Cl_2]$ 10	0.88±0.75a	18.51±1.62de	21.54±1.45f	24.71±0.71d	24.98±1.63 zx
$[Co(L^{3})_2Cl_2]$ 5	0.48±0.027ab	22.65±0.32b	23.33±1.21d	25.31±0.44c	29.68±1.54 c
$[Co(L^{3})_2Cl_2]$ 10	0.49±0.65ab	32.9843±1.47a	30.32±1.12b	35.32±0.61b	42.60±0.290a
$[Ni(L^{2})_2Cl_2]$ 5	0.47±0.03b	18.91±1.19bc	20.07±1.43e	21.96±1.25d	27.38±1.68
$[Ni(L^{2})_2Cl_2]$ 10	0.48±0.32ab	20.87±056b	25.87±77e	32.87±2.98b	36.90±0.43b
$[Cu(L^{2})_2Cl_2]$ 5	0.49±0.32a	12.65±1.43de	15.78±1.98g	19.87±1.48e	20.54±0.54e
$[Cu(L^{2})_2Cl_2]$ 10	0.49±0.76ab	17.65±0.78cd	18.54±0.43ef	23.76±1.76c	28.65±2.54c
$[Zn(L^{2})_2Cl_2]$ 5	0.49±0.76a	15.43±1.54de	17.42±1.87g	20.45±1.41e	20.54±0.08e
$[Zn(L^{2})_2Cl_2]$ 10	0.49±0.67ab	16.32±0.78cd	19.83±0.75ef	23.82±1.32c	27.41±2.97c

Table 3 displays the antioxidant activity of newly synthesized compounds.

Groups IC50 (µg/ml) for Scavenging	**DPPH**	**IC50 (µg/ml) for antilipid peroxidation**
$[Co(L^{1})_2Cl_2]$	9.87±0.64	15.65±2.12
$[Ni(L^{2})_2Cl_2]$	10.72±0.54	16.81±2.71
$[Cu(L^{2})_2Cl_2]$	12.64±0.41	22.53±3.2
$[Zn(L^{2})_2Cl_2]$	14.61±0.72	23.62±2.31
$[Co(L^{2})_2]Cl_2$	15.26±0.44	22.67±3.51
$[Ni(L^{2})_2]Cl_2$	11.54±0.67	18.67±1.43
$[Cu(L^{2})_2]Cl_2$	10.26±0.43	20.21±2.87
$[Zn(L^{2})_2]Cl_2$	13.54±0.71	19.56±1.83
$[Co(L^{3})_2]$	12.98±0.76	17.84±2.65
$[Ni(L^{3})_2]$	13.11±0.54	20.75±3.45
$[Cu(L^{3})_2]$	14.26±0.44	21.55±2.66
$[Zn(L^{3})_2]$	15.76±0.87	22.12±1.43
Ascorbic acid	13.71±0.75	25.72±1.23

CONCLUSION

The Schiff bases ligands L1–L3 that have recently been prepared act as tridentate ligands. These are connected to the metal ion via the hydroxyl-O, triazole ring –N, azomethine-N, and. All synthesized metal(II) complexes had an octahedral geometry with the exception of the Cu(II) complexes, which did not. According to biological research, linkage of heteroatoms and/or azomethine (-HC=N-) in these compounds may be to blame for the metal(II) complexes' moderate to significant activity compared to that of Schiff base ligands against a variety of bacterial and fungal strains. The results of biological activity revealed that when ligands were combined with various metal elements, most of them became more active. Based on chelation theory and Overtone's concept, the improvement in biological activity after coordination can be explained. Furthermore, we discovered that compounds $[Cu(L^{1})_2]Cl_2$ and $[Zn(L^{1})_2]Cl_2$ showed

considerable antioxidant action, with compound $[Cu(L^{I})_2]Cl_2$ having the strongest inhibitory activity when compared to the standard reference medication [IC50 of 5.12 and 0.56 M for COX^{-1} and COX^{-2}, respectively, vs 5.54 and 0.90 for standard celecoxib. Compound $[Zn(L^{I})_2]Cl_2$ inhibited COX^{-2} with an IC50 of 0.95. Compounds $[Co(L^{2})_2Cl_2]$ and $[Ni(L^{2})_2Cl_2]$ suppressed COX^{-1} and COX^{-2} nearly as well as the conventional medication. Compound$[Cu(L^{I})_2]Cl_2$ demonstrated the strongest inhibitory potential for 5-lipoxygenase, with an IC50 of 4.71 M compared to the typical anti-inflammatory medication meclofenamate sodium's (6.15 M).

REFERENCES

1. Firoozpour L, Edraki N, Nakhjiri M, Emami S, Safavi M, Ardestani SK, Khoshneviszadeh M, Shfee A, Foroumadi A (2012) Cytotoxic activity evaluation and QSAR study of chromene—based chalcone. Arch Pharm Res 35:2117–2125
2. Baviskar BA, Baviskar B, Shiradkar MR, Deokate UA, Khadabadi SS (2009) Synthesis and antimicrobial activity of some novel. Benzimidazolyl chalcones. Eur J Chem 6:196–200
3. Munawar MA, Azad M, Siddiqui HL (2008) Synthesis and antimicrobial studies of some quinolinylpyrimidine derivatives. J Chin Soc 55:394–400
4. Azad M, Munawar MA, Siddiqui HL (2007) Antimicrobial activity and synthesis of quinoline-base chalcones. J Appl Sci 7:2485–2489
5. Kalirajan R, Sivakumar SU, Jubie S, Gowramma B, Suresh B (2009) Synthesis and biological evaluation of some heterocyclic derivatives of chalcones. Int J ChemTech Res 1:27–34
6. Talia JM, Debattista NB, Pappano NB (2011) New antimicrobial combinations: substituted chalcones-oxacillin against methicillin resistant Staphylococcus aureus. Braz J Microbiol 42:470–475
7. Eumkeb G, Siriwong S, Phitaktim S, Rojtinnakorn N, Sakdarat S (2012) ynergistic activity and mode of action of favonoids isolated from smaller galangal and amoxicillin combinations against amoxicillin-resistant Escherichia coli. J Appl Microbiol 112:55–64
8. Do TH, Nguyen DM, Truong VD, Do THT, Le MT, Pham TQ, Thai KM, Tran TD (2016) Synthesis and selective cytotoxic activities on rhabdomyosarcoma and noncancerous cells of some heterocyclic chalcones. Molecules 21(3):329. https:// doi.org/ 10.3390/ molecules21030329
9. Sato Y, Shibata H, Arakaki N, Higuti T (2004) 6,7-dihydroxyfavone dramatically intensifes the susceptibility of methicillin-resistant or –sensitive Staphylococcus aureus to beta-lactams. Antimicrob Agents Chemother 48:1357–1360
10. Babasaheb PB, Sachin AP, Rajesh NG (2010) Synthesis and biological evaluation of nitrogencontaining chalcones as possible anti-infammatory and antioxidant agents. Bioorg Med Chem Lett 20:730–733
11. Vogel S, Barbic M, Jürgenliemk G, Heilmann J (2010) Synthesis, cytotoxicity, anti-oxidative and anti-infammatory activity of chalcones and infuence of A-ring modifcations on the pharmacological efect. Eur J Med Chem 45:2206–2213
12. Tran T-D, Park H, Kim HP, Ecker GF, Thai K-M (2009) Inhibitory activity of prostaglandin E2 production by the synthetic 21-hydroxychalcone analogues: synthesis and SAR study. Bioorg Med Chem Lett 19:1650–1653

13. Kim BT, Kwang-Joong O, Chun JC, Hwang KJ (2008) Synthesis of dihydroxylated chalcone derivatives with diverse substitution patterns and their radical scavenging ability toward DPPH free radicals. Bull Korean Chem Soc 29:1125–1130

14. Doan TN, Tran T-D (2011) Synthesis, antioxidant and antimicrobial activities of a novel series of chalcones, pyrazolic chalcones, and allylic chalcones. Pharmacol Pharm 2:282–288

15. Sivakumar PM, Prabhakar PK, Doble M (2011) Synthesis, antioxidant evaluation, and quantitative structure–activity relationship studies of chalcones. Med Chem Res 20:482–492

16. Vogel S, Ohmayer S, Brunner G, Heilmann J (2008) Natural and nonnatural prenylated chalcones: synthesis, cytotoxicity and anti-oxidative activity. Bioorg Med Chem 16:4286–4293

17. Echeverria C, Santibañez JF, Donoso-Tauda O, Escobar CA, Ramirez-Tagle R (2009) Structural antitumoral activity relationships of synthetic chalcones. Int J Mol Sci 10:221–231

18. Modzelewska A, Pettit C, Achanta G, Davidson NE, Huang P, Khan SR (2006) Anticancer activities of novel chalcone and bis-chalcone derivatives. Bioorg Med Chem 14:3491–3495

19. Vogel S, Heilmann J (2008) Synthesis, cytotoxicity, and antioxidative activity of minor prenylated chalcones from Humulus lupulus. J Nat Prod 71:1237–1241

20. Kamal A, Kashi Reddy M, Viswanath A (2013) The design and development of imidazothiazole-chalcone derivatives as potential anticancer drugs. Expert Opin Drug Discov 8:289–304

21. Do TH, Nguyen DM, Truong VD, Do THT, Le MT, Pham TQ, Thai KM, Tran TD (2016) Synthesis and selective cytotoxic activities on rhabdomyosarcoma and noncancerous cells of some heterocyclic chalcones. Molecule 21:329. https:// doi.org/ 10.3390/ molecules21030329

22. Neves MP, Lima RT, Choosang K, Pakkong P, de São José Nascimento M, Vasconcelos MH, Pinto M, Silva AM, Cidade H (2012) Synthesis of a natural chalcone and its prenyl analogs—evaluation of tumor cell growth-inhibitory activities, and efects on cell cycle and apoptosis. Chem Biodivers 9:1133–1143

23. Forejtníková H, Lunerová K, Kubínová R, Jankovská D, Marek R, Suchý V, Vondrácek J (2005) Chemoprotective and toxic potentials of synthetic and natural chalcones and dihydrochalcones in vitro. Toxicology 208:81–93

24. Orlikova B, Tasdemir D, Golais F, Dicato M, Diederich M (2011) Dietary chalcones with chemopreventive and chemotherapeutic potential. Genes Nutr 6:125–147

25. Ekhlass N, El-Badry YA, Eltoukhy AMM, Ayyad RR (2016) Synthesis and antiproliferative activity of 1-(4-(1H-Indol-3-Yl)-6-(4-Methoxyphenyl) Content courtesy of Springer Nature, terms of use apply Pyrimidin-2-yl)hydrazine and its pyrazolo pyrimidine derivatives. Medicinal chemistry. Med chem 6:4. https://doi.org/10.4172/2161-0444.1000350

26. Murakami N, Takase H, Saito T, Iwata K, Miura H, Naruse T (1998) Efects of a novel non-steroidal anti-infammatordrug (M-5011) on bone metabolism in rats with collageninduced arthritis. Eur J Pharmacol 352(1):81–90

27. Kulandasamy R, Adhikari AV, Stables JP (2009) A new class of anticonvulsants possessing 6Hz activity: 3,4-dialkyloxy thiophene bishydrazones. Eur J Med Chem 44(11):4376–4384

28. Lu X, Wan B, Franzblau SG, You Q (2011) Design, synthesis and antitubercular evaluation of new 2-acylated and 2-alkylated amino-5-(4-(benzyloxy) phenyl)thiophene-3-carboxylic acid derivatives. Part 1. Eur J Med Chem 46(9):3551–3563.

29. Kaushik NK, Kim HS, Chae YJ et al (2012) Synthesis and anticancer activity of di(3-thienyl)methanol and di(3-thienyl)methane. Molecules 17(10):11456–11468

30. Shehab WS, Saad HA, Mouneir SM (2017) Synthesis and antitumor/ antiviral evaluation of 6-thienyl-5-cyano-2-thiouracil derivatives and their thiogalactosides analogs. Curr Org Synth 14:291–298

31. Shehab WS, Mouneir SM (2015) Design, synthesis, antimicrobial activity and anticancer screening of some new1,3-thiazolidin-4-ones derivatives.Eur J Chem 6:157

32. Shehab WS (2009) Synthesis of tetrahydro pyrimidone derivatives and their glycosides. Curr Org Chem 13:14 33. Corral C, Lissavetzky J, Manzanares I et al (1999) Synthesis and preliminary pharmacological evaluation of thiophene analogues of viloxazine as potential antidepressant drugs. Bioorg Med Chem 7(1):349–1359

34. Abdel-Wahab BF, Abdel-Aziz HA, Ahmed EM (2009) Synthesis and ntimicrobial evaluation of 1-(benzofuran-2-yl)-4-nitro-3-arylbutan-1-ones and 3-(benzofuran-2-yl)-4, 5-dihydro-5-aryl-1-[4-(aryl)-1, 3-thiazol-2-yl]- 1H-pyrazoles. Eur J Med Chem 44:2632–2635

35. Kulmacz RJ, Lands WEM (1983) Requirements for hydroperoxide by the cyclooxygenase and peroxidase activities of prostaglandin H synthase. Prostaglandins 25:531–540

36. Jacob J, Prakash Kumar B (2015) Dual COX/LOX inhibition: screening and evaluation of efect of medicinal plants of Kerala as Antiinfammatory agents Pharmacogn. Phytochemistry 3:62–66

37. Kuroda T, Suzuki F, Tamura T, Ohmori K, Hosoe H (1992) A novel synthesis and potent antiinfammatory activity of 4-hydroxy-2(1H)-oxo-1-phenyl1,8- naphthyridine-3-carboxamides. J Med Chem 36:1130–1136

38. Simone RD, Chini MG, Bruno I, Riccio R (2011) Benzimidazole-1,2,3-triazole hybrid molecules: synthesis and evaluation for antibacterial/antifungal activity. J Med Chem 54:1565–1575

39. Khalil NA, Ahmed EM, Mohamed KO, Nissan YM (2014) Synthesis and biological evaluation of new pyrazolone–pyridazine conjugates as antiinfammatory and analgesic agents. Bioorg Med Chem 22:2080–2089

40. Lokwani D, Azad R, Sarkate A, Reddanna P, Shinde D (2015) Structure based library design (SBLD) for new 1, 4-dihydropyrimidine scafold as simultaneous COX-1/COX-2 and 5-LOX inhibitors. Bioorg Med Chem 23:4533–4543

41. Abdelgawad MA, Bakr RB, Azouz AA (2018) Novel pyrimidine-pyridine hybrids: synthesis, cyclooxygenase inhibition, anti-infammatory activity and ulcerogenic liability. Bioorg Chem 77:339–348

42. Nam TG, Nara SJ, Zagol-Ikapitte I, Cooper T, Valgimigli L, Oates JA, Porter NA, Boutaud O, Pratt DA (2009) Pyridine and pyrimidine analogs of acetaminophen as inhibitors of lipid

peroxidation and cyclooxygenase and lipoxygenase catalysis. Org Biomol Chem 7(24):5103–5112

43. Kotb ER, Soliman HA, Morsy EMH, Abdelwahed NAM (2017) New pyridine and triazolopyridine derivatives: synthesis, antimicrobialand antioxidant evaluation. Acta Pol Pharm 74(3):861–872
44. Mojarrab M, Soltani R, Aliabadi A (2013) Pyridine based chalcones: synthesis and evaluation of antioxidant activity of 1-phenyl-3-(pyridin-2-yl) prop-2-en-1-one derivatives. Jundishapur J Nat Pharm Prod 8(3):125–130
45. Rani J, Saini M, Kumar S, Verma PK (2017) Design, synthesis and biological potentials of novel tetrahydroimidazo[1,2-a]pyrimidinederivatives. Chem Cent J 11:16

SYNTHESIS AND STUDY OF THE MECHANICAL AND THERMAL PROPERTIES OF ABS/RICE HUSK ASH BIOCOMPOSITE USING MALEIC ANHYDRIDE AS COMPATIBILIZER

Pratibha Barik, Deepti Rekha Sahoo and Trinath Biswal
Veer Surendra Sai University of Technology, Burla-768018, India

ABSTRACT
In this study a new green composite material was synthesized by using the rice husk ash (RHA) as filler material, acrylonitrile butadiene styrene (ABS) as matrix with maleic anhydride as compatibilizer. ABS is a copolymer and belongs to thermoplastic nature, which is widely used in various applications and exhibits high-performance. ABS shows good chemical stability, interfacial properties, toughness and processability. The insulating properties of RHA promotes for the production of refractory bricks. RHA fillers are mainly utilized for making low-cost and light-weight insulating panels. Maleic anhydride can act as an excellent compatibilizer which increases the interfacial forces between the matrix and filler. The mechanical and thermal properties of the prepared biocomposites are measured using ASTM techniques. The different test results confirm that the tensile strength, flexural strength and hardness of the samples were increased marginally. The TGA report of the synthesized biocomposite increases gradually with the increase in filler content.

Keywords: ABS, Rice Hush Ash, Mechanical & Thermal properties, Compatibilizer.

1. INTRODUCTION
Plastic industry is now considered as one of the largest industry developed world wide. The use of plastic in many fields exhibits several benefits because of many unique amazing properties, low cost of manufacturing, excellent performance, therefore plastic materials are now replacing metals, ceramics and earthenware materials [1]. Today the massive use of plastic materials in various sectors is the cause of releasing huge amount of solid non-biodegradable plastic wastes. These large volume of plastic wastes dumping on land surface results infertility of the soil. On addition with surface water and marine water, it gradually converted into microplastics and nanoplastic particles. These plastic particles are wrongly consumed by phytoplankton, fishes and other aquatic biota and finally entered into the food chain. Hence, it is now treated as an emerging global issue [2, 3]. A large number of studies available regarding the synthesis and characterization of engineering materials having improved thermal and mechanical properties, for which these materials are efficiently used in various sectors such as construction and automobile. In order to solve this global issue researcher are focusing on biodegradable, cost effective materials, which can be used as a proper substitute of traditional metals, alloys, ceramics and other blended materials. Rice husk ash (RHA) is a highly thermally stable, low cost material and used as a good filler material for synthesis of stable biocomposite material. In this work the rice husk powder was reinforced on the matrix of ABS and maleic anhydride was added as a compatibilizer to increase the interfacial forces in between matrix and reinforcing phase. The biocomposite synthesized is also termed as a form of form polymer alloy [4]. The biocomposite prepared by reinforcing rice husk is light weight and shows improved thermal, mechanical properties, therefore used as an excellent candidate material for automobile and construction [5].

The main objectives of this work is to use rice husk ash as filler & maleic anhydride as a coupling agent with ABS as base or matrix phase, to investigate the behavior and performance of the

ABS/ RHA biocomposite with its application for various fields. The influence of rice husk with the mechanical and thermal properties of the synthesized biomaterial was studied [6].

2. MATERIALS AND METHODS

The ABS was dried in hot air oven for about 2hrs in 80^0C. The moisture present in the ABS is removed and the material becomes dry, then the dried form of ABS used for synthesis of the target biomaterial. Figure 1 shows ABS drying in an oven

Fig.1 ABS material in hot oven after drying

2.1 Surface Treatment

RHA was subjected for thermal treatment in a muffle furnace at temperature of about100°C for 1 hour. After being removed from the furnace, RHA was quickly cooled up to room temperature.

2.2 Sample preparation

The biocomposites containing different weight percentage of ABS, RHA and MA was designed by using a two-roll mill at a speed of about 15 rpm for 10 minutes at a temperature of 220°C. The melt blended biocomposite was kept at room temperature for cooling and the sheets were designed from the two roll mill using brass rod [7, 8].

Table-1 Sample preparation (different wt. %)

Sample	ABS%(in gm)	RHA%(in gm)	MA%(in gm)
1	100	0	0
2	95	05	2
3	85	15	2
4	75	25	2
5	70	30	2

2.3 Sheet Preparation:

The polymer matrix and composite materials (ABS/Rice hush ash) have been moulded into 3 mm thick sheets by using a compression moulding equipment at a temperature of 220°C and a pressure of 120 kg/cm^2 for about 15 minutes, then after that the temperature of the samples was reduced under same pressure and finally different required test samples were cut from the sheets using a hexa blade [9].

Fig. 2 Preparation of sheets using the compression molding technique

2.4 Tensile Testing

The tensile strength of the synthesized biomaterials is tested by using a universal testing machine, ASTM F2099. During this testing method, the 5 different samples of the synthesized biocomposite materials with wt. percentage of RHA varies from 0 to 30 wt. % were tested.

2.5 Flexural Testing

Flexural testing machine (ASTM D790) was used for measuring flexural strengths. Using this test method, the values of pure ABS & the synthesized biomaterial samples containing varying wt.% of ABS and RHA were determined.

2.6 Hardness Testing

The most widely used method for the measurements of Hardness of a material is the Rockwell hardness test, which is done by using ASTM E-18. The hardness values of virgin ABS material and ABS with different wt. % RHA with maleic anhydride (compatibilizer) was determined.

2.7 Thermogravimetric Analysis (TGA)

Thermo gravimetric analysis (TGA) includes heating a sample to a specific temperature and determining its weight with time. In this work TGA was used to assess the rate of breakdown and thermal stability of rice husk ash loaded ABS composites. The TGA experiment was carried out in an inert N_2 atmosphere by using STA-8000, a Perkin Elmer Instrument from the US, with a temperature range of 30°C to 1000°C at 10°C min^{-1}.

3. RESULTS AND DISCUSSION

3.1 Tensile Strength

The tensile strength value of virgin ABS is 29.8Mpa. With the addition of RHA, the strength increases and reaches its maximum value (30.5 Mpa) at RHA= 30 wt.%. But the tensile strength of the composites slightly increases at the point of 30 wt.% ash (strength is 30.5 Mpa) [10].

Table 2 Tensile strength of Samples

Sample	Composition %	Tensile Strength (in Mpa)
1	ABS	29.8
2	ABS/RHA/MA(95:5:2)	25.6
3	ABS/RHA/MA(85:15:2)	27.8
4	ABS/RHA/MA(75:25:2)	29.3
5	ABS/RHA/MA (70:30:2)	30.5

3.2 Flexural Test

The results of flexural test show that, the flexural strength of virgin ABS is 46.17 Mpa but this value gradually decreases with the addition of 5 wt. % of RHA. But, however after that the value gradually increases from 43.19 to 48.08 Mpa with subsequent addition of RHA.

Table 2 Flexural test of Samples

Sample no.	Batch %	Flexural strength(inMpa)
1	Virgin ABS	46.17
2	ABS/RHA/MA (95:5:2)	43.19
3	ABS/RHA/MA(85:15:2)	45.08
4	ABS/RHA/MA(75:25:2)	47.29
5	ABS/RHA/MA(70:30:2)	48.80

3.3 Hardness

The hardness of the virgin ABS material is found to be 74.5 in Rockwell L scale, but after adding different wt. % of RHA, the value decreases having 5wt% RHA. After that hardness value increases from 15 wt.% ash to 30wt.% ash up to the value 76.9 in Rockwell L scale.

Sample no.	Batch%	Hardness (in Rockwell L scale)
1	Virgin ABS	74.5
2	ABS/RHA/MA (95:5:2)	73.4
3	ABS/RHA/MA (85:15:2)	75.2
4	ABS/RHA/MA (75:25:2)	76.1
5	ABS/RHA/MA (70:30:2)	76.9

3.4 TGA

The initial temperature of pure ABS is 410ºC and final degradation temperature is 680.2ºC and the amount of residue obtained is 0.29 g. With the addition of different wt. % of RHA and maleic anhydride also be used as a good compatibilizer, which gradually enhances the degradation temperature of the synthesized biocomposites. The ultimate degradation started in the biocomposite sample containing 30 wt. % of RHA at a temperature range of 470 ^{0}C to 1002.9ºC and the amount of residue obtained is 15.8873 % [11, 12].

Sample no.	Batch%	1st degradation Temp(°C)	Medium degradation Temp(°C)	final degradation Temp(°C)	% of Residue
1	Virgin ABS	410.22	450	680.2	0.29
2	ABS/RHA/MA (95:5:2)	412.29	638.61	809.84	10.3217
3	ABS/RHA/MA (85:15:2)	420.73	789.32	910.94	12.4732
4	ABS/RHA/MA (75:25:2)	425.87	811.37	993.26	14.5621
5	ABS/RHA/MA (70:30:2)	427.95	853.30	1002.92	15.8873

4. CONCLUSION

In this work a novel and interesting biocomposite material ABS/Rice husk was prepared by using rice husk powder as filler material on the surface of ABS matrix. Appropriate quantity of maleic anhydride was added in it to reduce the interfacial tension between the matrix phase and reinforcing material, therefore act as a good compatibilizer. The biocomposite materials are synthesized with varying RHA 5 wt. % to 30 wt.% maintaining a constant composition of maleic anhydride. The various mechanical and thermal characteristics of the synthesized biomaterial was studied by adopting suitable procedure. The developed ABS/RHA biocomposite shows improved thermal and mechanical properties with exceptional thermal stability than virgin ABS. The maximum tensile strength of ABS/RHA is observed in the wt. % of 70:30. The maximum flexural strength is observed in the wt. % of 75:25. Again the

maximum hardness (76.9 L scale) was found in the composition ratio of 70:30. The TGA analysis studies confirmed that there is an increase in initial, intermediate & final temperature from 427.95 ℃ to 1002.92 ℃ which demonstrates high thermal stability of ABS/RHA biocomposites.

REFERENCES

1. Yang, Y., Boom, R., Irion, B., van Heerden, D. J., Kuiper, P., & de Wit, H. (2012). Recycling of composite materials. Chemical Engineering and Processing: Process Intensification, 51, 53-68.
2. Singh, N., Hui, D., Singh, R., Ahuja, I. P. S., Feo, L., & Fraternali, F. (2017). Recycling of plastic solid waste: A state of art review and future applications. Composites Part B: Engineering, 115, 409-422.
3. Chauhan, V., Kärki, T., & Varis, J. (2019). Review of natural fiber-reinforced engineering plastic composites, their applications in the transportation sector and processing techniques. Journal of Thermoplastic Composite Materials, 0892705719889095.
4. Adeniyi, A., Agboola, O., Sadiku, E. R., Durowoju, M. O., Olubambi, P. A., Reddy, A. B., ... & Kupolati, W. K. (2016). Thermoplastic-thermoset nanostructured polymer blends. In Design and Applications of Nanostructured Polymer Blends and Nanocomposite Systems (pp. 15-38).
5. Nagaraj, A., & Rajan, M. (2020). Future needs and trends: influence of polymers on the environment. In Polymer Science and Innovative Applications (pp. 593-634). Elsevier.
6. Zaaba, N. F., & Ismail, H. (2019). A review on peanut shell powder reinforced polymer composites. Polymer-Plastics Technology and Materials, 58(4), 349-365.
7. Arjmandi, R., Hassan, A., Majeed, K., & Zakaria, Z. (2015). Rice husk filled polymer composites. International Journal of Polymer Science, 2015.
8. Kenechi, N. O., Linus, C., & Kayode, A. (2016). 'Utilization of Rice Husk as Reinforcement in Plastic Composites Fabrication-A Review. American Journal of Materials Synthesis and Processing, 1(3), 32-36.
9. Fávaro, S. L., Lopes, M. S., de Carvalho Neto, A. G. V., de Santana, R. R., & Radovanovic, E. (2010). Chemical, morphological, and mechanical analysis of rice husk/post-consumer polyethylene composites. Composites Part A: Applied Science and Manufacturing, 41(1), 154-160.
10. Kishore, R., Bhikshma, V., & Prakash, P. J. (2011). Study on strength characteristics of high strength rice husk ash concrete. Procedia engineering, 14, 2666-2672.
11. Krishnadevi, K., Devaraju, S., Sriharshitha, S., Alagar, M., & Keerthi Priya, Y. (2020). Environmentally sustainable rice husk ash reinforced cardanol based polybenzoxazine bio-composites for insulation applications. Polymer Bulletin, 77(5), 2501-2520.
12. Fernandes, I. J., Santos, R. V., Santos, E. C. A. D., Rocha, T. L. A. C., Domingues Junior, N. S., & Moraes, C. A. M. (2018). Replacement of commercial silica by rice husk ash in epoxy composites: a comparative analysis. Materials Research, 21.

GREEN BIOSYNTHESIS OF SILVER NANOPARTICLES FROM WILD MUSHROOM (G.LUCIDIU) FIRST TIME IN IRAQ

Sara Qahtan Sulaiman and Shadman Tariq Sadiq
Ministry of Higher Education & Scientific Research, Tikrit University, College of Science, Biology Department, Tikrit-Iraq

ABSTRACT

Know days there is an increasing interests about nanotechnology and nanoparticle in vast medical and industrial applications, producing nanoparticles consider important branch of green rout for recent life technology, silver nanoparticles (AgNPs) one of the most safe compound to human and environment due to its low effect an low toxicity even with direct contacting and consuming release low particles of silver, for these reasons , the availability and low costing technology we produced silver nanoparticles from eco-friendly mushroom (Ganoderma lucidiu) first time in Iraq.

AgNPs were prepared by using aqueous extract of G. lucidium as a reducing agent for silver nitrate. The characteristics of silver nanoparticles were determined, including: Determining the highest absorption of silver nanoparticles by UV-VIS spectrophotometer, the shape and size of silver nanoparticles by atomic force microscopy (AFM), as well as determining the aggregates Functionalization of proteins bound to AgNPs by Fourier-transform infrared spectroscopy (FTIR). Particle size and shape were confirmed by Scanning Electron Microscopy (SEM).

The results showed the emergence of a spectral imaging beam using a spectrophotometer that ranged between 350-900 nm, where the best absorption beam was at a wavelength of 450 nm, while the result of AFM showed the surface topography of silver nanoparticles with an average size of 62.78 nm. The protein aggregates were determined with a range between 1091-3434 cm^{-1}, as well as their role in the stability of these molecules. The size of spherical particles ranged between 17.15 - 25.81 nanometers under SEM.

Keywords: Nanoparticles by gonoderma, Gonoderma, AgNPs, FTIR.

INTRODUCTION

Nanotechnology has been a well-known and important field of research since the last century. Its idea dates back specifically to the American physicist Richard P. Feynman, the Nobel Prize winner, when he presented a research paper before the American Physical Society entitled "There's Plenty of room at the Bottom" in 1959 (Feyman, 1960) during which an evolutionary revolution occurred in the field of nanotechnology (Khan et al, 2019). It was followed by researcher Norio Taniguchi by coining the term nanotechnology for the first time in 1974 in reference to the ability to manufacture and develop materials into nanoparticles (Bayda S et al.2019).

The biological preparation of nanoparticles from fungi is known as Myconanotechnology, which is usually made from fungal biomass and the metabolites such as enzymes and proteins (Sudher et al. 2022). In addition, the cell wall plays an important role in the manufacture of nanoparticles through the absorption and reduction of metal ions (Khandel and Shahi, 2018). However, the mechanism and nature of the biological manufacture of nanoparticles are largely unknown because fungi can manufacture nanoparticles inside their bodies (inVivo and inVitro) (Sudheer et al, 2022).

The genus Ganoderma is considered one of the most important medicinal fungi due to the content of some species of active compounds (about 400 active compounds). The past studies indicate that these species have different biological activities, including anti-cancer, anti-

oxidant, anti-bacteria and liver protection effects. The globally famous type G. lucidium (Reishi or Lingzhi) is known in Asia as the king of medicinal herbs for its medicinal value due to its effective content of terpenoids, sterols, steroids, carbohydrates, fatty acids, trace elements, proteins and peptides. On the basis of the foregoing, the current study aimed to prepare and characterize silver nanoparticles for the first time in Iraq from the large Iraqi wild mushroom G. lucidium (Wachtel-Galor S et al.2011).

MATERIALS AND METHODS

Specimens Collection

The mushroom was obtained from the laboratories of the College of Science / Department of Life Sciences / Tikrit University which previously diagnosed by Assistant Professor Dr. Sara Qahtan Suleiman.

PREPARATION OF SILVER NANOPARTICLES

1- Preparation of the aqueous extract of G. lucidium large

Initially, the fruiting body of the pre-dried mushroom was ground by an electric grinder to obtain a fine powder. 15 g of the above powder was dissolved in 150 ml of deionized water with the aid of a shaking water bath under a constant speed and temperature of 55 ° C for 48 hours.

The mixture was filtered by whatman No.1 type filter paper and then filtered again using 0.22 micron micro filters. The mushroom extract was stored in the freezer until its use (Al nasiri et al.2020 ;Nguyen et al.2021).

2-Preparation of Silver Nanoparticles

An aqueous solution of 1 Mmol silver nitrate was prepared as follows:

-0.169 g of silver nitrate added to 1000 ml of deionized water.

-Heating the silver nitrate solution under 30^{o}C for half an hour with continuous shaking.

- The bio-nano particles were prepared by distilling 50 ml of mushroom extract prepared in section 1 to 950 ml of 1 mmol silver nitrate solution under ultrasonic conditions, with an ultrasonic power of 100 watts and a frequency of 42 kHz. Then, after sonication for 20 minutes, the solution was stirred at 800 rpm at 25°C for 30 minutes, and placed in a shaking incubator at 25°C for 120 hours. The color changes were observed, which is evidence of the formation of nanoparticles (Mohanta et al. 2018).

Purification of silver nanoparticles:

The solution containing silver nanoparticles prepared in paragraph 2 was placed in foggy test tubes, then placed in a cooled centrifuge device at a speed of 10,000 rpm for 10 minutes. The distilled was placed in the centrifugal device at a speed of 10,000 rpm for a period of 10 minutes, and the process was repeated 3 times until the filtrate became free of any color. The sediment is collected after drying and kept until used (Agrawal et al., 2014).

Diagnostics of silver nanoparticles

Some characteristics of the prepared silver nanoparticles were studied by following technologies

Spectrophotometer UV-VIS

The optical properties of the silver particles were determined by taking 2 ml of the prepared solutions and diluting them 10 times with deionized water to reduce the false readings. The samples were transferred for examination by a spectrophotometer and UV rays with a wavelength range from 190 to 850 nm and the appropriate wavelength was fixed (Al-Shammari, 2016).

Fourier Transforms Infrared FTIR-

This technique used for identifying active groups that make up the biomass extract of the fungus alone and the mixture of silver nitrate solution and the mushroom extract (silver nanoparticles). The samples were prepared by depositing a drop of each sample on a glass slide and dried at a temperature of 60 degrees Celsius inside the electric oven for 30 minutes, then it was made into a paste with a high-viscosity liquid substance such as paraffin oil (Nujol) after which a small amount of this paste was placed Between two discs of potassium bromide to form a very thin layer then examined by Fourier transform infrared (Al-Shammari, 2016).

Atomic Force Microscope - AFM

As we know Atomic force microscopy stabilizes shape and size of nanoparticles. The process included placing a thin film of a sample of nanoparticles on a glass slide by dropping 100 µl of the sample onto the slide and allowing it to dry for 5 minutes. Then the slides are scanned using AFM (Kaman et al. 2019).

Scanning Electron Microscopy-SEM

The SEM used for study of the surface of nanoparticles.

RESULTS AND DISCUSSION

Visual Change Detection

The optical and spectral characteristics of the prepared silver nanoparticles were studied by observing the presence of color changes when adding the aqueous extract of the fungus G.lucidium to the silver nitrate solution compared with the solution containing the aqueous extract of the fungus without AgNo3. These color changes ranged from Hyaline transparent color (colorless) to settle to light yellow color as shown in Figure (1). It was also noted that the color change process took 120 hours at a temperature of 26±2°C.

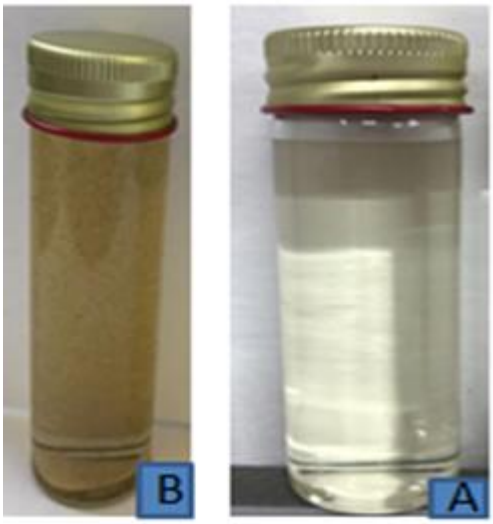

Figure (1) color change of extract containing nanoparticles, A-extract without AgNo3. B-extract with AgNPs .

The occurrence of these changes is evidence of the formation of those particles and the appearance of this color is due to the excitation of the surface plasmon resonance(SPR) of formed particles. It has the direction of electron movement over time with the same oscillation of the incident electromagnetic wave. This property, which depends on the size and shape of the particle is clearly found in gold, silver and copper in the visible light region which responsible for changing their colors when these elements reach the nano size and have many properties and applications (Xia et al, 2005).

UV-VIS Spectra Analysis

Ultraviolet spectroscopy was used to measure the surface plasmon excitation of the nanoparticles in the solution to record the highest absorbance at the wavelength of 450 nm, as shown in Figure (2). This absorption peak was recorded by several studies (AlSalhi et al, 2016; Alfuraydi et al, 2017; AL-Ansari et al 2020) this peak confirms the formation of silver nanoparticles and the spherical nature of them. In addition, fungi are characterized by their ability to help form larger quantities of nanoparticles compared to bacteria due to their ability to secrete large amounts of nanoparticles. There are a large number of enzymes that reduce silver to metal particles and form nanoparticles (Mohanpuria et al., 2008).

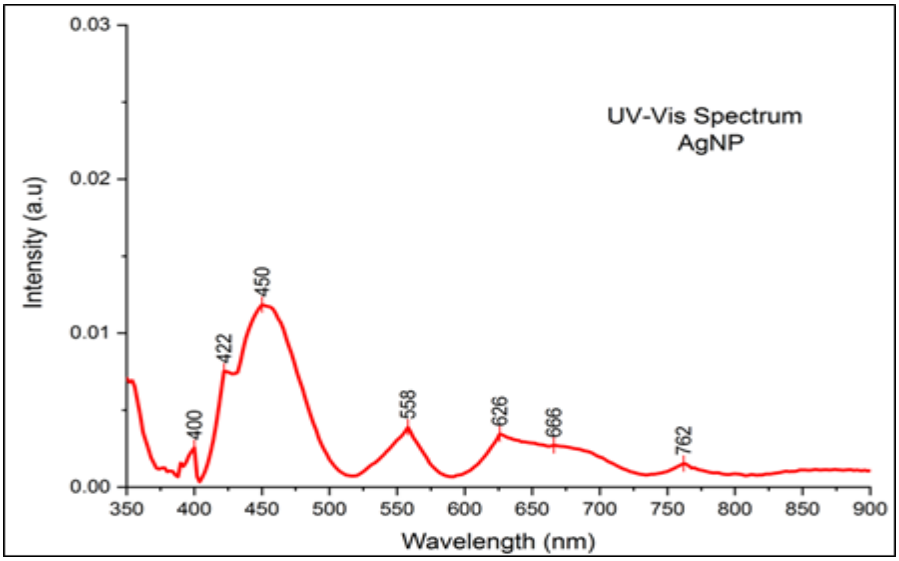

Figure (2). Absorption spectrum of bio-silver nanoparticles prepared using ultraviolet and light spectroscopy

Fourier-Transform Infrared:

Infrared spectroscopy is a powerful tool for identifying the types of chemical bonds in a molecule by producing an infrared absorption spectrum that resembles a molecular "fingerprint".

Numerous curves appeared which indicate the presence of bonds when analyzing the aqueous extract as well as the prepared nanoparticles, Figure 3.

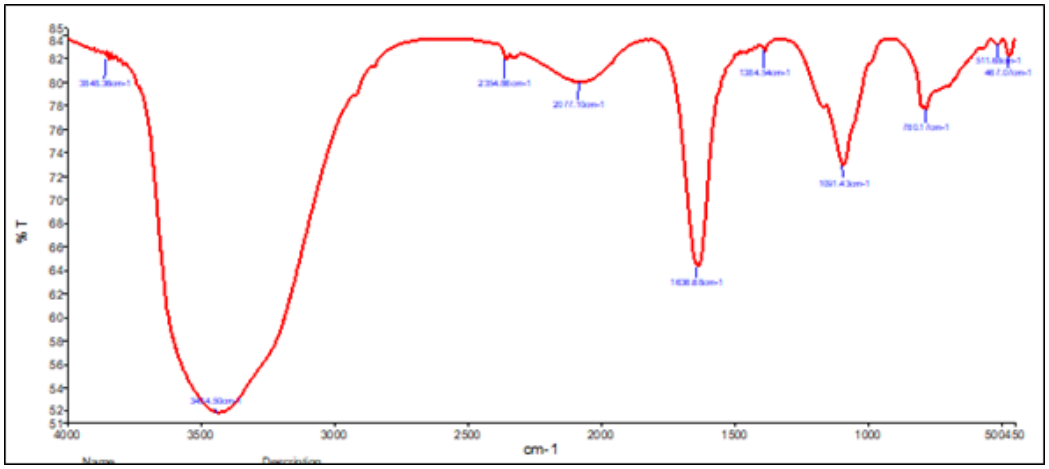

Figure 3: Infrared spectroscopy of silver nanoparticles prepared by aqueous extract of the fungus.

Infrared spectroscopy proved that the appearance of an absorption band at frequency (3434) cm-1 is due to the (OH) bond pattern, and the appearance of an absorption band at frequency (2354) cm-1 belongs to a group (CO2), as well as the appearance of an absorption band at frequency (2077).) cm-1 belongs to the isothiocyanate group (N=C=S), with the appearance of an absorption band at frequency (1636) cm-1 belonging to the azomethine group (C=N), and the appearance of an absorption band at frequency (1384) cm-1 belonging to the group (C-O) alcoholic, and the appearance of an absorption band at the frequency (1091) cm-1 belongs to the etheric (C-O) group. These results were similar to those found in other studies (Aftan et al., 2021a; Aftan et al., 2021b).

Atomic Force Microscope

Atomic force microscopy has been adopted as a powerful tool for studying the morphology of biofunctional particles (Debnath et al., 2019).

The process of revealing the nature of the surface of the synthesized nanoparticles using an atomic absorption microscope showed the nature of the synthesized nanoparticles as in Figure 4.

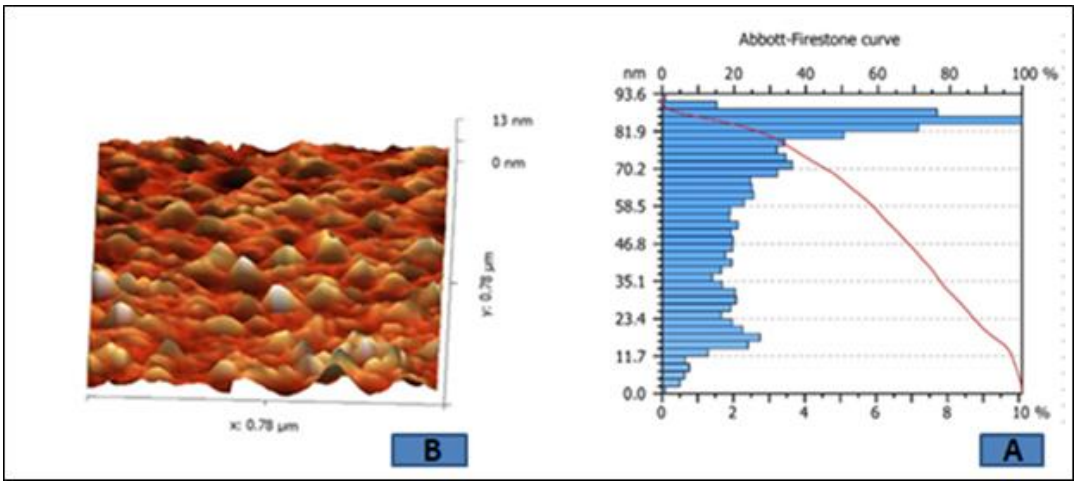

Figure 4: Atomic force microscopy result. (A) Graph of the size of silver nanoparticles, (B) 3D image of silver nanoparticles

The above figures show that the nanoparticles prepared by the aqueous extract of the fungus were characterized by spherical shapes, and Figure (4) shows the size distribution of silver AgNPs nanoparticles, where the average size of the nanoparticles was (62.78 nm).

The shape, size and distribution of nanoparticles depends on physical and chemical properties such as temperature, time, and pH. The size and shape of nanoparticles play an important role in determining the physical, chemical and biological properties of those particles, according to Kredy 2018 study.

Scanning Electron Microscopy

The shape and size of nanoparticles determined by electron microscope. Figure 5 shows that the nanoparticles have spherical shape and size that ranged between 17.15-25.81 nanometers.

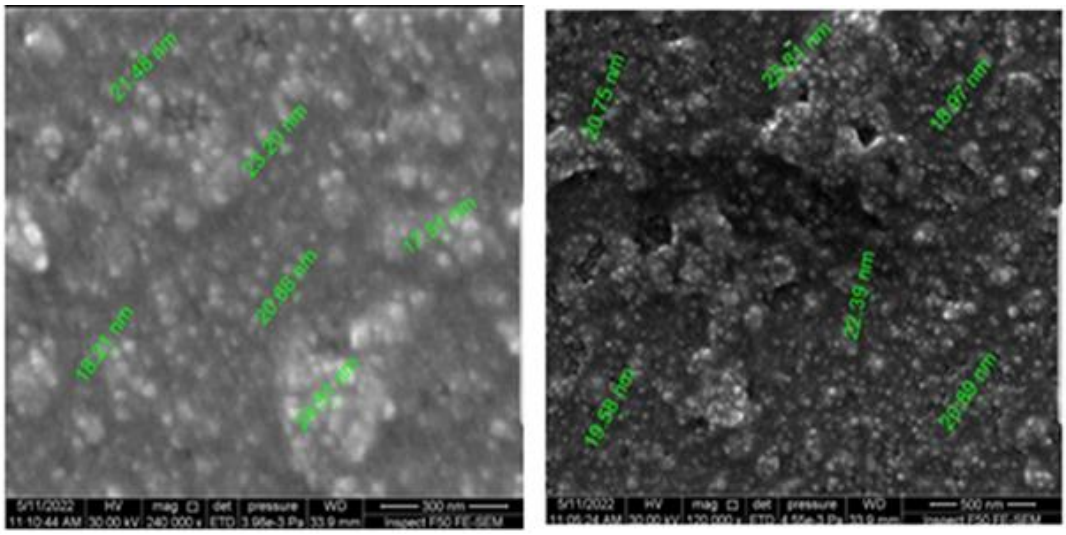

Figure 5: Scanning electron microscope results (**240000X)**

These results were close to the results of Devi and Joshi (2015), in which the electron microscope revealed the spherical shape of the bio-silver nanoparticles, as well as several studies that indicated the same shape for the silver nanoparticles (Salehi, 2017). It also coincided with the study of Nagajyothi et al 2013 in which the use of a scanning electron microscope revealed the formation of spherical nanoparticles ranging from 14.7 - 35.2 nm, which were synthesized from the extract of the fungus Inonotus obliquus.

CONCLUSIONS

In this study, we demonstrated an ecofriendly and economical way for the Biosynthesis of AgNPs using aqueous extraction of G. lucidum.

The produced particles affected by several parameters like pH, reaction time, concentration, and temperature, silver nanoparticles AgNPs produced in 28 hrs. The obtained particles were stable and characterized by FTIR ,UV-Vis, SEM and Furthermore, The results proposed a potential of utilizing AgNPs in the medical fields, especially as antimicrobial , anticancer treatment and furthermore.

REFERENCES

Aftan, M. M., Jabbar, M. Q., Dalaf, A. H., & Salih, H. K. (2021a). Application of biological activity of oxazepine and 2-azetidinone compounds and study of their liquid crystalline behavior. Materials Today: Proceedings, 43, 2040-2050.

Aftan, M. M., Toma, M. A., Dalaf, A. H., Abdullah, E. Q., & Salih, H. K. (2021b). Synthesis and characterization of new azo dyes based on thiazole and assess the biological and laser efficacy for them and study their dyeing application. Egyptian Journal of Chemistry, 64(6), 2903-2911.

Agrawal, N. K., Singh, M., Vijay, Y. K., & Swami, K. C. (2014). Synthesis and characterization of colloidal TiO2 nanoparticles: through titanium chloride rich solutions. Advanced Science, Engineering and Medicine, 6(5), 595-602.

Al-Ansari, M. M., Dhasarathan, P., Ranjitsingh, A. J. A., & Al-Humaid, L. A. (2020). Ganoderma lucidum inspired silver nanoparticles and its biomedical applications with special reference to drug resistant Escherichia coli isolates from CAUTI. Saudi Journal of Biological Sciences, 27(11), 2993-3002.

Alfuraydi, A. A., Devanesan, S., Al-Ansari, M., AlSalhi, M. S., & Ranjitsingh, A. J. (2019). Eco-friendly green synthesis of silver nanoparticles from the sesame oil cake and its potential anticancer and antimicrobial activities. Journal of Photochemistry and Photobiology B: Biology, 192, 83-89.

AlSalhi, M. S., Devanesan, S., Alfuraydi, A. A., Vishnubalaji, R., Munusamy, M. A., Murugan, K., ... & Benelli, G. (2016). Green synthesis of silver nanoparticles using Pimpinella anisum seeds: antimicrobial activity and cytotoxicity on human neonatal skin stromal cells and colon cancer cells. International journal of nanomedicine, 11, 4439.

Al-Shammari, Hazim Idan, Al-Zubaidi, Hamza Kahdum.(2016). Toxicity of silver nanoparticles prepared by extract of Eucalyptus sp in some biological aspects of Citrus mealybug Planococcus citri (Risso), Hemiptera: Pseudococcidae, European Academic Research, Vol. IV, Issue 9.

Bayda S, Adeel M, Tuccinardi T, Cordani M, Rizzolio F. (2019) The History of Nanoscience and Nanotechnology: From Chemical-Physical Applications to Nanomedicine. Molecules.

Debnath, G., Das, P., & Saha, A. K. (2019). Green synthesis of silver nanoparticles using mushroom extract of Pleurotus giganteus: characterization, antimicrobial, and α-amylase inhibitory activity. Bionanoscience, 9(3), 611-619.

Devi, L. S., & Joshi, S. R. (2015). Ultrastructures of silver nanoparticles biosynthesized using endophytic fungi. Journal of Microscopy and Ultrastructure, 3(1), 29-37.

Feynman, R. P. (1960). " There's Plenty of Room at the Bottom". Engineering and Science (California Institute of Technology).

Kámán, J., Huszánk, R., & Bonyár, A. (2019). Towards more reliable AFM force-curve evaluation: a method for spring constant selection, adaptive lever sensitivity calibration and fitting boundary identification. Micron, 125, 102717.

Khan, I., Saeed, K., & Khan, I. (2019). Nanoparticles: Properties, applications and toxicities. Arabian journal of chemistry, 12(7), 908-931.

Khandel, P., & Shahi, S. K. (2018). Mycogenic nanoparticles and their bio-prospective applications: current status and future challenges. Journal of Nanostructure in Chemistry, 8(4), 369-391.

Kredy, H. M. (2018). The effect of pH, temperature on the green synthesis and biochemical activities of silver nanoparticles from Lawsonia inermis extract. Journal of Pharmaceutical Sciences and Research, 10(8), 2022-2026.

Mohanpuria, P., Rana, N. K., & Yadav, S. K. (2008). Biosynthesis of nanoparticles: technological concepts and future applications. Journal of nanoparticle research, 10(3), 507-517.

Mohanta, Y.K., Nayak, D., Biswas, K., Singdevsachan, S.K., Abd Allah, E.F., Hashem, A., Alqarawi, A.A., Yadav, D., & Mohanta, T.K. (2018). Silver Nanoparticles Synthesized Using Wild Mushroom Show Potential Antimicrobial Activities against Food Borne Pathogens. Molecules : A Journal of Synthetic Chemistry and Natural Product Chemistry, 23.

Nagajyothi, P. C., Sreekanth, T. V. M., Lee, J. I., & Lee, K. D. (2014). Mycosynthesis: antibacterial, antioxidant and antiproliferative activities of silver nanoparticles synthesized from Inonotus obliquus (Chaga mushroom) extract. Journal of Photochemistry and Photobiology B: Biology, 130, 299-304.

Nguyen, V. P., Le Trung, H., Nguyen, T. H., Hoang, D., & Tran, T. H. (2021). Synthesis of biogenic silver nanoparticles with eco-friendly processes using Ganoderma lucidum extract and evaluation of their theranostic applications. Journal of Nanomaterials, 2021.

Sudheer, S., Bai, R. G., Muthoosamy, K., Tuvikene, R., Gupta, V. K., & Manickam, S. (2022). Biosustainable production of nanoparticles via mycogenesis for biotechnological applications: A critical review. Environmental research, 204, 111963.

Wachtel-Galor S, Yuen J, Buswell JA, et al. Ganoderma lucidum (Lingzhi or Reishi): A Medicinal Mushroom. In: Benzie IFF, Wachtel-Galor S, editors. Herbal Medicine: Biomolecular and Clinical Aspects. 2nd edition. Boca Raton (FL): CRC Press/Taylor & Francis; 2011. Chapter 9

Xia, Y., & Halas, N. J. (2005). Shape-controlled synthesis and surface plasmonic properties of metallic nanostructures. MRS bulletin, 30(5), 338-348.

ENVIRONMENTAL DAMAGE OF POLYMER PRODUCTS THAT HAVE BEEN TURNED INTO ASSEMBLY AFTER BEING OUT OF USE

Shixaliyev Karam Sefi
Doctor of Technical Sciences, Professor-Academician of the European Academy of Natural Sciences & Professor, Department of Organic Substances and Technology of Macromolecular compounds, Azerbaijan State Oil and Industry University, Baku, AZ1010, Azerbaijan, 20 Azadlig Avenue

ABSTRACT
In this study, the reasons for the decommissioning of polymer materials are shown and recycling methods are analyzed. Polymer materials do not rot, corrode, etc. if their characteristics are taken into account, their recycling is an economic problem as well as an ecological problem that needs to be solved. Taking into account all this, the methods of obtaining purposeful compositions from some polymer wastes have been studied. its destruction mainly occurs as a result of high temperature. As a result, the molecular mass of RS (rubber scrub) decreases. When studying this in an oxygenated and non-oxygenated environment, the maximum stability of RS is observed in the temperature interval of 180°C. Therefore, we adopted the temperature of 180°C to modify road oil bitumen with RS waste. The most effective field of use of polymer materials is the modification of road bitumen

Keyword: Waste of polymer materials, ecology, modification, road oil bitumen, polymer-bitumen composition, polymer asphalt concrete mixture

INTRODUCTİON
Every year, the amount of polymer products used in households in the world is constantly increasing, and these products become waste after use, causing ecological damage to our flora and fauna (0. The waste of polymers used in technology is also increasing every year with the same intensity. ..... Subject to biological decomposition The recycling of residual polymer waste is of both ecological and economic importance. However, the lack of full study of recycling methods limits the use of these valuable raw materials.

During the last 20 years, the use of plastic mass-based products in European countries has reached 80-90 kg per person per year. Calculations have shown that by 2025, the amount of plastic used annually by each person will be 130-140 kg.

150 types of plastic mass are produced on an industrial scale. 30% of them are mixtures of different polymers. .....In order to improve the physical and mechanical properties of plastic masses, various chemical substances are added to them, which are called "ingredients". At the current stage, the production of plastic mass is increasing every year by about 6-10%, and by 2027, its production volume is expected to reach 250 million tons.

41% of produced plastics are used as coating materials..... The quality and cheapness of plastic mass-based products expands their areas of use. After use, polymer products become waste. The recycling of these wastes is of both economic and environmental importance. Currently, the recycling and modification of plastic masses and rubbers has entered the highest stage of development.

Plastic mass recycling technology includes the following operations:

a) Chemical transformations by adding ingredients to the initial plastic mass and creating the required material;

b) Forming the obtained material and obtaining the intended finished product from the formed material.

The field of recycling of rubber and plastic masses includes the preparation of the material for processing and its further processing, calculation of technical and economic indicators...

1.METHOD AND DISCUSSION

Preparation Of Polymer-Bitumen Composition And The Main Content Of The Application Work

1.1. Modification of road oil bitumen with Polystyrene and Polyethylene waste

If their structure remains and they are not destroyed, recycling of polymers with the same composition is quite easy. Of course, the destruction process is such that as a result of it, important changes can occur in the macromolecule and morphology of the polymer. As a result of these changes, all the physical properties of the polymer deteriorate.Therefore, the use of a mechanical method when recycling polymer waste does not give the desired results. Because during mechanical processing, macromolecules are destroyed more and lose their physical and mechanical properties. The method of preparation of bitumen modified with polymers, as a rule, involves the process at high temperature (150-200°C) and intensive mixing of the components. The decomposition temperature of most of the polymers used for bitumen modification (polyethylene, polypropylene, ethylene-propylene rubber, thermally flexible plastic) is higher than the temperature of their compatibility with bitumen. Therefore, thermal and mechanical destructive reaction of polymers does not occur in the bitumen mass. If it does, it is very weak. When heated, bitumens soften, and thermoplastic polymers go into a viscous-flow state, regardless of whether they are crystalline or amorphous. High temperatures accelerate the swelling or dissolution of the polymer in the bitumen.

Dissolution of polymeric materials occurs in the swelling phase. The swelling process consists of dissolving the polymer in the solvent with the increase in volume and mass

Models of the dispersed structure of road bitumen (Figure 1) form 3 types of gel. In type I gels, the type I environment in which the asphalt-concrete is located is more dispersed. The type III structure is structured with more resins than the type I environment of structural connections of individual aggregates. Type III structure is a system consisting of a dispersed medium. Type II structure is composed of electron pairs [28-67].

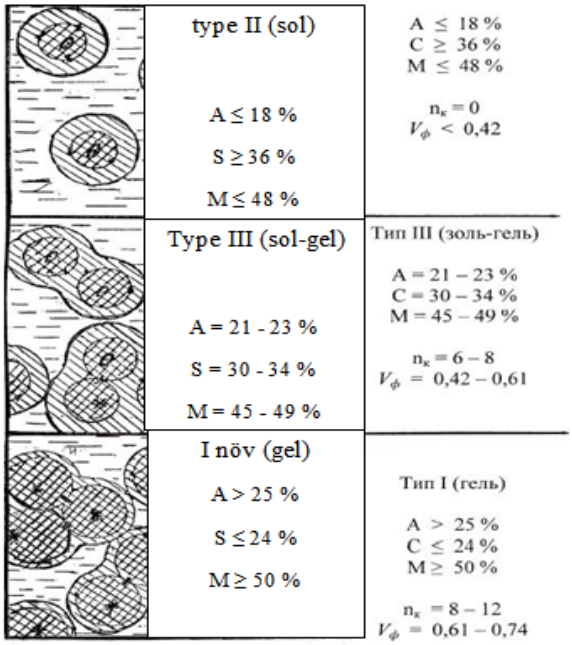

Figure 1. Models of road bitumen dispersion structure

- localized unpaired electron;

- delocalized unpaired electron;

- weak covalent bond.

Taking into account that there are 40-50 thousand tons of polyethylene and polystyrene waste every year in our republic, we determined that the method of their disposal is the modification of road oil bitumen.

Polystyrene destruction mainly occurs as a result of high temperature. As a result of destruction, PS molecular mass decreases. This can be seen more clearly in Figure 2.

Polystyrene recycling and utilization methods. Recycling of homogeneous polymers is quite simple if their structures have not been destroyed. If the structure of the polymer is destroyed, then its molecular mass decreases and the physical-mechanical properties of the polymer deteriorate [51-52].

If the polystyrene waste has preserved its original physical and mechanical properties, it can be used only for special purposes.

Polystyrene is used in various fields [53-54]. Polystyrene is the main raw material in the production of packaging material, coating, electrical and electronic structures, toys and other products.

In this work, the polystyrene waste shown in table 1 was used to obtain a polymer-bitumen composition.

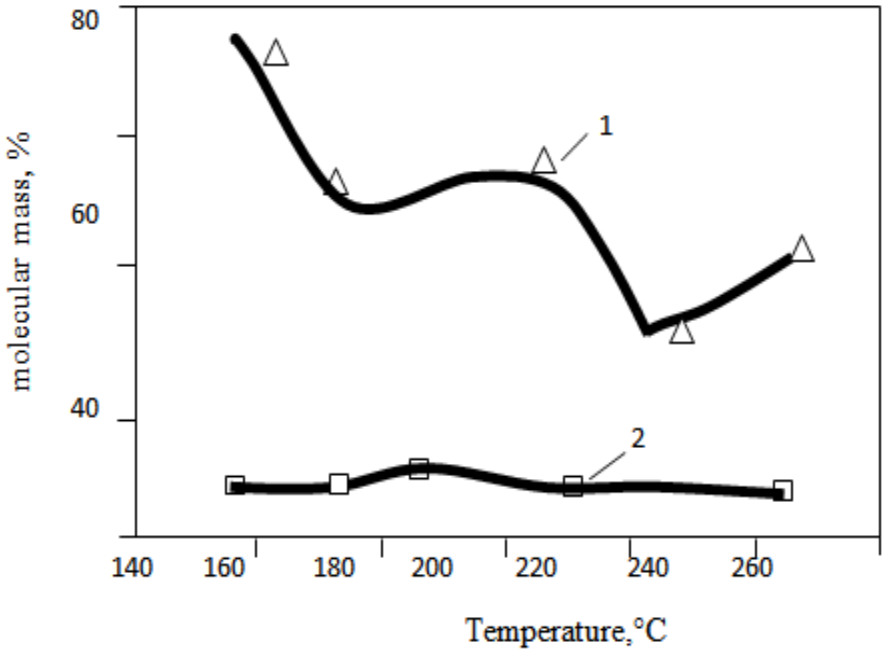

Figure 2. PS destruction in oxygenated and non-oxygenated environment 1-with oxygen, 2-without oxygen.

The combined use of PS and polyethylene waste is also of great ecological and economic importance.

"Baku" brand bitumen was modified with polymer waste. The physical and mechanical properties of the obtained polymer-bitumen binder were studied by 2 modern research methods, and the obtained results are shown in table .1., .2., .3. and given in .4.

Table .1. Physical and mechanical properties of the polymer-bitumen composition obtained with "Baku" brand oil bitumen modified with polystyrene waste

Name of indicators	**Requirements for Standard 52 056.2003**	**Baku «25\85» bitumen**	**Polymer bitumen composition modified with 2.5 mass parts of polystyrene waste**
Depth of penetration of the needle into the sample, 0.1 mm At25°C At0°C	 60 32	 74 25	 62 27
Length, sm At25°C At0°C	 25 11	 140 3,5	 103 23
Yumşalma temperaturu, °C	54	42	68
Elastiklik, % at 25°C a t0°C	 80 70	 4 3	 89 70
Sticking to sand and stone	**it sticks well**		
Kinematic viscosity at 135°C	455	-	1159
Dynamic viscosity at 60°C	270	-	931
After testing according to ASTM P 1734			
change in volume,in % by mass	-	0,3	0,21
Softening temperature, ºC	-	45	108

Table 2. Polymer-bitumen modified with polyethylene waste physical and mechanical properties of its composition

Name of indicators	**Requirements for Standard 52 056.2003**	**Amount of polyethylene in polymer-bitumen composition, mass part .**		
		2 mas. part	**4 mas. part .**	**6 mas. part**
Depth of penetration of the needle into the sample, 0.1 mm At25°C At0°ə	 40 25	 74 25	 43 22	 41 20
Length, sm At 25°C At 0°C	 15 8	 20 3,5	 18 10	 16 9
Softening temperature, °C	48	63	69	76
Brittleness temperature, °C	-18	-22	-26	-40
Elasticity, % at25°C af0°C	 80 70	85 Not checked	95	60
Change in softening temperature after heating, ºC	5	3	2	1
Ignition temperature, °C	210	300	320	350
Kinematic viscosity at 135°C	-	455	4768	5940

Table 3. Physical and chemical indicators of polyethylene waste

№ .	Characteristics	Brands of polyethylene waste: :					
		A-1	A-2	A-3	B-1	B-2	B-3 B-4
1	Primary raw material	Household waste, caps, packaging materials, plastics			Low-pressure polyethylene waste, production waste		
2	density, q/sm^3	0,915	0,915	0,915	0,945	0,945	0,945
3	Alloy flow index: 21.17 H (2.16 kgs) at load 49.0 H (5.0 kgs) in cargo	0,1-10 -	0,1-10 -	0,1-10 -	- 0,1-35	- 0,1-35	- 0,1-2,0
4	Mass fraction of volatile substances, %	0,30	0,30	0,30	0,30	0,30	0,30
5	Mass fraction of sol, %	5,0	5,0	7,0	5,0	5,0	0,1
6	Maximum tensile strength, MPa	8,0	8,0	8,0	15,0	15,0	15,0
7	Relative elongation at break , MPa	300	300	300	250	250	250
8	Compaction density kg/m3	400	400	250	400	400	400

Table .4. - Physico chemical properties of industrial wastes produced on the basis of industrial wastes

№	Characteristics	Industrial waste consisting of low and high pressure polyethylene mixtures					
		: Brands					
		B-1	B-2	B-3	Q-1	Q-2	Q-3
1	Primary raw material	Polyethylene industrial waste			Industrial waste consisting of low and high pressure polyethylene mixtures		
2	density,, q/sm^3	0,915	0,915	0,915	0,915	0,915	0,915
3	Alloy flow index: 21.17 H (2.16 kgs) at load 49.0 H (5.0 kgs) in cargo	0,1-35 0,1-35	0,1-35 0,1-35	0,1-35 0,1-35	0,1-35 0,1-35	0,1-35 0,1-35	0,1-35 0,1-35
4	Mass fraction of volatile substances, %	0,30	0,30	0,30	5,0	5,0	5,0
5	Mass fraction of sol, %	5,0	5,0	5,0	7,0	7,0	7,0
6	Maximum tensile strength , MPa	8,0	8,0	8,0	8,0	8,0	8,0
7	Relative elongation at break , MPa	8,0	8,0	8,0	8,0	8,0	8,0
8	Compaction density kg/m3	300	300	300	250	250	250
9	Density of scattering and pouring (ball formation), kg/m3	400	400	400	300	300	300

1.2. Polymer-Bitumen Binder

Polymer-bitumen binder (BBM) is the most important element of the top layer of the asphalt-concrete surface of a modern highway. The life of the road built on the basis of polymer asphalt concrete mixture prepared using PBE is at least 7-8 years longer. We have used the tread rubbers of old tires that are out of service to produce PBU.

The waste of tires that are out of operation increases many times the basic properties of oil road bitumen. The experiments we conducted showed that the received polymer bitumen has strength, water and cold resistance, anti-cracking, heat resistance (up to 85°C), displacement

resistance, etc. it was possible to increase the indicators several times. . Although we increase the price of asphalt concrete by 1% by using PBE, its other properties: the long life of the paved road, its environmental friendliness, and the fact that the road surface meets world standards confirm that its use is effective [55-58].

Rubber scrub|RO| The physical-mechanical property of the polymer-bitumen composition prepared on the basis depends on the property of the primary bitumen. Even 2.5% mass of bitumen rubber scrub. h. by giving, the elasticity of such a composition can be raised above 70% at 25°C. RO added to bitumen dramatically increases its viscosity. The aging resistance of the polymer-bitumen composition was studied by the ASTMD 1754 methodology. The obtained results are shown in table 5. As can be seen from table 5, kinematic viscosity at 135°C and dynamic viscosity at 60°C with 2.5% RO addition of kraton DT 1101CS blunt. increases by 2.4 and 3.65 times, respectively.

As can be seen from Table 5, the amount of RO in the polymer-bitumen composition is 2.5%. 4.0% k from h. Increasing h increases both the kinematic viscosity and the dynamic viscosity. At the same time, the physical and mechanical properties of the composition fully meet the requirements of DÜIST 52058-2003.

The high degree of structuring of the polymer-bitumen binder does not allow it to be fully studied. The amount of RO in the polymer-bitumen composition is 6% k. When it reaches h, the "softening temperature" increases sharply and it becomes difficult for the needle to enter the sample.

Thus, by changing the amount of RO in the polymer-bitumen binder, it is possible to obtain a modified PBE with any characteristic.

Table .5. Polymer-bitumen obtained using RO physical and mechanical properties of its composition

Name of indicators	Bakı $85/25$ bitumun göstəriciləri	DÜIST 52056 əsasən tələbat	RO miqdarını -lə modifikasiya olunmuş polimer-bitum		
			2 k. h. RO miqdarını	4 k. h. RO miqdarını	6 k. h. RO miqdarını
The depth of penetration of the needle into the sample (Penetration), 0.1 mm at25°C at0°C	 40 25	 47 25	 64 26	 78 27	 68 25
Don't lie downı, sm at25°C at0°C-	 15 8	 40 3,5	 50 13	 48 12	 53 14
Yumşalma temperaturu, °C	56	48	53	72	78
Change in annealing temperature after heating , °C	3	2	2	1	1
Brittleness temperature , °C	-15	-19	-23	-24	-26
Elasticity ,% at25°C at0°C	 40 30	 80 70	 75 65	 85 74	 85 75
Ignition temperature , °C	230	300	340	360	400
Adhesion (sticking) to sand or marble	**meets demand**				

Fire hazard	**it is dangerous**				
Kinematic viscosity at 135°C	-	455	980	1914	2102
Dynamic viscosity at 60°C	-	210	1806	2947	3048
olume change by ASTMD 1754 method, % mass	**after testing**				
Residual penetration, %	-	72	80	93	96
Softening temperature, °C	40	53	63	76	85
Elongation at 25°C, %	110	47	45	38	32
Kinematic viscosity at 135°C	661	670	1017	1134	1340
Dynamic viscosity at 60°C	604	610	3029	3134	3680

3.3. Polymer Asphalt Concrete Based on Oil Refinery and Rubber Waste Preparation and Application

Comparison of polymer asphalt concrete and asphalt concrete. The main properties of asphalt concrete prepared on the basis of modified bitumen are manifested only during use. The tested polymer asphalt concrete fully met the parameters of DÜIST 28-97 bitumen under operational conditions. Compared to asphalt concrete, polymer asphalt concrete has high deformation, strength, water and mine resistance.

Polymer asphalt concrete has shown to have better deformation properties than asphalt concrete at 20ºC (table. 6).

In the mechanical process, Mu P-100 research conducted under dynamic conditions (piston travel speed 1200 mm/min) showed that the temperature at which the brittle disintegration of asphalt concrete takes place is indeed in the negative temperature region. One of the most important indicators is its tolerance to temperature changes. Physical and mechanical properties of polymer asphalt concrete DÜIST 28-97 prepared on the basis of bitumen modified with HRS were mainly determined and the obtained results are given in table 7. Deformation of asphalt concrete and polymer asphalt concrete was studied under both static and dynamic loading mode.

Table 6. Properties of polymer asphalt concrete

Name of indicators	**Yükün təsir etmə vaxtı, san**	**Temperatur ºC**	**Istifadə olunan əlaqələndirici**			
			Neft bitumu	**Istifadə olunan bitum**	**5%-li HRS**	**10%-li HRS**
Balance module $E_m\left(\frac{kq\cdot s}{sm^2}\right)\cdot 10^{-3}$	-	+20	1,09	0,77	1,57	3,13
	-	-20	36,5	8,5	5,92	19,5
Deformation module $E\left(\frac{kq\cdot s}{sm^2}\right)\cdot 10^{-3}$	10	+20	0,24	0,16	0,36	0,96
		-20	18,3	4,7	3,4	9,4
	0,02	-20	133	32,2	22	50,5
Plasticity, P	-	+20	0,34	0,39	0,34	0,28
	-	-20	0,151	0,149	0,142	0,107

The highest viscosity of the conditional-dispersion structure $\eta_o^x \cdot 10^{-10} \frac{kqs \cdot s}{sm^2}$	- - -	+20 -20 -	11,6 488 42	7,6 270 35	15,6 340 22	31,2 1300 42
Aging factor α_0 - until old age α_1 - after aging	-	-20	1,76	1,73	1,39	-

In this case, the bending strength of polymer asphalt concrete is greater than that of asphalt concrete at a positive temperature.

Polymer asphalt concrete prepared on the basis of bitumen modified with HRS has more deformation properties at negative temperature and good brittleness and high dynamic resistance at positive temperature.

To determine the aging of polymer asphalt concrete, we heated it and determined its acoustic indicators.

As an indicator of aging, it is calculated according to the ratio of the attenuation coefficients of the sound waves in the sample before and after heating at 120ºC for 40 hours.

The elastic-viscous-plastic characteristics of polymer asphalt concrete samples at 50ºC were determined. The obtained results are given in table 7.

Table 7. Polymer asphalt prepared on the basis of bitumen modified with HRS indicators of brittle-viscous-plastic characteristics of concrete

Name of indicators	**BND brand bitumen (prototype)**	**Polymer – bitumen-based binder (suggested)**
The highest plastic viscosity, $\eta_o 10^{-4}$, Pa· san	8,5	54,0
Ən aşağı plastik özlülük $\eta_m 11^1$, Pa· sec	4,9	23,7
Dynamic displacement limit , $P_{1<2}$, Pa	4,4	24,0
Equilibrium fragility modulus Gm, $P < P_{1<2}$ when it happens Pa	139	463
Voltage reaction cycle q· η_o /Gm· sec	611	1166

Analysis of rheological characteristics shows that the viscosity and brittleness of polymer asphalt concrete prepared on the basis of modified bitumen is 5-6 times higher than that of asphalt concrete.

The effect of HRS viscosity and the granulometric composition of the mineral part was studied for the preparation of polymer asphalt concrete mixture according to the requirements of DÜIST 52056 – 2003. The obtained results were compared with the properties of asphalt concrete prepared on the basis of standard BND 60/90 and BND 200/300 brand bitumens. 5 k. h. The rheological curve of polymer bitumen and petroleum bitumen prepared on the basis of HRS is given in figure 3. As can be seen from the figure, polymer asphalt concrete obtained on the basis

of HRS modified bitumen is more than the actual strength of asphalt concrete obtained on the basis of petroleum bitumen.

Figure 3 shows that polymer asphalt concrete is more resistant to movement and vibration than asphalt concrete. This is explained by the fact that bitumen modified on the basis of HRS reaches such a high level that it is not found in petroleum bitumen.

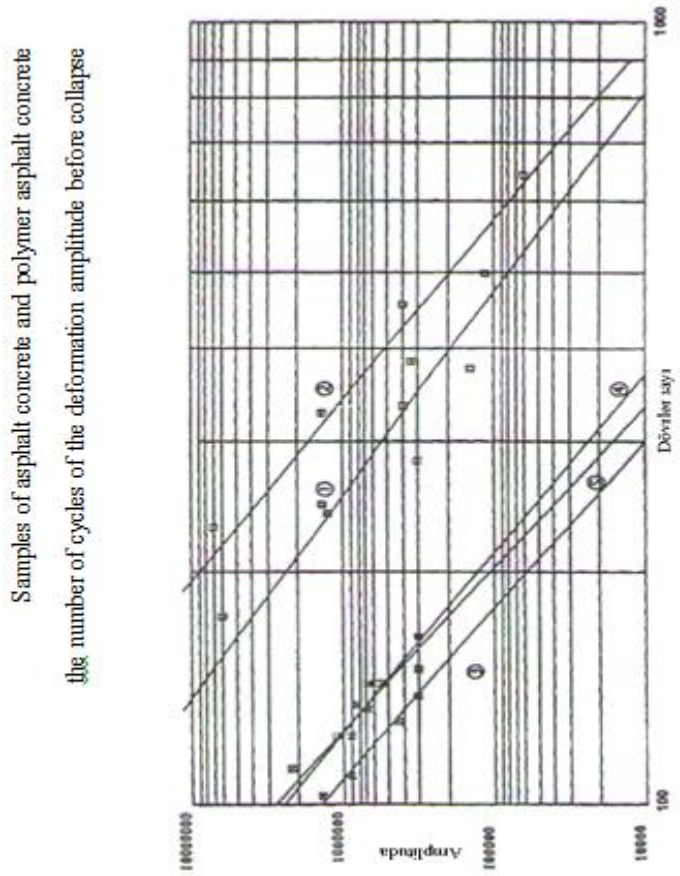

Figure 3. 5 k. h. Rheological curve of polymer bitumen and oil bitumen prepared on the basis of HRS

To prepare polymer asphalt concrete mixture according to the requirements of DÜIST 52056 – 2003

The obtained indicators allow us to say that the displacement tolerance of polymer asphalt concrete (and) is more durable than asphalt concrete. The sum of ΣR=R20+R50 is taken as strength. Because displacement can occur at 20ºC. We take P=2tg 4+c as the sum of displacement continuity.

Polymer asphalt concrete prepared on the basis of modified bitumen based on HRS (type B) P25=98 ΣR=5.61 MPa is less than asphalt concrete type B prepared on the basis of BND 60/90 (P25=48) ΣR=6.4 MPa - P2 .18 and as many as 2.02. In this case, polymer asphalt concrete is more than asphalt concrete.

These indicators make it possible to reduce R50 and R20 norms for polymer asphalt concrete by 10% compared to asphalt concrete. Polymer asphalt concrete can maintain its basic properties even at high temperatures. This fact can be confirmed by analyzing R0/R50 ratios.

CONCLUSION

We modified "Baku 85/25" branded bitumen with polyethylene, polystyrene, SBS and rubber coating. As a result, we received a high-quality polymer-bitumen composition.

By adding polymer waste to bitumen, it was possible to increase its viscosity by 2 times and its strength by 4 times.

After modifying the bitumen with polymer waste, we studied the properties of the obtained composition. The obtained results show that the penetration of the prepared sample is 1.4 times higher than the standard, and its elasticity is 4 times higher.

Since the physical and chemical properties of bitumen are very low, the asphalt-concrete road surfaces made of them soften in high temperature conditions in the summer months and release toxic chemicals into the atmosphere. In order to prevent all this, we managed to obtain ecologically clean bitumen by modifying road-oil bitumen with polymer-based waste. It has been proven by the results of our scientific research that the eco-friendly bitumen we offer is 4 times more flexible than the bitumen currently produced on an industrial scale, and it is possible to increase its heat resistance up to 120°C, which creates fertile conditions for its application in the industry.

REFERENCES

[1]. Alizade Aydan(2022)**.** SKN-40 Rubber with the Participation of Simple and Complex Eternals Purchase Of Chemically Resistant RUBBERS International Journal of Engineering Technology Research & Management/vol 06-issue.01.pp54-63

[2]. Amirov Fariz. Shixaliyev Kerem. (2020).Properties of Linear Low-Density Polyethylene. International Journal of Innovative Technology and Exploring Engineering (IJITEE). Volume-9 Issue-9,pp348-352

[3]. Bilalov Ya.M, Shikhaliev KS,(1973) investigation of the regularities of the reaction of grafted copolymerization of ethylene-propylene rubber and methacrylic acid in an emulsion. Scientific notes AzINEFTEKHIM. pp.36-47.

[4]. Bazhenov S.L., Berlin A.A., Kul'kov .(2010) kompozitsionnyye materially [Polymer composite materials]. Dolgoprudnyy: Intellekt Publ., No. 8 .pp..- 84-87

[5]. Kuperman E. F(2011). New rubber for tires with a high content of venous links. Solution rubbers with a high content of vinyl units, an alternative to SBR emulsion. Transpolymers and copolymers of isoprene and butadiene. Moscow, 2011. 367 p. (in Russian).

[6]. Cooperman E.F. Novye kauchuki dlya shin [New rubber tires. Priority requirements. Assessment methods]. M.oscow, 2005. 329 p. (In Russ.).

[7]. Ososhnik I.A. Karmanova O.V., Shutilin Yu.F. (2004)Tekhnologiya pnevmaticheskikh shin. [Technology tires]. Voronezh, VGTA, 508 p. (In Russ.).

[8]. Ryzhikova, IG, Volkov, A.M., Bauman, NA, Kazakov, Yu.M., Wolfson, SI . (2015) Influence of the concentration of ponents of the peroxide TUMP system modifier and Mooney viscosity of the SKEDT rubber on the yield balance and impact resistance of masterbatches of EPDM in a polypropylene matrix. Bulletin of the technological university-№4.- pp148-150.

[9]. Shixaliyev K.S (2021)Method of Group Decision Making for Production Planning of the Oil Refinery Plant Indian Journal of computer Graphics and Multimedia(LJCGM) Volume-1 Issue2, August 2021ISSUL-2Angust.pp. 1-5

[10]. Shatin D.A., Wolfson S.I., Makarov TV.V. (2010).The effect of the modification of ethylene-propylene triple rubber on the physicomechanical properties of rubber. Vestnik Kazan technological university.№4.pp.5- 7

[11]. Sitnikova D.V., Bukanov A.M., Kovaleva A.N. (2013), Influence of technological additions on the properties of rubbers based on a mortar and emulsion styrene-butadiene kauchkov in blends with highly dispersed silicic acid filler. Kaushik I retina. no. 2, pp. 14 (In Russ.).

[12]. Turaev ER, Beknazarov Kh.S., Akhmedov UK, Dzhalilov AT.(2018) Interphase interactions of three-phase polypropylene composite materials. Universum.Technical sciences .№12.-pp. 57

[13]. Kasatkin M.M. Recycling of depreciated car tires and rubber waste. - M: Signal, 2000, - from 29-30

[14]. Rudensky A.V. Road asphalt concrete pavement. - M: Transport, 1992. - 256 p.

[15]. Zolotarev V.A. On the quality indicators of bitumen modified with polymers. - KUIB: Collection of scientific papers, 2006. - Issue 5 - P. 200-201

[16]. Shikhaliev K.S., Amirov F.A., Movkhasv I.G., Talybova N.R., Mustafayeva R.E. Study of the process of tire operation and methods for recycling worn tires, Ecoenergy, 2008. No. 2, - p. 33-38

[17]. Shikhaliev K.S. Composition based on bitumen and rubber dust. rubber industry. Moscow 2005, -p. 131-134

[18]. Shikhaliev K.S., Ibragimova S.M., Bafadarova Z.M., Novruzova F.M. Modification of bitumen with rubber-containing waste and the use of rubber-bitumen compositions in road construction. VTUZ News: 2008. No. 6, - p. 29-32

SPEECH EMOTION RECOGNITION FOR AUDIO AND TEXT

N. Sirisha, D. Mounika, Roja, Dattatreya, Himansh and Pavan
Department of Computer Science & Engineering, MLR Institute of Technology, Hyderabad-500043, India

ABSTRACT
Nowadays due to internal politics and discrimination in MNC's, few employees are suffering mentally because of their colleagues and the higher authorities. For the growth and well- being of the company, employee mental health is needed to be taken care of. As we know that Human beings emotions are numerous. Unlike other living beings they can express their views by speaking. Human speech depends on various factors like voice, pitch, language, emotion etc. Sometimes it becomes unpredictable what a person is going through. Also the type of emotion they express to the other person might be varied. It may be positive or it can be negative or neutral. Over the previous few years, there is a lot of testing going on right now, emotion

Recognition in speech and it is a key component of human-computer interaction. Computers can't be feeling what humans can. But they can be trained accordingly for getting the desired results. We are building a model on "Speech based emotion recognition for text and audio" where we are implementing sentimental analysis for text based communication and deep learning techniques like CNN for Speech Recognition. In the end, the model will be able to predict the type of emotion based on the given user input. Using this, appropriate actions can be taken by the company based on the acquired output.

Keywords: CNN, emotions, human-computer interaction

I. INTRODUCTION
From a quantitative perspective, human feelings are incredibly difficult to grasp. One of the easiest ways to deduce a person's emotional state is to look at their facial expressions. Another choice is to use speech as a modality. Speech is a multi- dimensional signal that includes details regarding the emotions (through facial expressions), message, speaker and the language [1]. We all know several different types of emotions that can be expressed by word. SER is a system which determines the individual's emotional state based on the individual voice. When it comes to speech, even for us humans, it can be hard to deter- mind the speaker's emotions. The impulse to intensify the spontaneity and performance of HMI (human and machine interaction) is a big motivator. Only four emotions were effectively recognized by the reference paper that was selected. The work discussed here has identified eight feelings, all of which have a high rate of acceptance. In general, speech analysis systems use a variety of techniques to derive properties from raw signals. Pitch, Prosody, and Voice Quality all provide important details about emotions. The subsequent stage in this methodology is to discover the highlights that segregate discourse information (preparing names) and dispose of the non-discriminative highlights.

II. EXISTING SYSTEM
SER has evolved from a minor component of design technology to a significant component of human-computer interaction, for example. These systems aim to motivate direct voice interaction allows for natural interaction with machines. Call centre conversations, on-board car driving systems, and the use of feeling designs from discourse in clinical applications are instances of such employments. These systems, however, have a number of weaknesses that must be addressed. Human listeners to reply rather than utilizing traditional gadgets as input to interpret spoken information and make it simple for human audience members to answer.

Disadvantages:
i. The existing system recognizes or classifies low number of emotions less than six.

ii. They are not computationally efficient.

iii. Accuracy of these systems is very less.

III. PROPOSED SYSTEM

Since human speech signals are highly variable due to speaker differences, it's a difficult task., as well as other factors. To reflect the person's emotion/sentiment, we use the proposed CNN structure to remove the most important frames from the entire series.

This project not only concentrates on the emotion of the speaker or the voice it also analyses the sentiment of a text, regardless, of whether it is positive negative, or neutral dependent on the catch phrases.

IV. LITERATURE SURVEY

Human emotions are complex. A person can guess what other person is feeling but there are lower chances of guessing the correct feeling they're experiencing at that moment. With the help of their facial movements and gestures sometimes it becomes easier to understand the feeling. In general, a lot of research has been done on these emotions. But due to the faster trends in the technology, the concepts of machine learning were introduced in identifying these emotions. Using Convolutional Neural Networks, the process of classification is made easier [2]. Generally CNN is used for the purpose of image classification so here we are using the same concept by converting the audio files (.wav) in to the spectrograms. From this, a chart is produced with time on the X-point and recurrence on Y-point. It can also be done by calculating a cepstrum co-efficient and sampling rate [3]. Audio files are larger in size. Because of this reason, loading files into the model can take huge time. So using technology like big data can solve these type of problem to some extent [4]. For knowing the opinion, sentiment analysis is used for texts. It results out in positive or negative or neutral [5]. The emoFBVP data set of multimodal chronicles looks, body motions, vocal articulations, and physiological signs, of entertainers establishing different articulations of feelings[6]. To see feeling it has been removed Mel Frequency Cepstral Coefficients (MFCC) from the signs. Likewise, we portrayed with k-NN computation[7]. Human-machine recipient recognition (H-M Advertisement) is an advanced paralinguistics and discourse challenge that emerges in multiparty discussions between a few group and an expressed exchange framework (SDS) since the clients may likewise converse with one another and even to themselves while interfacing with the framework[8]. Middle channel will be utilized to eliminate the commotion and pass signal without clamor[9].

To know the state of mind i.e. feelings and emotions, a model is developed using neural networks and knn classifier for classification [9]. Another way to deal with include extraction dependent on examination of two measurements time-recurrence portrayal of a discourse signal have been introduced. The calculation was tried with Emotional Data set[10].

V. ARCHITECTURE

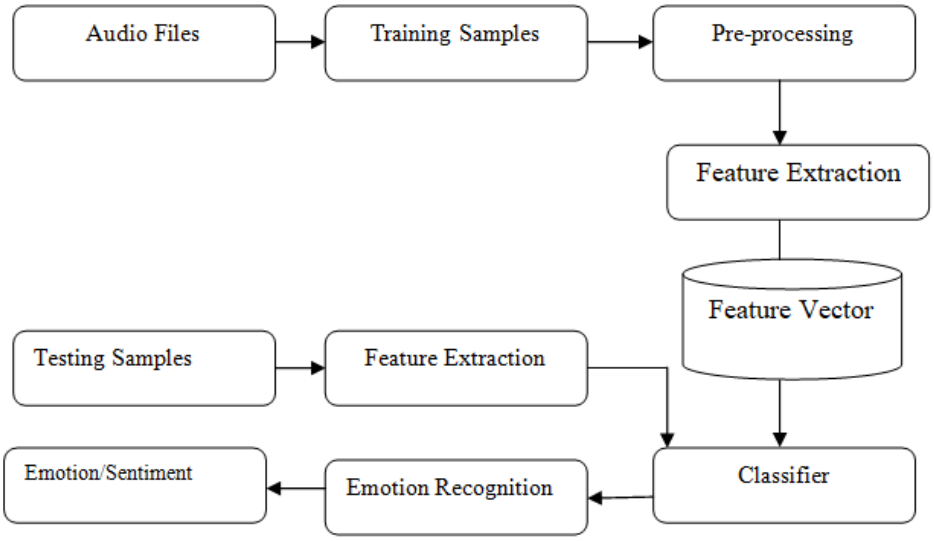

Fig 1: Architecture of speech emotion recognition

VI. SYSTEM DESIGN

System design for speech processing and classification.

Stage 1 (Sound or Speech or Audio):

We can send the audio file existing recordings or the live recorded files.

Stage 2 (Implementing CNN Algorithm) : When an media containing audio file is sent to a person, the algorithm first analysis the recording, converting the audio into an spectral image with the help of MFCC. Then with the help of CNN the image classification[11] can be done.

Stage 3 (Emotions and sentiment):

When he audio undergo testing, it shows the emotion of the sender, whether he/she/they are angry, sad, depressed, happy etc

Modules:

Module 1: Audio feature extraction and visualization

Module 2: To train the module for accuracy calculation.

Module 3: Implementation process of CNN model Module 4: Classification of speech emotions.

VII. DATA DESCRIPTION

We are using 1440 audio files containing both male and female voices with eight different emotions.

They are

1) Angry
2) Neutral
3) Calm
4) Happy

5) Sad

6) Fearful

7) Disgust

8) Surprised

a) Preprocessing

The audio sound wave has three- dimensions with time, amplitude, and frequency represented on three axes. The speech signal is converted into frequency domain using time series analysis.

b) Feature extraction

Sampling Frequency

The number of samples considered from a continuous signal to generate a discrete or digital signal per second is known as sampling frequency. It is also known as sampling rate.

c) MFCC

Mel Frequency Cepstral Coefficients are abbreviated as MFCCs. By converting a standard frequency to Mel Scale, MFCC is ideal for speech recognition[12] tasks because it takes into account human intuition for sensitivity at acceptable frequencies. and is thus suitable for speech recognition tasks.

The knowledge of rate of change in spectral bands is known as cepstrum.

d) CNN ALGORITHM

Step 1: The sample audio is provided as input.

Step 2: The spectrogram and waveform is plotted from the audio file

Step 3: Using the LIBROSA, a python library we extract the MFCC (Mel Frequency Cepstral coefficient).

Step 4: Remixing the data, dividing it in train and test and there after constructing a CNN model and its following layers to train the dataset.

Step 5: Predicting the human voices emotion from that trained data

e) Sentiment Analysis

It's a method for determining whether the data is positive, negative, or neutral. For example: When we pass an expression like “You are not doing well”. This expression shows negative traits and the output will be negative.

VIII. RESULTS AND DISCUSSIONS

The framework in this paper recognizes eight different emotions based on features extracted using a CNN classifier. Based on the given text inputs and audio inputs, the model has detected the emotion and has given the predicted output. As shown in the figure 5.1 when the speech input is given, the model detects the gender and the type of emotion they are expressing it in.

Also, the count is maintained and stored so that if anyone in the organization raises any complaint against a person, this acts as a proof and one can take a proper action against that person.

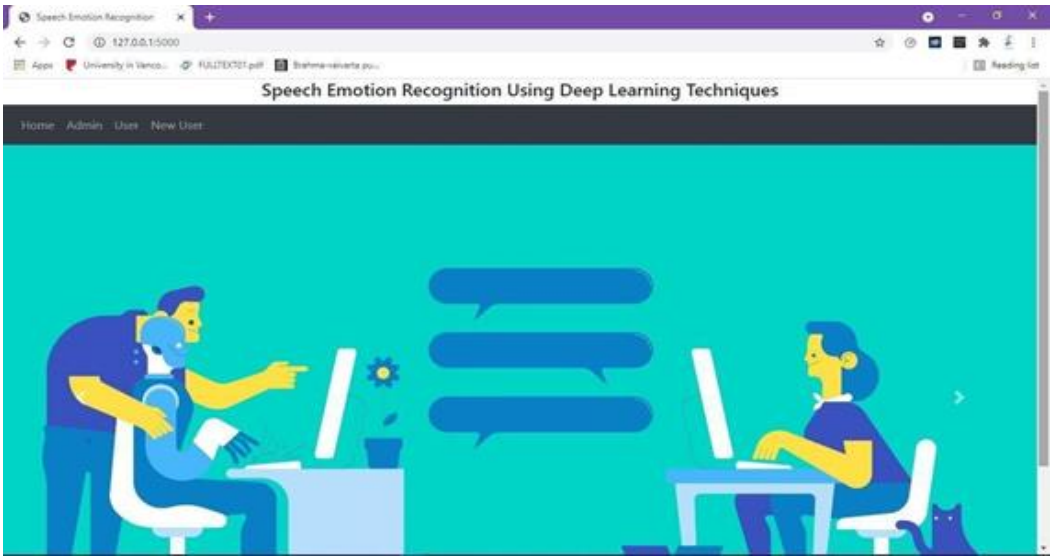

Fig. 2: Home page of the speech recognition application

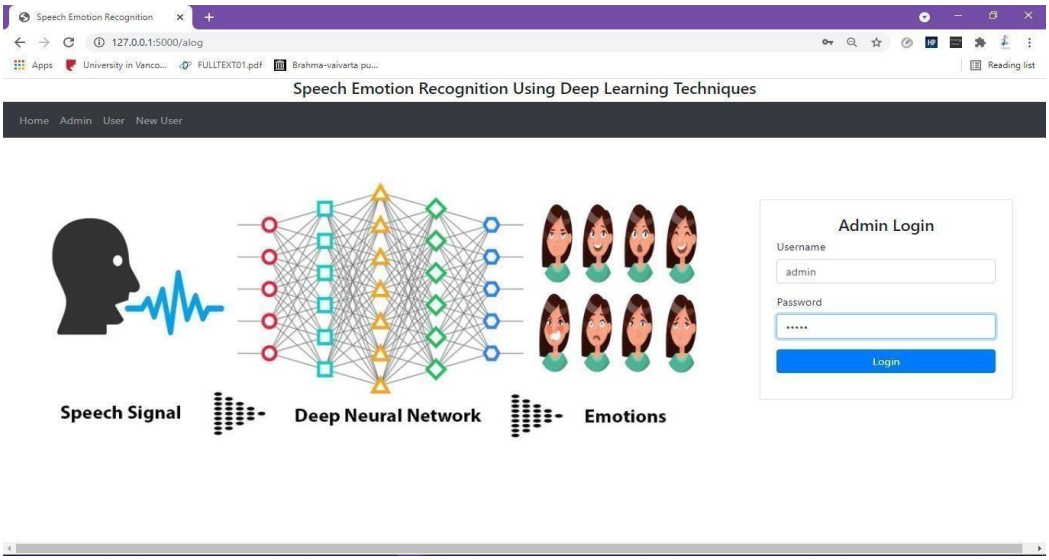

Fig. 3: UI for admin login

IX. LIMITATIONS AND FUTURE ENHANCEMENTS

- The data used were only from English language. So it can be trained to predict in otherlanguages as well.
- The accuracy [13] is quite low when small data sets are used. So we believe that larger data setscan result in high accuracy rate.
- When multiple voices are given to the module the accuracy [14] will be decreased.

X. CONCLUSION

We've found that the model is better at predicting surprise, anger and disgust emotions, which makes sense considering that speech files for these emotions differ in a number of ways, including pitch, tempo, and volume. Overall, we got 71% accuracy on our test results, which is good, but we can boost it even further by using more augmentation techniques and other feature extraction techniques. Speech emotion recognition has many applications in real time. Here we have implemented it as a useful chat application for MNC's so that nobody should face the internal politics in the company.

XI. REFERENCES

[1] K. R. Scherer, "What are emotions? and how can they be measured?" Social science information, vol. 44, no. 4, pp. 695–729, 2005.

[2] A. B. Nassif, I. Shahin, I. Attili, M. Azzeh, and K. Shaalan, "Speech recognition using deep neural networks: A systematic review," IEEE Access, vol. 7, pp. 19 143–19 165, 2019.

[3] D. Ververidis and C. Kotropoulos, "Emotional speech recognition: Re- sources, features, and methods," Speech communication, vol. 48, no. 9, pp. 1162–1181, 2006.

[4] A. Satt, S. Rozenberg, and R. Hoory, "Efficient emotion recognition from speech using deep learning on spectrograms." in INTERSPEECH, 2017, pp. 1089–1093

[5] A. M. Badshah, J. Ahmad, N. Rahim, and S. W. Baik, "Speech emotion recognition from spectrograms with deep convolutional neural network," in Platform Technology and Service (PlatCon), 2017 International Con- ference on. IEEE, 2017, pp. 1–5.

[6] M. S. Hossain and G. Muhammad, "Emotion recognition using deep learning approach from audio–visual emotional big data," Information Fusion, vol. 49, pp. 69–78, 2019.

[7] M. Swain, A. Routray, and P. Kabisatpathy, "Databases, features and clas- sifiers for speech emotion recognition: a review," International Journal of Speech Technology, vol. 21, no. 1, pp. 93–120, 2018.

[8] A Abbasi, H Chen and A. Salem, Sentiment analysis in multiple languages: Feature selection for opinion classification in Web forums[M], ACM, 2008.

[9] H. Ranganathan, S. Chakraborty, and S. Panchanathan, "Multimodal emotion recognition using deep learning architectures," in 2016 IEEE Winter Conference on Applications of Computer Vision (WACV). IEEE, 2016, pp. 1–9.

[10] K. Han, D. Yu, and I. Tashev, "Speech emotion recognition using deep neural network and extreme learning machine," in Fifteenth annual conference of the international speech communication association, 2014.

[11] S. Demircan and H. Kahramanlı, "Feature extraction from speech data for emotion recognition," Journal of advances in Computer Networks, vol. 2, no. 1, pp. 28–30, 2014.

[12] J. Deng, S. Frühholz, Z. Zhang, and B. Schuller, "Recognizing emotions from whispered speech based on acoustic feature transfer learning," IEEE Access, vol. 5, pp. 5235–5246, 2017.

[13] M. Sidorov, S. Ultes, and A. Schmitt, "Emotions are a personal thing: Towards speaker-adaptive emotion recognition," in Acoustics, Speech and Signal Processing (ICASSP), 2014 IEEE International Conference on. IEEE, 2014, pp. 4803– 4807.57

[14] H. M. Fayek, M. Lech, and L. Cavedon, "Evaluating deep learning architectures for speech emotion recognition," Neural Networks, vol. 92, pp. 60–68, 2017.

[15] M.Prabu, Aditi Tiwari, Ritesh Kumar Singh, Rohan Yadav. Speech Emotion Recognition and Features Extraction Based on NN Classifier. IJAST **2020**, 29, 2852 - 2857.

[16] K. Tarunika and R.B Pradeeba "Applying Machine Learning Techniques for Speech Emotion Recognition".

[17] Sathit Prasomphan "Improvement of Speech Emotion Recognition with Neural Network Classifier by Using Speech Spectrogram".

COMPARATIVE STUDY ON THE EFFECTIVENESS OF PNF (HOLD-RELAX TECHNIQUE) WITH MOBILISATION VERSUS CONTRAST BATH WITH MOBILISATION IN THE MANAGEMENT OF VOLAR PLATED WRIST

Nithyanisha, Shathurshini,Vennilavan and Pavithra
Dr.Mgr Educational and Research Institute, Deemed to BeUniversity, Chennai, Tamilnadu

ABSTRACT

Objective of the Study:
The aim of the study is to compare the effectiveness of PNF (hold-relax technique) with mobilisationversus contrast bath with mobilisation in the management of volar plated wrist.

Background Study:
PNF (proprioceptive neuromuscular facilitation) helps in regaining muscle strength and also helps inre-education of the muscle action. Improves coordination and develops certain skills of the population. Contrast bath is an alternate heat and cold therapy which helps in the stimulation of the weak muscle group and prepares them for better action, so that the range of motion can be improved.It also helps in limiting the deformity of the individual in the society.

Methodology:
The Study design is Comparative Studywith a pre and post type based on inclusion and exclusion criteria 30 subjects were selected and using randomized sampling method it was conducted in Out Patient Department ACS Medical College and Hospital for a period of 6 weeks.

Procedure:
30 subjects were selected and divided into two groups Group A and Group B.

Group A:
PNF (Hold-relax technique), hold (5-10 secs), repetition (5-10 times).

Groupb:
Contrast Bath (Alternate Cold And Heat Therapy),,hotpack(3mins), cold pack (1min).

Result:
Comparing pre and post tests within Group A and Group B on VAS and Patient related wrist handevaluation scores shows a highly significant difference in the mean values at $P \leq 0.001$.

Keywords: Fracture, Plating, Proprioceptive neuromuscular facilitation, Contrast bath, Range of motion,Muscle strength, Goniometer, Patient Rated Wrist Evaluation.

INTRODUCTION

Volar locking plates are the most commonly used metallic device in the open reduction and internal stabilization distal radius fractures. These Devices allow immediate post operative return of motion and are good at preventing angular displacement. Their careful positioning is however key toprevent iatrogenic injuries during surgery or chronic sequelae such as slate onset tenosynovitis.

Volarlockingplate implantations have multiple early and late complications, many of which can be picked up on plain film, stress penetrating the dorsal cortex of the radius may damage extensor tendons, whilst the flexor compartment can be injured during volar plate positioning.

According to the International PNF association, PNF (proprioceptive neuromuscular facilitation) stretching was developed by Dr. Herman kebat in the 1940s as a means to treat neuromuscular conditions. PNF stretching may be the most effective stretching technique for

increasing range of motion. One of the PNF techniques is hold-relax. This involves putting a muscle in a stretched position (also called as passive stretch) and holding for a few seconds. Contracting theMuscle without moving (also called as isometric), such as pushing gently against the stretch without actually moving. Relaxing the stretch and then stretching again while exhaling. This second stretch should be deeper than the first. Relax the joint or muscle and then gently stretch for 30 seconds, thenthere is 30 seconds rest and process is repeated again several times. The progressive stretching and change between the contraction and relaxation allows the muscle to adapt to its new position each time it is held in position. This allows it to stretch further next time. The normal range of movement of wrist is given by., Wrist flexion - 0-90 degrees, Wristextension - 0-80 degrees, Radial deviation - 0-20degrees,Ulnar Deviation - 0-30degrees

Contrast bath therapy is a form of treatment where a limb or the entire body is immersed inhot water followed by the immediate immersion of the limb or body in cold ice water. This procedureis repeated several times, alternating hot and cold. This works under the principle of Lewis hunting reaction. Contrast bath is performed using a whirlpool tub. One tub is filled with warm water and another tube with coldwater. The warm tub should be between 98-100 degrees Fahrenheit and the cold tub should be between 50-60 degreesFahrenheit.

Once both the tubs are at the correct temperature, place the injured body part in the warm whirlpool, where it should stay for 3-5 minutes. We can also perform gentle motion exercises at that time. Then quickly move the part being treated to cold water for about one minute.This sequence isrepeated for 20-30 minutes.The theory behind the use of the contrast bath is that the rapid change from warm to cold helps quickly open up and close tiny capillaries (blood vessels) in the body.

Warmth causes these small capillaries to open, whereas the cold causes them to close. Thisrapid opening and closing of blood vessels near the site of your injury creates a pumping action thatis thought to help decrease swelling and inflammation around injuries. Decreasing the swelling and inflammation helps to alleviate the pain and improve mobility.

PROCEDURE

Study Design: Comparative Study STUDY TYPE: Pre and post-test type SAMPLE SIZE: 30 Subjects

Study Method: Randomized sampling method

Study Setting: Out Patient Department ACS Medical College and HospitalSTUDY

Duration: 6weeks

Inclusion Criteria:

- Both male and female
- All age group
- Within two weeks after volar plating

Exclusion Criteria:

- Mentally retarded patients
- Hypersensitive skin (peripheral neuropathy)
- Unconsciouspatients
- Un co-operative patients
- Muscular Dystrophy

- Drug Abuse

OUTCOME MEASURES

- Pain measurement using Visual Analogue Scale (VAS)
- Patient Rated Wrist Evaluation (PRWE)
- Evaluation of range of motion by goniometry.

INTERVENTION

GROUP A- PNF (HOLD RELAX TECHNIQUE)TECHNIQUE:

Hold Relax: Direct Treatment

The therapist or the patient moves the joint or the body segment to the end of the passive or pain free range of motion. Active motion is preferred.The therapist asks for an isometric contraction of the restricting muscles or pattern(antagonists).The contraction should be maintained for at least 5 to8 seconds.The resistance is increased slowly.No motion is intended by either the patient or the therapist.The joint or the body part is repositioned either actively or passively to the new limit of range. Active motion is preferred if it is free.The motion may resist if that does not cause pain. The final stretch must be held for 10 to 15seconds.

Hold Relax: Indirect Treatment

In the indirect treatment with hold relax, the therapist resists the synergists of theshortenedorpainfulmusclesandnotthatpainfulmusclesorpainfulmotion.If that still causes pain resistthe synergistic muscle of the opposite pattern instead.

GROUP B- CONTRAST BATH DESCRIPTION:

STEPS:

Water in the cold container should be between 50-59°F (10-15°C), and water in the hotcontainer should be between 95-113°F(35-45°C).

Immerse the injured part in warm water for 1 to 3minutes. Immediately follow with a 1-minute dip inColdwater. Repeat this process for approximately 20 minutes, ending with cold-water.

DATA ANALYSIS

The collected data were tabulated and analyzed using both descriptive and inferential statistics. All theparameters were assessed using the statistical package for social science (SPSS) version 24. Paired t- test was adopted to find the statistical difference within the groups & Independent t-test (Student t- Test) was adopted to find statistical difference between the groups.

RESULT

On comparing Pre test and Post test within Group A & Group B on VAS and Patient Rated WristEvaluation Score shows highly significant difference in mean values at $P \leq 0.001$.

Table 1: Comparison of Visual Analogue Scale Score between Group – AandGroup - B in Pre and Post Test

TEST	GROUP-A		GROUP-B		t-TEST	df	SIGNIFICANCE
	MEAN	S.D	MEAN	S.D			
PRE TEST	6.06	.961	6.13	.743	-2.31	28	.833*
POSTTEST	2.46	1.06	3.53	.639	-3.33	28	.000***

Thistableshowsthatthereisnosignificantdifferenceinpretestvaluesbet ween Group A & Group B (*****P >0.05).

This table shows that statistically highly significant difference inpost test values between Group A & Group B **(***- P ≤ 0.001)**

GRAPH– I

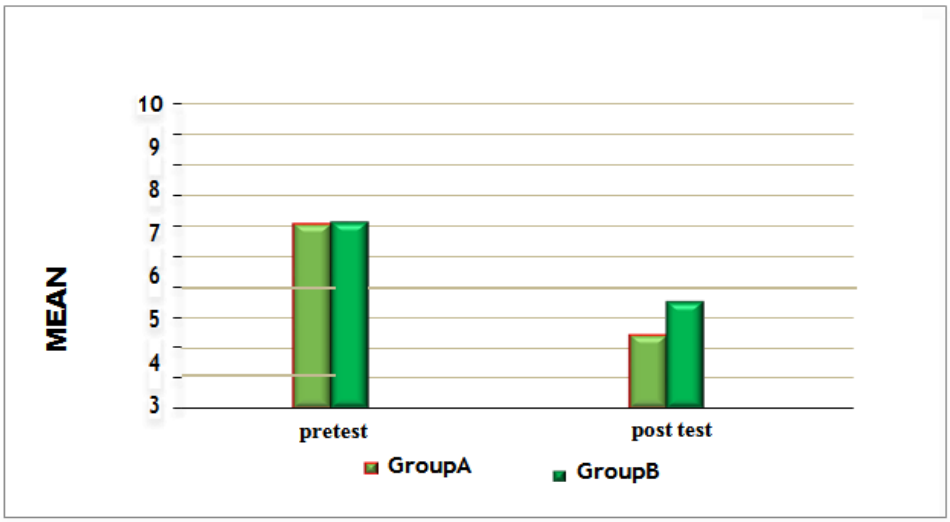

COMPARISON OF VISUAL ANALOGUE SCALE SCOREBETWEENGROUP –AAND GROUP -BIN PREANDPOSTTEST

Table 2: Comparison of Patient Rated Wrist Evaluation ScoreBetweengroup –A and Group-Bin Preandpost Test

#TEST	#GROUP -A		#GROUP -B		t-TEST	df	SIGNIFICANCE
	MEAN	S.D	MEAN	S.D			
PRETEST	70.86	4.50	71.33	5.00	-.268	28	.790*
POSTTEST	40.00	2.77	54.26	3.41	-12.56	28	.000***

Thistableshowsthatthereisnosignificantdifferenceinpretestva luesbetween GroupA &GroupB (*****P >0.05).

This table shows that statistically highly significant differenc in post testvaluesbetween GroupA&GroupB **(***-P ≤0.001)**

GRAPH– II

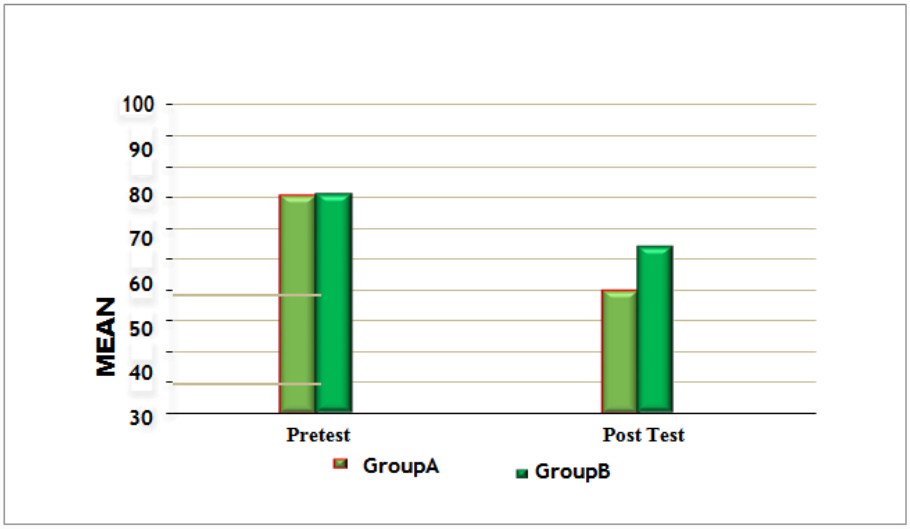

COMPARISON OF PATIENT RATED WRIST EVALUATION SCORE BETWEENGROUP –A AND GROUP-BIN PRE ANDPOST TEST

Table 3: Comparison of Visual Analogue Scale Score within Group – Aandgroup-B Betweenpretestand PostTest

#GROUP	PRE TEST		POST TEST		t- TEST	SIGNIFICANCE
	MEAN	S.D	MEAN	S.D		
GROUP-A	6.06	.961	2.40	1.06	-22.04	.000***
GROUP-B	6.13	.743	3.53	.639	-38.14	.000***

There is a statistically highly significant difference between the pre test and post testvalues withinGroup A and GroupB (***-P≤0.001).

GRAPH-III

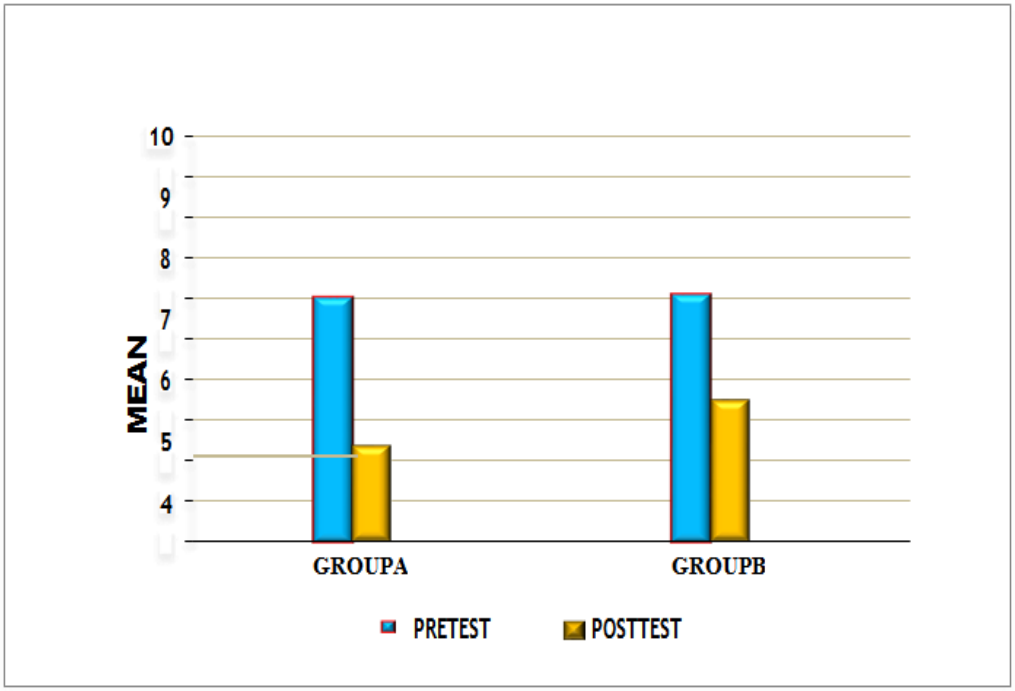

COMPARISON OF VISUAL ANALOGUE SCALE SCORE WITHIN GROUP – A &GROUP –B BETWEEN PRE &POST TEST VALUES

Table 4: Comparison of Patient Rated Wrist Evaluation ScoreWithingroup –A &Group– Bbetweenpre& Posttestvalues

#GROUP	PRE TEST		POST TEST		t- TEST	SIGNIFICANCE
	MEAN	S.D	MEAN	S.D		
GROUP-A	70.86	4.50	40.00	2.77	-15.92	.000***
GROUP-B	71.33	5.00	54.26	3.41	-19.74	.000***

There is a statistically highly significant difference between the pre test and post testvalues withinGroup AandGroupB(***-P≤0.001).

GRAPH-IV

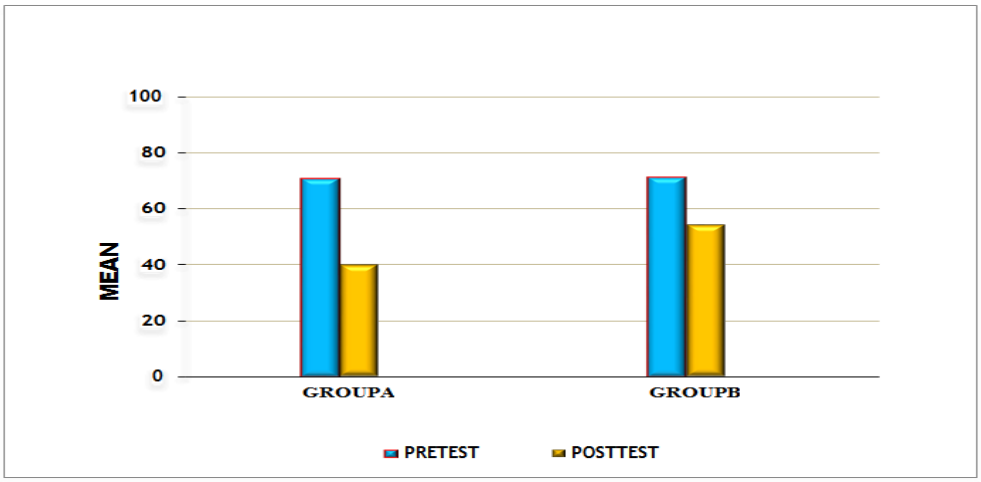

COMPARISON OF PATIENT RATED WRIST EVALUATION SCORE WITHINGROUP –A &GROUP– BBETWEENPRE& POSTTESTVALUES

DISCUSSION

In this study, VAS score and PRWE score significantly improved as a result of 6weeksPNF (hold relax technique). These findings are in agreement with the previous findings by FlorianSchneideretal.,(2009)fromdeterminingtheeffectsof2differentpost-operativetherapyapproachesafteroperativestabilizationofthewristfractures.Aftera6-weekperiodofpostoperativetreatment,thepatients(n=23)performinganindependenthomeexercise programusingatrainingdaryshowedasignificantlygreaterimprovementofthefunctionalityofthewrist.Gripstrengthreached54%(p=0.03) and ROM in extension and flexion 79% (p<.001)of the uninjured side. Patientswhowereperformingthehometrainingafteroperationrecordedan improved functionwithanearly50%lowervalue(p<.001)inthePRWE score.

However,eventhoughourresultsinpainreductionandimprovementinPRWEscoreareconsistent withthesesimilarfindingswithincreaseinfunctionalityofwrist,rangeofmotionandgripstrength,there isalsosomeevidencethatcan'tbeassociated with ourresult. Contrary findings by ErcoleCRubinietal.,shows the rewasnosignificantdifferencebetween thestretchingprotocols.Therewasnosignificant effect on RT,MTshowedanegativemain effectfor time(p<0.05) showing3.4%.

Peanchai Khamwong et al., (2011) reviewed that stretching with proprioceptive neuromuscular facilitation (PNF) is frequently used before exercise. 28 healthy males wererandomlydividedintothePNFgroup(n=14)andcontrol group(n=14).PNFwas used before eccentric exercise induction in the wrist extensors. All subjects were tested to examine muscle damage characteristics including sensory-motor functions at baseline immediately, and from 1st to 8th days after the exercise-induced muscle damage(EIMD).TheresultsdemonstratedthatthePNFgroupshowedalesserdeficit in some sensory-motor functions(p<0.05) than the controlgroup.

Table-3revealstheMean,StandardDeviation(S.D),t-value andp-valuebetweenpre- test and post-test within Group – A & Group – B. There is a statistically highly significant differencebetween the pre-test and posttest values within Group A and Group B (***- P ≤0.001).

Table- 4 reveals the Mean, Standard Deviation (S.D), t-value and p-value between pre-test and post-test within Group – A & Group – B. There is a statistically highly significant difference between the pre-test and post test values within Group A and Group B (***- P ≤0.001).

Although earlier studies recommended that PNF techniques are an adjunct to conventional disability, improving range of motion when compared to conventional therapy alone in conservatively managed distal radius fractures, they are consistent with our findings in the pain reduction and limitation of disability. Overall, because of findingasignificantchangeintheVASscoreandPRWEscoreofthePNF(holdrelax technique) group when compared to contrast bath, it seems that well effective interventions are needed to reduce the treatment duration and improve the independency of an individual in doing their activities of dailyliving.

REFERENCE

- Mahieu NN, et al. Scand J .Effect of proprioceptive neuromuscular facilitationstretchingon the plantar flexor muscle- tendontissueproperties. Med Sci Sports. 2009. PMID: 18627559 ClinicalTrial.
- Kham Wong P, et al. A active effect of proprioceptiveneuromuscularfacilitation (PNF)stretchingonsymptomsofmuscledamageinducedby eccentricexercise of the wristextensors. 2011.PMID:21943625ClinicalTrial.
- Rubini EC, et al. Immediate effect of static and proprioceptive neuromuscularfacilitation stretching on hip adductor flexibility in female ballet dancers. J Dance MedSci.2011.PMID: 22687658 Clinical Trial.
- SErhart, SToth, PKaiser, TKastenberger…Comparisonofvolarlyanddorsallydisplaceddistalradiusfracturetreatedbyvolarloc kingplatefixationArchivesoforthopaedic…, 2018-Springer
- KC Chung, L Squitieri, HM Kim Comparative outcomes study using the volarlocking plating system for distal radius fractures in both young adults and adults olderthan60year-The Journal ofhand surgery, 2008-Elsevier
- EKarlsson,PWretenberg,PBjörling…Combinedvolaranddorsalplatingvs.volar plating of distalradius fractures. A single-centerstudyof105case-HandSurgeryand …, 2020-Elsevier
- GD Krischak, A Krasteva, F Schneider, D Gulkin… Physiotherapy after volarplating of wrist fractures is effective using a home exercise program - Archivesofphysical …,2009-Elsevier
- CVillarivera,KWinchell,AFerguson,MHelfandPhysicalTherapyInterventionsintheHospitalSetting -ehc-Django-testing.s3.Amazonas…
- DonnaEBregerStanton,RolandoLazaro,JoyCMacdermid.ASystematicReviewoftheEffectivenesso fContrastBathsNovember2008JournalofHandTherapy22(1):57-69; quiz70
- Debra Sullivan ,Ph.D.,MSN,R.N.,CNE, COI Medically reviewed What to KnowAboutContrastBathTherapyWrittenbyRebeccaJoyStanborough,MFAonJuly29,2020
- Paul Ingraham Contrast Hydrotherapy "Exercising" tissues with quick changesin temperature, to help with pain and injury rehab (especially repetitive straininjuries)• Dec 12,2018
- PeggyPletcher,M.S.,R.D.,L.D.,CDEMedicallyreviewedPNFStretching:AHow-ToGuide—Written byKristenBarta—Updatedon July8,2017.
- BradWalkerWhatisPNFStretching?ProprioceptiveNeuromuscularFacilitation – How to do it, precautions to take, safety guidelines, and PNFstretching examples |First Published February 16,2004| Updated October 17,2019.

FORMULATION AND SPECTROSCOPY OF CU(II) NANO COMPLEXES OF MONOBASIC TRI- OR BIDENTATE (NNO, NO) AZO DYE LIGANDS

Rehab Kadhim Raheem Al-Shemary
Department of Chemistry, College of Education for Pure Sciences, Ibn -Al-Haitham, University of Baghdad

ABSTRACT
A collection of copper (II) azo complexes with the formula [$CuL^{1-4}(nH_2O)$] OAc xH_2O have been created utilizing azo dyes that contain the thiadiazole and triazole moieties. Thermal analyses molar conductance magnetic moment measurements, Elements, electronic mass, IR, and ESR spectra were used to describe azodyes and their metal complexes. IR spectra revealed tridentately organized ligands with a triazole moiety with copper(II) ion, naphthyl OH donor sites, azo group N-atoms, triazole moiety. Comparatively, azodyes with thiadiazole moiety had ON donor positions of the azo moiety's N-atom and the naphthyl OH. The TG curves were used to determine the thermodynamic activation constants ΔE, ΔH*, ΔS*, and ΔG*. Electronic spectroscopy and transition electron microscopy included as analyze the produced spherical copper nanoparticles (TEM). The spectrum data revealed that the (OH) attaching group formed a surface complex between azodye ligands and colloidal copper nanoparticles. Resulting in greater surface area of the produced copper nanoparticle complexes, their stability constant of the produced copper nanoparticles complexes is higher than the equivalent bulk ones.*

INTRODUCTION
Metal complexes of heterocyclic azo compounds are widely used in various practical uses, including technology to operate, nonlinear optical components, and storage devices for molecular memory. Additionally, It's possible that heterocyclic azo dyes and their metal complexes are important. Because of their bioactivity and analytical uses. Nowadays, much emphasis has been placed on and 1,3,4-thiadiazole ,1,2,4-triazole derivatives are a significant family of N-including aromatics. The heterocycles have piqued the interest of researchers as a result of their bioactive components like antitumor,antimycotic,anti-inflammatory, antibacterial, antimicrobial, and powerful agents of antifungal. These derivatives, on either side, are a significant characteristic of heterocyclics that exhibit a wide range of biocidal actions, presumably attributed to the combination of the toxophoric ANACAS group. Metal complexes of these derivatives are now of attention, owing to their importance in metal connections with biomolecules. Nanoparticle coordination chemistry is a relatively young field of study in contemporary chemistry. Nanoparticles are massive pseudomolecules with complicated internal structures; they are primarily made up of the core and shell. They often include active surface sites.Cu(II) nanoparticles are attractive because of their low cost (relative to Ag and Au), catalytic, optical, mechanical, magnetic, and electrical properties. Heat conduction properties differ from those of bulk metals. We successfully synthesized and described Cu(II) complexes with four azo dyes derived from 1-Methyl-1H-1,2,4-triazol-3-amine,5-Phenyl-1H-1,2,4-triazol-3-amine,5-Methyl-1,3,4-thiadiazole-2-thiol or 2-Amino-5-(ethylthio)-1,3,4-thiadiazole with β-naphthalene. Also, the favorable conditions for complex structure, complexation, and spectroscopy measurement of Cu(II) ion as part of our ongoing work on hetero azo dyes and their metal complexes. The study of the financial institution of the examined azo dyes based on elemental analyses, magnetic moments, spectral techniques (UV–Vis, ESR, and IR), conductance, and thermal properties are also of importance. Because the interaction between metallic nanoparticles and organic ligands piqued our interest, we evaluated the interaction between the researched azo ligand and the colloidal solution of copper nanoparticles.

2. EXPERIMENTAL

2.1. Materials and Analyses

The solvents and reagents were of sample solution purity and employed just as specified. Sigma–Aldrich provided starting material. The conductivity studies for the synthesized solid Cu(II) azo complexes were taken using a Hana model 1331 conductometer. In this study, $Hg[Co(SCN)_4]$ was used as a calibrant for the Sherwood Scientific Magnetic Susceptibility Balance. Shimadzu Qp-2010 plus mass spectra were recorded. Perkin–Elmer model 2400 automated analyzer was used for (C, H, and N) analysis. We used Shimadzu TG-50 thermal analyzer to record both TG and DTG curves. A spectrophotometer of Shimadzu UV-visible acquired UV-Vis absorption spectra. The observations were made in a nitrogen environment with a heating rate of 10˚C min^{-1} using platinum crucibles. The morphology of the copper nanoparticles was studied using a JEOL-JEM-100SX transmission electron microscope. Image analysis provided the particle size and size distribution. Also, the spectrophotometer of IR-generated as a KBr disk. The Cu ion content was calculated using an atomic absorption spectrophotometer.

2.3. Preparation of the Ligands

1-Methyl-1H-1,2,4-triazol-3-amine(0.134g,1mmol),5-Phenyl-1H-1,2,4-triazol-3-amine (0.133g,1mmol**),** 2-Amino-5-methyl-1,3,4-thiadiazole (0.115g,1mmol), or2-Amino-5-(methylthio)-1,3,4-thiadiazol(0. 147 g,1mmol) was dissolved in 3 ml of a(1M) HCl solution and slowly stirred into diazotized with (0.069 g, 1 mmol) of $NaNO_2$ in a mixture of water and ice (6 ml). The resultant diazonium salt solution was mixed with β-naphthalene (0.144 g, 1 mmol) diluted in 30 ml sodium hydroxide solution (30 %) and chilled 5 to 0 ˚C in an ice bath. The colored solids were suction purified and rinsed with bidistilled water, refined by recrystallization, finally, the purified ligands were dried in a desiccator over anhydrous $CaCl_2$. The purity of the azo dyes was determined initially using the m.p constancy, followed by elemental examination and, finally, differential equations (Scheme 1).

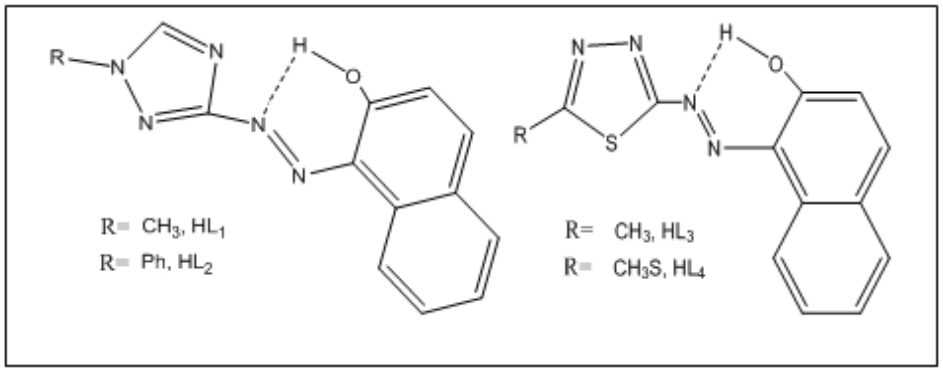

Fig. 1: Structure of azo-dye ligands ($HL_{1–4}$).

2.4. Synthesis of Solid Complexes

The formed colored solids were suction purified and rinsed with bidistilled water many times, refined by recrystallization, and finally, the purified ligands were dried in a desiccator over anhydrous $CaCl_2$. Thus, the dyes' purity (azo dyes) (Scheme 2) was determined using the m.p constancy, followed by means of elemental analysis, and then lastly differential equations. Next, to defining the end of the response, the reaction mixture was stirred over many hours utilizing TLC plates. Finally, to extract Cu(II)complexes, the precipitated particles were recovered by filtering, over anhydrous $CaCl_2$ and rinsed with twice distilled water in a dried desiccator. Table 1 provides detailed information about every complex.

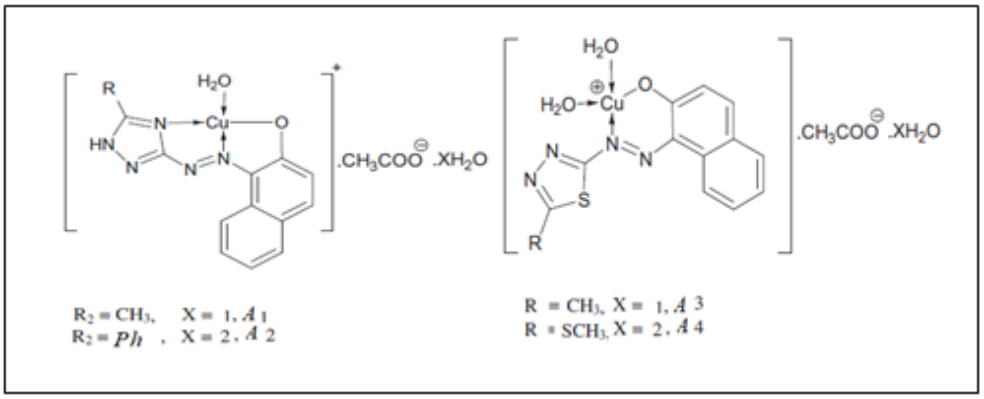

Scheme 2: Structure of complexes (A1–A4).

2.5. Synthesis of Copper Nanoparticles

The reaction was performed in an open 125 ml flask. Dropwise adding of a 10ml amount of 0.003 M Cu $(NO_3)_2$ generated in solution of IPA (approximately 1 drop/s) to 0.090 M of CTAB/IPA solution in a typical reaction. Specifically, a dropwise (1 drop/s) addition of (0.003 M) Cu $(NO_3)_2$ generated in solution of IPA (10ml) to (0.090 M) of solution CTAB/IPA. Then, use a board of magnetic stir, the reaction mixture was vigorously swirled. After adding 2 ml $Cu(NO_3)_2$, the changed colour after adding 5 ml copper nitrate, and dark violet after adding the entire volume of $Cu(NO_3)_2$. The emergence of colour revealed the existence of Cu nanoparticles. A spectrum measured minutes after the colour appeared revealed the plasmon absorption at 560 nm. The product remained stable for a week when sealed in a vial. After one week, however, the violet colour and plasmon band began to fade.

3. RESULTS AND DISCUSSION

3.1. UV.-vis. Spectra of ligands and their complexes Figure 2 displays the UV.-vis. spectra of compounds in methanol. The absorption spectra readings were calculated by subtracting the absorption maxima of the azo-copper complexes from the ligand. UV.-vis. spectra of azo bonds, using electronic spectroscopy, except for HL_2, showed just two bands. The frequency range 210-800 nm revealed three major absorption bands. The 1st peak observed in the reign (220–280)nm is attributed to a moderate energy π–π* transformation within the moiety of phenyl representing the ($^1La \rightarrow {}^1A$) state. The 2nd peak detected in the 285–345nm reign is due to decreased energy π– π* electronic transition of the phenyl ring and heterocyclic structure. Both solvent and substituent kind utilized have little effect on these two bands. The 3rd peak in the reign 460–550 nm represents the n-π* electronic transition in which the electron system is involved and charge transfer. Cu(II) complexes spectra showed that the significant ligand-associated band had moved to higher-frequency wavelengths. The peaks at 540, 570, 580, and 600 nm differed by a bathochromic change of LMCT. The resulting finding supports modern molecular orbital theory by suggesting that the Cu(II) central ion influences the complexes bands according to this hypothesis. Any factor affecting the electronic density of a conjugated system, electron negativity, for instance. the radius, or the metal(II) ion's electrical configuration, must result in a band variation.

3.2. Mass Spectroscopy

The spectrum of mass for HL^1 revealed a molecular ion peak $[M]^+$ at m/z = (253,76%) corresponding to its molecular mass of $C_{13}H_{11}N_5O$. Fragments of the molecular ion $[M^+]$ occur at various sites. However, the base peak was observed at m/z = (130, 100%), indicating the chemical formula C_9H_6O. The peaks represented the other fragmentation at m/z = 114, 83, and 69. Peak $[M]^+$ at m/z=(316, *64* %) indicated that HL^2 had a molecular mass of $C_{18}H_{13}N_5O$, which provided a starting peak at m/z=(2*9*8,100%) because of OH-radical loss followed by H-

radical loss, respectively. The peak fragments lose $C_{10}H_6$ to generate a peak at m/z= (1*72*, *42* %), which then loses N_2 and C_6H_5 H-radical is then made to increase a 2nd peak at m/z = (68, 48%), which corresponds to $C_2H_2N_3$.This molecular mass was represented by HL^3 with the empirical formula $C_{13}H_{10}N_4OS$ at m/z = (270). This peak was also the starting peak, with 100% abundance of relative. A peak confirmed a fragmentation ion at m/z =145 (32%) corresponding to the formula of $C_{10}H_7O$. N2 gas may leak from the fragment ion with m/z =100(56%), due to the C_2N_2S formulas, the CH_3 group produces a fragment ion at m/z =84(40 %). Finally, the peak of molecular ion $[M]^+$ at m/z = (302,48 %) for HL^4 is related to the formula $C_{13}H_{10}N_4OS_2$. This ligand is more plentiful than the previous ones. A large, great peak at m/z = (159, 100%) announced the break of connection between the azo group and the ring of naphthalene.

3.3. The Production of Cu (II) Complexes in Solution

"The continuous variation method" CVM, "mole-ratio method" (MRM) was used to determine the structure of the complexes in solution. According to the findings, Cu (II) complexes developed in solution at a molar ratio of 1:1 (M/L). Harvey and Manning's Equation was used to derive the conditional formation constants stated in Table 2. The (DG) of Cu(II) complexes production was also computed. Conductometric titrations revealed a 1:1 (M/L) Cu(II)complex stoichiometry. The rise in conductance has demonstrated a covalent association to the O-atom of the OH moiety, which is the reaction between azo dyes and Cu(II) ion. In addition, specific absorptivity, Beer's law's validity limits, molar extinction coefficient, correlation coefficient, and standard deviation were determined. Cu(II) ion-dependent EDTA ligand measurement revealed that possible Cu(II) titration indicators are ligands for this ion-dependent titration. Table2 demonstrated that the existing spectrophotometric approach could determine the Cu(II) ion.. The obeyance to Beer's law and Ringbom plot is shown in Fig3. The absorption of long-wavelength absorption peaks produces Cu (II) complexes. For cells with a 1 cm optical path length, the equation of Benassi–Hildebrand (B–H) was used to calculate the formation constant of azo-complexes with a 1:1 stoichiometry (acceptor-donor):

$$\frac{[L_O]}{A - A_O} = \frac{1}{\varepsilon_{ML} - \varepsilon_L} + \frac{1}{(\varepsilon_{ML} - \varepsilon_L)K[M_O]}$$

ε_L and ε_{ML}, respectively, are the coefficients for the molar extinction and Cu complexes. A_0 and A are free ligand absorbents and Cu complexes at the ligand and Cu complexes' given wavelength. Also, $[M_0]$ is the Cu ion concentration, $[L_0]$ is the initial ligand concentration and the final coefficients.

Table 1: Spectrophotometric data (ε, a), For Cu(II) with HL1–4, the Sandell sensitivity (S), standard deviation (SD), correlation coefficient (CC), and Beer's law range are all positive

Data	HL^1	HL^2	HL^3	HL^4
λmax (nm)	540	550	560	580
Beer's range (ppm)	0–2.31	0–3.84	0–3.80	0–3.76
Ringbom range (ppm)	-0.08 to 0.27	0.28 – 0.56	0.20–0.61	0.24–0.62
CC	0.99986	0.9973	0.9964	0.9961
SD	0.00543	0.02654	0.02785	0.01965
ε (μmol^{-1} cm^{-1})	$18.9x\ 10^3$	$13x10^3$	$10.6\ x\ 10^3$	$11.1\ x\ 10^3$
a (ml g^{-1} cm^{-1})	0.334	0.197	0.179	0.184
S (μg cm^{-2})	0.004	0.006	0.0054	0.0067
MRM	1:1	1:1	1:1	1:1
CVM	1:1	1:1	1:1	1:1
CM	1:1	1:1	1:1	1:1
Logβn	5.76	5.43	5.11	7.31
ΔG*	7352	7105	6894	8875

Yx 10^{-5}	5	5	5	5
X x 10^{-5}	5	5	5	5
K (bulk-copper)	35,764	23,378	13,535	8312
K (nano-copper)	35E+7	131E+7	30E+7	81E+7

ΔG*, Gibbs free energy; X represents the concentration of the prepared sample (mol L^{-1}); βn, complex stability constant; ‘‘EDTA-titration" denotes the presence of EDTA in the sample. Y represents the concentration of the sample. (mol L^{-1}) was calculated through practical means. ‘‘EDTA-titration’’.

Under 1:1 donor-acceptor complexes, Equation (1) is valid. A straight line is obtained when only a 1:1 complex is generated; a curve is obtained when a system contains a mixture of 1:1 and 1:2 complexes. Then, To obtain a linear plot, we must employ another equation. The data of the formation constant (K) for Cu(II) complexes are determined using plots of $[L_0]/(A\ A_0)$ vs. 1/ [M0]. Figure 4 Table 2 displays the results. The findings showed that copper (II) complexes with ligands are more stable than copper(II) complexes with ligands., led to the expansion of two rings that provide more stability than one ring, providing adequate proof to the proposed structure of the produced complexes

3.4. Solid Copper Complexes are Being Studied for Their Properties

The proposed formulae $[CuL^{1–4}(nH_2O)]AcO.\ XH_2O$ were confirmed by the elemental analyses shown in Table 1, where n = 1 for A1, A2; n = 2 for A3, A4, and x = 1for A1,A3; x = 2 for A2,A4 Table 1. The majority of organic solvents are insoluble in Cu complexes, except for DMF and DMSO. Table 2 shows molar conductivity data that are in the electrolyte region (1:1).

Table (2): Several physical characteristics and microanalysis techniques

Compounds	formula	Molecular Weight	Colour	Yield %	M.P. ˚C	%Elemental Analysis Found % (Calculated)			
						C	H	N	M
HL^1	$C_{13}H_{11}N_5O$	253.27	orange	70	197	61.13 (61.65)	3.54 (4.38)	27.13 (27.65)	-
$[Cu\ L^1(H_2O)]AcO.H_2O$(A1)	$C_{15}H_{17}CuN_5O_5$	410.88	Light violet	60	286	42.95 (43.85)	3.90 (4.17)	16.76 (17.05)	14.76 (15.47)
HL^2	$C_{20}H_{13}CuN_5O$	315.34	red	65	170	52.83 (53.15)	3.88 (3.82)	17.05 (17.71)	-
$[Cu\ L^2(H_2O)]\ AcO.\ 2H_2O$ (A2)	$C_{20}H_{21}CuN_5O_6$	490.00	violet	75	265	48.34 (48.93)	3.90 (4.31)	4.18 (14.26)	12.39 (12.94)
HL^3	$C_{14}H_{12}N_4OS$	284.34	Pink	72	180	61.83 (59.14)	3.87 (4.25)	24.03 (19.76)	-
$[Cu\ L^3(H_2O)_2]\ AcO\ .H_2O$ (A3)	$C_{15}H_{18}CuN_4O_6S$	445.94	violet	81	273	40.84 (40.40)	3.99 (4.07)	12.11 (12.56)	14.53 (14.25)
HL^4	$C_{14}H_{12}N_4OS_2$	316.40	Redith Orange	68	205	53.23 (53.15)	3.67 (3.82)	17.13 (17.71)	-
$[Cu\ L^4(H_2O)_2]\ AcO.2H_2O$(A4)	$C_{15}H_{20}CuN_4O_7S_2$	495.01	Dark violet	78	289	36.75 (36.51)	4.26 (4.09)	19.12 (18.93)	10.97 (10.73)

3.4.1. IR Spectra

The IR spectra of compounds were compared., evidence for complex formation was established. Table 3 shows the most distinctive bands and their assignments. For example, the bands in the range 1460-1500cm^{-1} associated with υ (N=N) stretching were displaced to a smaller number of different frequency bands 1443-1464 cm^{-1} indicating N=N as evidenced by the formation of new bands the t(Cu-N) bond in the reign 426-464 cm^{-1}. Because of υ(C=N) of triazole nitrogen, the IR spectrums of HL_1 and HL_2, respectively, showed a frequency of 1655and 1670 cm^{-1}. This band was reduced to a lower frequency in the complexes, demonstrating the engagement of N-azomethine in the chelation of the Cu(II) ion. The vibrational mode of υ(O-H) was observed at 3456-3480 cm$^{-1,}$ caused by the presence of lattice water in complexes A1–A4. The appearance of bands in the spectra of all complexes at 3323–3311, 1709–1686, 845–819, and 624–582 cm^{-1} were due to the pooled water's υ (O-H), δ(H_2O), ρr(H_2O), and ρw(H_2O) vibrations, respectively. The phenolic υ (C-O) band was observed in the region 1250–1282 cm^{-1} in the free ligands $HL^{1–4}$ and (as a moderate to the high band) in complexes A1–A4 Cu-O bonds through hydrolysis. The emergence of υ (Cu-O) at 520–545cm^{-1} showed coordination via O- phenolic moiety. According to the initial results and micro-analyses, the triazole azo is associated with the Cu(II) ion via N-azo moiety, N-triazole. O-phenolic, the $HL_{1,}$ and HL_2 act as monobasic tridentate ligands. The chelation centres for the thiadiazole of ligands are the O-phenolic moieties and N- azo moieties, respectively. Thus, the ligands HL_3 and HL_4 act as monobasic bidentate ligands shown in Scheme 2.

Table 3: IR data (cm^{-1}) of the significant compounds.

Compound	υ OH	υ(NH)	δ(H_2 O)	υ (C=N)	υ (N=N)	υ (C-O)	ρr(H_2 O) ρw(H_2 O)	υ (C-S)	υ Cu-N) υ (Cu-O)
HL^1	-	-	-	1655	1460	1265	-	-	-
[Cu L^1(H2O)]OAC. H_2O(A1)	3456 3323	-	1709	1634	1448	1280	8*34* 595	-	443 520
HL^2	-	3160	-	1673	1485	1250	-	-	-
[Cu L^2(H2O)]OAC. 2H_2O (A2)	3463 33*18*	3158	1686	1651	1464	1276	845 611	-	464 434
HL^3	-	-	-	1593	1470	1282	-	634	-
[Cu L^3(H2O)2]OA C.H_2O (A3)	3480 3311	-	1701	1590	1443	1294	819 624	631	456 539
HL^4	-	-	-	1586	1500	1270	-	627	- -
[Cu $L^4(H_2O)_2$] AcO.2H_2O(A4)	3476 332*0*	-	1694	1584	1456	1297	84*0* 582	628	451 545

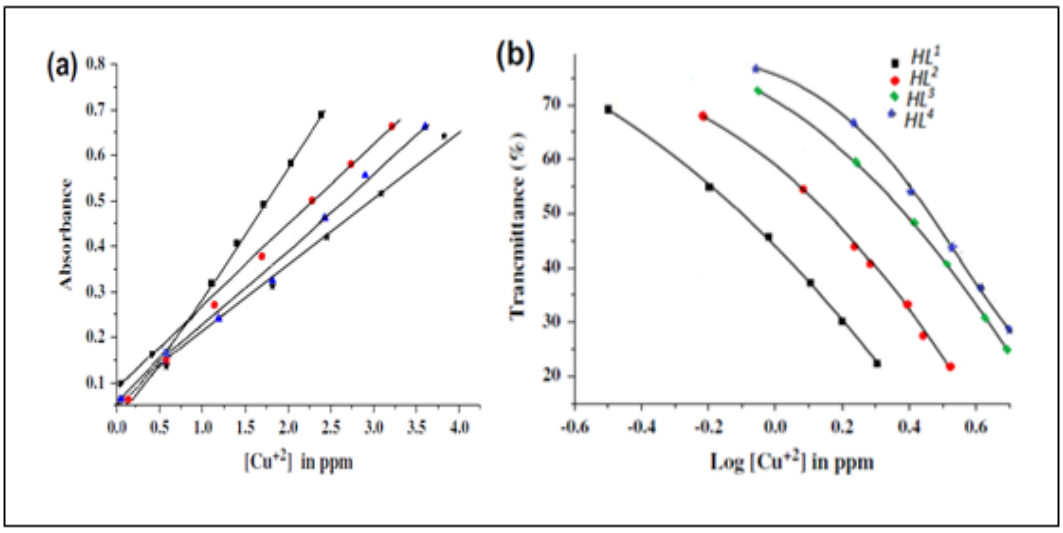

Fig. 3: (a) Beer's law is observed for complexes of ($L_{1–4}$) with Cu(II) .(b) Cu(II) compounds with ($L_{1–4}$) ringbom plots.

3.4.2. TGA studies of Cu(II)-complexes (A1–A4) were performed, and reasonable degradation was observed. Table 4 illustrates the mass lake, possible shards, and reign of temperatures for all Cu(II)azo- complexes investigated. In addition, the complex A1's thermogram is used to illustrate [Cu $L^1(H_2O)$]OAC.H_2O is complex. Therefore, complex A1 is used as a reflective thermogram. This complex [Cu $L^1(H_2O)$]OAC.H_2O thermally disintegrates four steps over a 25–800˚C temperature range. The 1st step takes place at *3*2.78– 151.74 ˚C with a mass loss estimate of approximately due to the loss of lattice H_2O molecules. The 2nd step occurs within the temperature range 151.74– 182.83˚C. It results in a mass loss of approximately 4.17% (calcd. 4.32%) due to the loss of H_2O chelated molecules. Therefore, this stage requires 14*3.643* kJ mol^{-1} as activation energy. The 3rd degeneration stage involved losing hetero ring at 182.83–460˚C with an approximated weight lake of 16.75% (calcd. 16.80%). This stage requires 2*87.543* kJ mol-^{1}as activation energy. The 4th degradation step responsible for the pyrolysis of the HL^1 molecule with the last CuO remains was the loss of $C_{10}H_6$, acetate, and N_2 gas within the temperature range 460–700.65˚C with an estimated weight lake of 2.42% (calcd.52.38%). This stage has 89,4 kJ mol^{-1} as activation energy. In the neutralization of Horowitz-Metzger and Coats- Redfern. The kinetic and thermodynamic parameters for the stages of thermal degradation were investigated.

Table 4: Thermochemical analysis (DrTGA and TGA) results for Cu(II) complexes(A1-A4)

Compounds	(TGA)				
	Step	Temperature (˚C)	wt.% loss (calcd.)/found	Assignment	DrTGA (˚C)
A1	1st	32.76–151.74	(4.38)/4.23	Loss of H_2O lattice	90
	2nd	151.74 – 182.83	(4.32)/4.17	Loss of H_2O coordinated	172
	3 rd	182.83–460	(16.80)/16.75	Loss of hetero ring	251
	4th	460–700.65	(52.38)/52.42	Loss of (N_2, $C_{10}H_6$, CH_3COO)	532
A2	1st	25.53–140.32	(7.33)/7.51	Loss of H_2O lattice	*7*5
	2nd	140.32– 174.64	(3.66)/4.02	Loss of H_2O coordinated	1*65*
	3 rd	174.64–450	(14.06)/14.19	Loss of hetero ring	2*31*

	4th	450–650.31	(43.83)/43.76	Loss of (N_2, $C_{10}H_6$, CH_3COO)	4*47*
A3	1st	30.34–150.63	(4.01)/4.15	Loss of H_2O lattice	8*0*
	2nd	150.63–180.53	(4.21)/4.19	Loss of H_2O coordinated	1*65*
	3 rd	180.53–440	(28.58)/28.79	Loss of hetero ring	24*0*
	4th	440–670.32	(38.87)/38.76	Loss of (N_2, $C_{10}H_6$, CH_3COO)	4*68*
A4	1st	35.42–153.76	(7.27)/7.31	Loss of H_2O lattice	85
	2nd	153.76–186.65	(7.21)/7.18	Loss of H_2O coordinated	187
	3 rd	186.65–430	(26.70)/26.79	Loss of hetero ring	242
	4th	430–680.54	(43.43)/43.55	Loss of (N_2, $C_{10}H_6$, CH_3COO)	486

Coats–Redfern equation: Where α denotes the decomposed fraction, β denotes the rate of heat, The absolute temperature is indicated by T, while the universal gas constant is R., A is the pre-exponential Arrhenius constant, while Ea is the activation energy. Thus, the expression (AR/βEa) (1-2RT/Ea) is nearly constant, as is the value of (1-2RT/Ea).

$$\text{For } n = 1: \ \log\left[\frac{-\log(1-\alpha)}{T^2}\right] = \log\left(\frac{AR}{\beta E_a}\right)\left(1-\frac{2RT}{E_a}\right) - \left(\frac{E_a}{2.303RT}\right) \quad (2)$$

$$\text{For } n \neq 1: \ \log\left[\frac{1-(1-\alpha)^{1-n}}{T^2(1-n^2)}\right] = \log\frac{AR}{\beta E_a}\left(1-\frac{2RT}{E_a}\right) - \left(\frac{E_a}{2.303RT}\right) \quad (3)$$

For n = 1, a straight line with a slope equal to (-Ea/2.303R) was obtained by plotting log(-log (1-)T2 vs. 1000/T, this can be used to compute activation energy. Moreover, an intercept equal to log(AR/βEa) can also be used to calculate the Arrhenius pre-exponential factor. For n–1, plotting log(-log (1-)T2) vs. 1000/T provided a straight line with a slope of (-Ea/2.303R), an intercept equal to log(AR/βEa), and A and ΔE.

Table 5: Heat capacity of Coats–Redfern and Horowitz–Metzger procedures were used to create complexes.

Complexes	Thermodynamic parameters								
	Step	Method	n	CC	E* (kJ mol^{-1})	H* (kJ mol^{-1})	A (S^{-1})	-ΔS (J mol^{-1} K^{-1})	ΔG* (kJ mol^{-1})
A1	1st	CR HM	1 2	0.96432 0.98654	22.78862 32.65213	555.46018 29.47437	25.96638 179.9404	0.107027 0.203803	63.69622 107.3714
	2nd	CR HM	1 0	0.98214 0.99864	143.643 155.9365	138.8779 152.1046	7.86E-05 8.98E+15	0.337091 0.123567	287.875 354.4321
	3rd	CR HM	1 2	0.98655 0.98987	287.543 321.876	293.543 315.765	6.97E-10 9.43E+21	0.56532 0.28750	530.8087 465.3245
	4th	CR HM	1 2	0.97876 0.99098	485.8762 596.7651	485.8642 521.0089	5.45E-12 3.62E+30	0.76532 0.65479	897.9471 487.7653
A2	1st	CR HM	1 2	0.99123 0.99543	13.8766 20.4321	10.75433 17.13215	4.59 E-10 1.854 E+09	0.14568 0.38765	39.6531 123.4322

	2nd	CR HM	1 2	0.98432 0.99212	165.5432 178.0985	148.7643 157.5466	7.23E-06 8.54E+14	0.43789 0.08712	290.5436 180.9870
	3rd	CR HM	1 2	0.98311 0.99012	289.9876 265.5432	276.4321 269.8976	1.37E-16 2.48E+26	0.76589 0.30651	478.890 357.244
	4th	CR HM	0 0	0.98098 0.99234	256.874 205.653	207.5325 213.7752	0.00542 4.54E+12	0.43268 0.01986	475.0973 296. 2471
A3	1st	CR HM	1 2	0.08761 0.98876	13.6542 19. 6633	7.190359 16.75734	0.00980 2.11E+07	0.08400 0.54387	54.7658 109.4907
	2nd	CR HM	1 2	0.98875 0.99109	176. 2058 154. 3956	135. 3973 187.0164	6.87E-07 9.68E+14	0.76544 0.18765	296.3386 178.4394
	3rd	CR HM	1 2	0.97543 0.99123	228.8568 203.0972	249.8750 257. 3784	1.76E-12 1.43E+24	0.56239 0.42152	456.2740 396.9432
	4th	CR HM	0 0	0.98763 0.99613	220.1205 265.8644	219.5421 243.5727	0.085432 1.43E+12	0.50678 0.00321	513.5799 234.2147
A4	1st	CR HM	1 2	0.98543 0.99321	14.11830 20.67633	9.105993 15.43717	3.65E+10 2.3589	0.08764 0.54321	39.95431 120.0323
	2nd	CR HM	1 2	0.96543 0.97321	20.78862 35.35261	72.9875 43.6432	31.9543 182.8652	0.37237 0.78383	70.98754 114.8543
	3rd	CR HM	1 0	0.97789 0.98907	23.22688 37.05813	23.19573 45.68131	1.78E+12 5.954506	0.006273 0.467805	63.9876 161.3125
	4th	CR HM	1 2	0.98654 0.99532	200.28264 309.0355	321.9196 387.3867	6.98E-10 8.51E+22	0.63210 0.21885	627.9812 427.5105

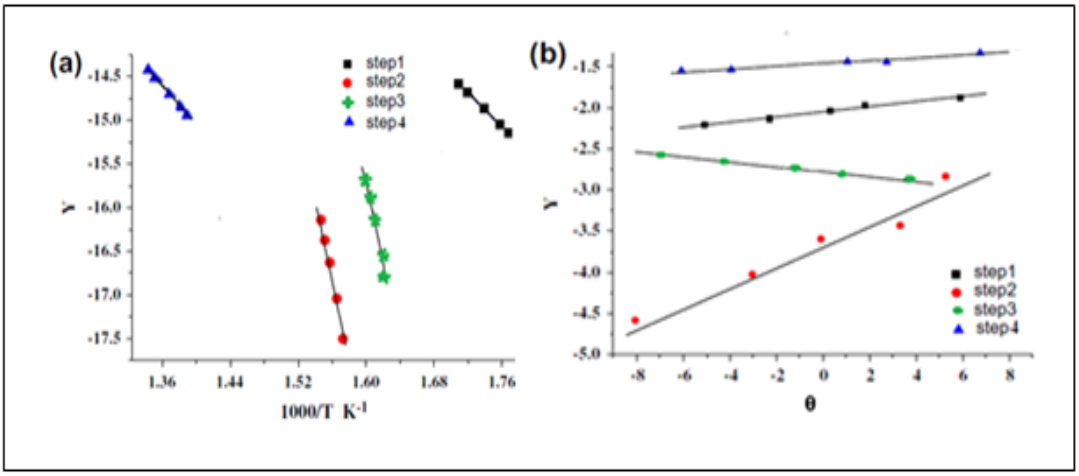

Fig1: (a) Use the Coats–Redfern equation to display Y = log(-log (1-)T2) vs. 1000/T (k1) for the different decomposition steps of complex A2. (b)shows the Horowitz–Metzger decomposition of complexA_2 using the Horowitz–Metzger equation.

Horowitz–Metzgar equation:

$$\text{For } n = 1: \quad \log[-\log(1-\alpha)] = \frac{E_a \theta}{RT_s^2} \qquad (4)$$

$$\text{For } n \neq 1: \quad \log\left[\frac{1-(1-\infty)^{1-n}}{1-n}\right] = \log\left(\frac{A}{\beta}\frac{RT_s^2}{E}\right) - \frac{\theta E_a}{RT_s} \qquad (5)$$

$$\Delta H = E - RT$$

$$\Delta S = R \ln[Ah/KT]$$

$$\Delta G = \Delta H - T\Delta S$$

The findings lead to the following conclusions:

1- The activation complexes have more energy data. Second, they demonstrate because of their covalent nature, the investigated compounds are extremely stable.

2- The final residue's free energy is greater than the first compound's was revealed by higher than the value of the first compound. Thus, all of the degradation stages are non-spontaneous.

3. With each consecutive level of a complex's breakdown, the data of ΔG increased. Thus, increasing the ΔG data of a complex indicated that the subsequent ligand was being eliminated slower than the primary ligand. Likewise, it was because the data of TΔS increase from one stage to the next that overrides the data of ΔH.

4. The ΔS data (-) showed a better ordered complex than a reactant or a sluggish reaction.

5. The endothermic nature of the breakdown process is indicated by the data (+) of ΔH.

6. In Table 5, the approximation method (Horowitz–Metzgar) provided higher kinetic parameter values than the integral method (Coats–Redfern).This is because the obtained data has been subjected to various mathematical approaches

3.4.3. Mechanistic Aspects

On the assumption that g(a) is constant, the thermal decomposition mechanism is assigned, that is dependent on the reaction mechanism. According to the Equation, using Satava's nine forms of g(a), the integral approach (Coats–Redfern) was employed to elucidate the thermal decomposition mechanism in each stage.

$$\ln[g(\alpha)/T^2] = \ln(AR/\beta E) - E/RT$$

The significance of the various symbols are well-known: where β is the heating rate, α is the fraction decomposed, T is the absolute temperature, R is the universal gas constant ,E is the activation energy, A is the Arrhenius pre-exponential and g(α) is the kinetic mode. As a function of (1/T), the quantity log[g()/T2] is displayed. For each of these nine forms, as well as the form of g(a), the correlation coefficient was determined. The maximum value for correlation is used as the reaction mechanism. The TGA process was repeated for the Cu(II) complex C1at various rates of heating, namely 5, 10, and 15 C/min.

At heating rates of 10 and 15 C/min or 5 C/min, respectively, 2or 3 distinct and the thermal decomposition reaction has well-defined steps. First, the decomposition is analyzed using the Coats–Redfern method. Second, The activation energy (E) and the Arrhenius pre-exponential function were calculated using the slope and intercept (A) .Next, the slope and the intercept were used to calculate the activation energy (E) and the Arrhenius pre-exponential (A). Additionally, the outcomes indicated that, except step II, the heating rate increased the thermodynamic functions of activation of the thermal decomposition.

3.4.4. Measurements of Magnetic Moments and Electronic Spectra

Cu(II) complexes (A1–A4) influential electronic absorption bands recorded as Nujol mull are shown in Table 3. Magnetic moments exist in complexes of Cu(II). Table 1 proposed square planar organization for complexes A1, A2, A3, and A4. Cu(II) complexes have a magnetic moment. For complexes A1, A2, A3, and A4, Table 1 suggested square planar chelation. Two bonds within 15,152–17,786 and 22,342–25,324cm^{-1}, usually in a square planar geometry

location that can be allocated ^{2} $B_1g\rightarrow$ ^2E_1g and $^2B_1g\rightarrow^2Eg$ respectively, exhibited the Cu(II) complexes spectrum in the solid-state.

3.4.5. ESR Spectra

The ESR spectra of Cu(II) complexes (C1–4) were recorded at room temperature (25˚C) and are displayed in Table 3. Complex ESR spectra are characterized dx^2–y^2 ground state with type of axial symmetry and monomeric structure, most prevalent for Cu(II) complexes. Cu(II)-azo complexes had two different g data in their ESR spectra. Because the azo and metal ions are covalently bound, all complexes have positive g-data compared to the free electron (2.0023). The g11 2.3 data suggest that the bonding of metal-ligand in the complex is covalent.

Additionally, the expression G= (g11 2)/ (g\ 2). If G > 4, the exchange interaction is negligible, whereas if G 4, the stable complexes exhibit a significant exchange interaction. The g-data of Cu (II)-complexes with a ^2B_1g ground state can be expressed as (g11 > g)by

$$k_{11}^2 = (g_{11} - 2.0023)\Delta_2/8\lambda$$

$$k_{\perp}^2 = (g_{\perp} - 2.0023)\Delta_1/2\lambda$$

$$k^2 = [k_{11}^2 + 2k_{\perp}^2]/3$$

Where $k^2\perp$ and k^2_{11} are the components of perpendicular and analogous of the factor of orbital lowering k, the electronic transitions $^2B_1g\rightarrow^2B_2g$ and $^2B_1g\rightarrow^2Eg$ are represented by Δ_2 and Δ_1, respectively. The computed data of $k^2\perp$ and k^2_{11} due to $k\perp < k_{11}$, that is convincing proof for the assumed ^2B_1g state of the ground. The fact that k is lower than the unit shows covalence, which aligns with the conclusion drawn from the g_{11} data. All complexes $k\perp > k_{11}$had bonding of in-plane π, $k\perp \sim k_{11} \sim 0.77$, which Hathaway claims is significant, and bonding of out-plane π, Hathaway claims is not significant.

3.5. Cu- Nanoparticle Coordination

Classical coordination chemistry is concerned with metal complexing, chelation numbers, ions, and electronic information structure, efficient charge, coordinating impact, ligands, size, and charges, distribution of charges, orbitals, appropriate for forming a bond with a metal ion, and appropriate for forming metal-ligand

To some extent, these concerns arise, when the chelation object is a spheroidal particle containing 10^3 to 10^5 atoms rather than a single metal ion or several combined ions as (atoms). Only the surface ions (atoms) of a particle will interact with its surroundings (ligands), not the atoms. The ligand of organic- nanoparticle interaction has the same fundamental interactions as the classic metal ion composition: acceptor-donor sites, the electrocution of ions and vacant metal orbitals, and the covalent connection. However, here dispersion interactions and nanoparticle surface spatial screening are far more critical.

The chemical process is copper (II) nitrate reduction with isopropyl alcohol:

$$Cu^{2+} + CH_3{-}CH(OH){-}CH_3 \rightarrow Cu^0 + (CH_3)_2C = O + 2H^+$$

According to TEM Fig. 3, the technique yields particles with a size of 20 nm. At 560 nm, the plasmon absorbance. From the ligand absorption spectra in the absence and existence of colloidal Cu^0 nanoparticles at various concentrations.

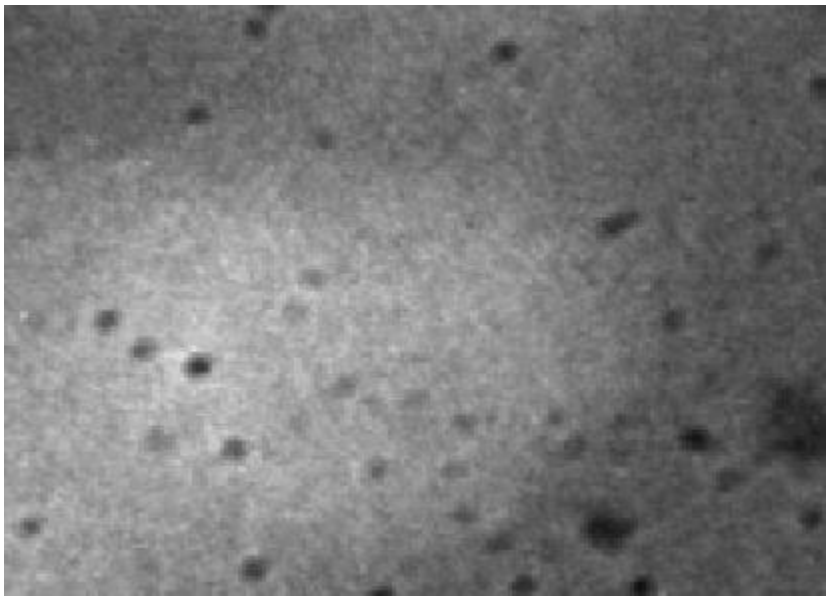

Fig.2: Transmission electron microscopy image of prepared copper nanoparticles,

We found that as the concentration of colloidal Cu^0 nanoparticles increases, The absorption of ligands ($HL_{1–4}$) consistently decreases due to ligand adsorption on the surface of Cu^0 nanoparticles as colloidal, a new peak has appeared. Thus, we result in the surface complex's configuration up to where the Cu^0 surface is saturated with ligand molecules.

Concentration There is no increase in the absorption spectrum, as evidenced by the image of TEM.

Equation (6) can be used to compute the equilibrium for complicated composition between azo-ligands and Cu^0 nanoparticles, where Kapp symbolizes the apparent constant of association (see Scheme 3)

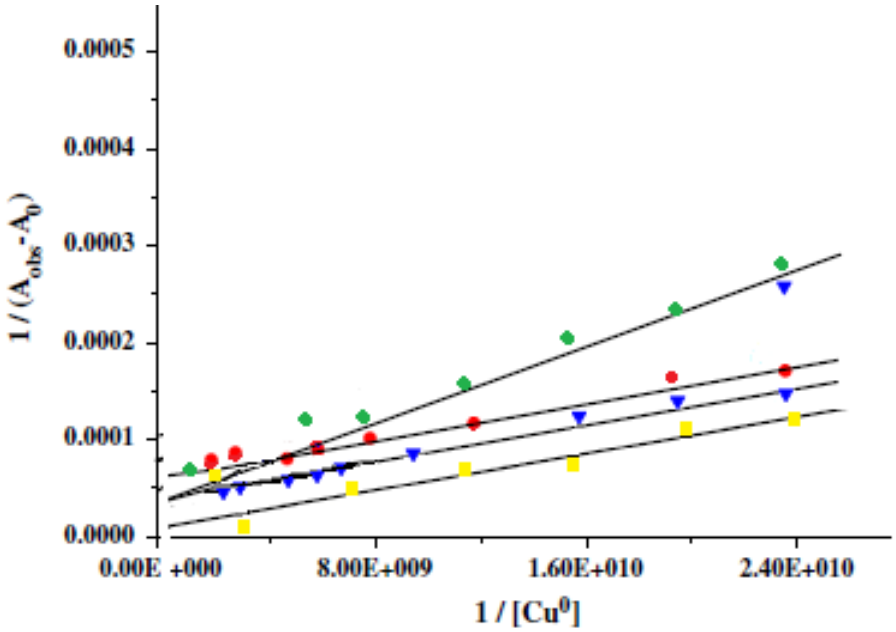

Fig. 3: According to equation of the Hildebrand and Benesi, the reciprocal concentration of colloidal copper nanoparticles coordinated with ($HL^{1–4}$) and the linear dependence of 1/(Aobs A^0) on the reciprocal concentration.

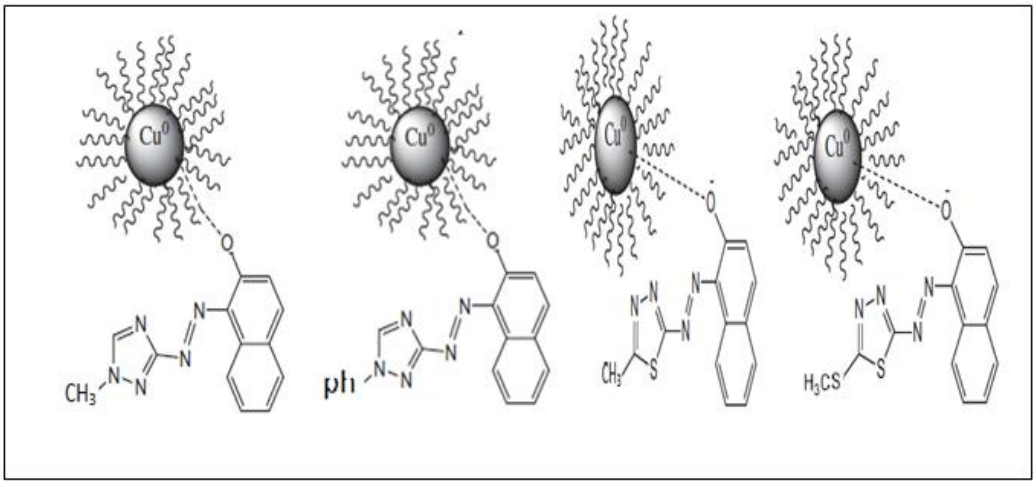

Scheme 3: The interactions of L1-4 with the surface of colloidal Cu^0.

$$\text{Azo-ligand} + Cu^0\text{nanoparticles} \leftrightarrow \text{Azo-ligand} \cdots Cu^0\text{nanoparticles}$$

$$K_{app} = \frac{[\text{Azo-ligand} \cdots Cu^0\text{nanoparticles}]}{[\text{Azo-ligand}] \cdot [Cu^0\text{nanoparticles}]} \qquad (6)$$

According to Benesi and Hildebrand the variation in the strength of the absorption peak resulting from the surface complex formation was used to calculate Kapp.

$$A_{obs} = (1 - \alpha)C_0\varepsilon_{\text{azo-ligand}} + \alpha C_0\varepsilon_{\text{complex}}$$

Eq. (7) can be written as Eq (8), where α is the degree of association between Cu^0 nanoparticles and azo-ligand, The measured absorbance of a solution containing varied concentrations of colloidal Cu^0 nanoparticles is denoted by Aobs, a is the degree of association between azo-ligand and Cu^0 nanoparticles, and Aobs is the observed absorbance of a solution containing different concentrations of colloidal Cu^0 nanoparticles. Moreover, b represents the degree of connection between the azo-ligand and the Cu0 nanoparticles. The molar extinction coefficients at the given temperature are Ɛcomplex and Ɛazo-ligand. As a result, in the water Equation (7), Azo-ligand and formed complex wavelengths, respectively, can be written as Equation (8), where Ac and A^0 denote the complex with a C^0 concentration and the ligand absorbance:

$$A_{obs} = (1 - \alpha)A_0 + \alpha A_c \qquad (8)$$

$$(K_{app}[Cu^0 \text{ nanoparticles}])/(1 + K_{app}[Cu^0\text{nanoparticles}]). \qquad (9)$$

$$\frac{1}{A_{obs} - A_0} = \frac{1}{A_c - A_0} + \frac{1}{K_{app}(A_c - A_0)[Cu^0\text{nanoparticles}]} \qquad (10)$$

Based on the strong linear relationship between 1/(Aobs- A0) and the reciprocal, the increase in absorbance was due to surface complex absorption, i.e., donor–adaptor behavior. Colloidal Cu^0 nanoparticle concentration (stock solution)

= 8.46 109 mole HL^1), The intercept is equal to 1/Kapp(Ac-A0), while the slope is 1/Kapp(Ac-A0) (Ac- A0). That obtained from this graphic, derives the apparent association constant (Kapp).

4. CONCLUSION

The some heterocyclic azo compounds reaction with $\underline{Cu}(OAc)_2$ resulted in coordination. Furthermore, the IR spectra revealed ligands with triazole moiety coordinate with the copper (II) ion tridentately with ONN donor sites. Azo-dyes containing a thiadiazole moiety coordinate with the copper (II) ion and ON donor sites in a bidentate manner. The UV spectra, magnetic moments, conductance, and thermal analysis are used to determine the structure of the complexes. Spectrophotometry is also used to investigate the reaction between the solution of Cu(II) ion and azodyes. We determine the constants of stability and stoichiometry. The findings suggest which the azo dyes under investigation can be used as a spectrophotometric indicator to determine Cu(II) ion. The interaction between azo dyes under investigations and the Cu nanoparticles are regarded. The data of spectral showed the surface complex formation between colloidal copper nanoparticles and azodye ligands by the (OH) anchoring moiety. The prepared copper nanoparticle complexes' stability constant has been calculated.

REFERENCES

[1] P.A. Kobielska, R. Telford, J. Rowlandson, M. Tian, Z. Shahin, A. Demessence, V.P. Ting, S. Nayak, Polynuclear complexes as precursor templates for hierarchical microporous graphitic carbon: an unusual approach, ACS Appl. Mater. Interfaces 10 (2018) 25967–25971, https://doi.org/10.1021/acsami.8b10149.

[2] F.A. Saad, A.M. Khedr, Greener solid-state synthesis of nanosized mono and homo bi-nuclear Ni(II), Co(II), Mn(II), Hg(II), Cd(II), and Zn(II) complexes with new sulfa ligand as a potential antitumor and antimicrobial agents, J. Mol. Liq. 231 (2017) 572–579, https://doi.org/10.1016/j.molliq.2017.02.046.

[3] A.A. Almaqwashi, T. Paramanathan, I. Rouzina, M.C. Williams, Mechanisms of small molecule-DNA interactions probed by single-molecule force spectroscopy, Nucleic Acids Res. 44 (2016) 3971–3988, https://doi.org/10.1093/nar/gkw237.

[4] C.Y. Lee, H.Y. Kim, S. Kim, K.S. Park, H.G. Park, A simple and sensitive detection of small molecule–protein interactions based on terminal protection-mediated exponential strand displacement amplification, Analyst 143 (2018) 2023–2028, https://doi.org/10.1039/C8AN00099A.

[5] P. Zhao, S. Zhai, J. Dong, L. Gao, X. Liu, L. Wang, J. Kong, L. Li, Synthesis, structure, DNA interaction, and sod activity of three nickel(II) complexes containing L-phenylalanine Schiff base and 1,10-phenanthroline, Bioinorg. Chem. Appl. 2018 (2018).

[6] A. Erxleben, Interactions of copper complexes with nucleic acids, Coord. Chem. Rev. 360 (2018) 92–121, https://doi.org/10.1016/j.ccr.2018.01.008.

[7] A. Hussain, M.F. AlAjmi, M. Rehman, A.A. Khan, P.A. Shaikh, R.A. Khan, Evaluation of transition metal complexes of the benzimidazole-derived scaffold as promising anticancer chemotherapeutics, Molecules 23 (2018) 1232–1249, https://doi.org/10. 3390/molecules23051232.

[8] F.A. Saad, H. El-Ghamry, M.A. Kassem, A.M. Khedr, Nano-synthesis, biological efficiency and DNA binding affinity of new homo-binuclear metal complexes with sulfa azo dye-based ligand further pharmaceutical applications, J. Inorg. Organomet. Polym. Mater. 29 (2019) 1337–1348, https://doi.org/10.1007/ s10904-019-01098-z.

[9] M.A. Malik, O.A. Dar, P. Gull, M.Y. Wani, A.A. Hashmi, Heterocyclic Schiff base transition metal complexes in antimicrobial and anticancer chemotherapy, Med. Chem. Commun. 9 (2018) 409–436, https://doi.org/10.1039/C7MD00526A. [10] F.A. Saad, H.A. El-Ghamry, M.A. Kassem, Synthesis, structural characterization and DNA binding

affinity of new bioactive nanosized transition metal complexes with sulfathiazole azo dye for therapeutic applications, Appl. Organometal. Chem. 33 (2019) e4965, , https://doi.org/10.1002/aoc.4965.

[11] S.M. Gomha, S.M. Riyadh, E.A. Mahmoud, M.M. Elaasser, Synthesis and anticancer activity of arylazothiazoles and 1,3,4-thiadiazoles using chitosan-grafted-poly (4-vinylpyridine) as a novel copolymer basic catalyst, Chem. Heterocycl. Compd. 51 (2015) 1030–1038, https://doi.org/10.1007/s10593-016-1815-9.

[12] M. Gaber, N.A. El-Wakiel, H. El-Ghamry, S.K. Fathalla, Synthesis, spectroscopic characterization, DNA interaction and biological activities of Mn(II), Co(II), Ni(II) and Cu(II) complexes with [(1H- 1,2,4-triazole-3-ylimino)methyl]naphthalene-2-ol, J. Mol. Struct. 1076 (2014) 251–261, https://doi.org/10.1016/j.molstruc.2014.06. 071. 28.

[13] R. K Al-Shemary, W.A. Jaafar, and A.N Niseaf. Structure, diagnosis, and in the Vitro Antimicrobial evaluation of 2-amino pyridine-derived Ligand Schiff base and its complexes with Cu (II), Hg (II), Ni (II), Mn (II) and Co (II), Rese. J. of Pharma, Biolog. and Chem. Sci (RJPBCS),, June ,2017, 8(3), 14-183

[14] W. A Jaafar., S. M. Fezea and R. K. Rahm Al- Shemary (2018)Employing the Physicochemical, Spectroscopy, Antimicrobial and Antifungal Efficacy Studies of P-Hydroxy Acetophenone Based Azo Schiff Base Complexes, J. of Global Pharma Technology, 10(06):503-512

[15] K. El-Baradie, R. El-Sharkawy, H. El-Ghamry, K. Sakai, Synthesis and characterization of Cu(II), Co(II), and Ni(II) complexes of a number of sulfa drug azo dyes and their application for wastewater treatment, Spectrochim. Acta A 121 (2014) 180–187, https://doi.org/10.1016/j.saa.2013.09.070.

[16] W. Al Zoubi, A.A.S. Al-Hamdani, S.D. Ahmed, Y.G. Ko, Synthesis, characterization, and biological activity of Schiff bases metal complexes, J. Phys. Org. Chem. 31 (2017) e3752, https://doi.org/10.1002/poc.3752.

[17] A.A. Osowole, E.J. Akpan, Synthesis, spectroscopic characterization, in-vitro anticancer and antimicrobial activities of some metal(II) complexes of 3-(4,6-dimethoxy pyrimidinyl) aminomethyl naphthalen-2-ol, Eur. J. Appl. Sci. 4 (2012) 14–20https://pdfs.semanticscholar.org/53fb/ ff7a0fd3e5e34de1767c8b81171723d47375.pdf.

[18] M.M. Al-Ne'aimi, M.M. Al-Khuder, Synthesis, characterization and extraction studies of some metal (II) complexes containing (hydrazoneoxime and bis-acyl hydrazone) moieties, Spectrochim. Acta A 105 (2013) 365–373, https://doi.org/10. 1016/j.saa.2012.10.046.

[19] P.N. Patel, D.J. Patel, H.S. Patel, Synthesis, spectroscopic, thermal and biological aspects of drug-based copper(II) complexes, Appl. Organomet. Chem. 25 (2011) 454–463, https://doi.org/10.1002/aoc.1786.

[20] L. K. Abdul Karem, F. H. Ganim and R. K. Rahem Al-Shemary (2018) Synthesis, Characterization, Structural, Thermal, POM Studies, Antimicrobial and DNA Cleavage Activity of a New Schiff Base-Azo Ligand and Its Complexation with Selected Metal Ions. Biochem.Cell. Arch. 18(1), 1437-1448

[21] The in-vitro antitumor activity of H2L and its complexes 1–5 toward MCF-7 cell lines compared with the applied standard 5-fluorouracil. A.M. Khedr, et al. Inorganic Chemistry Communications 108 (2019) 107496 6 8478152, https:// doi.org/ 10.1155/2018/8478152.

[22] J.K. Hui, M.J. MacLachlan, Metal-containing nanofibers via coordination chemistry, Coord. Chem. Rev. 254 (2010) 2363–2390, https://doi.org/10.1016/j.ccr.2010.02. 011.

[23] A. Salimi, J.R. Halla, S. Soltanian, Immobilization of hemoglobin on electrodeposited cobalt-oxide nanoparticles: direct voltammetry and electrocatalytic activity, Biophys. Chem. 130 (2007) 122–131, https://doi.org/10.1016/j.bpc.2007. 08.004.

[24] A.A. Fahem, Comparative studies of mononuclear Ni(II) and UO2(II) complexes having bifunctional coordinated groups: Synthesis, thermal analysis, X-ray diffraction, surface morphology studies, and biological evaluation, Spectrochim. Acta A 88 (2012) 10–22, https://doi.org/10.1016/j.saa.2011.11.037. [25] F.A. Saad, J.H. Al-Fahemi, H. El-Ghamry, A.M. Khedr, M.G. Elghalban, N.M. ElMetwaly, Elaborated spectral, modeling, QSAR, docking, thermal, antimicrobial and anticancer activity studies for new nanosized metal ion complexes derived from sulfamerazine azodye, J. Therm. Anal. Calorim. 131 (2018) 1249–1267, https:// doi.org/10.1007/s10973-017-6598-4.

[26] F.A. Saad, M.G. Elghalban, N. El-Metwaly, H. El-Ghamry, A.M. Khedr, Density functional theory/B3LYP study of nanometric 4(2,4dihydroxy-5-formylphen-1- ylazo)-N-(4-methyl pyrimidine-2-yl)benzenesulfonamide complexes: quantitative structure-activity relationship, docking, spectral and biological investigations, Appl. Organomet. Chem. 11 (2017) e3721, https://doi.org/10.1002/aoc.3721.

[27] R K.Al-Shemary Synthesis, Spectroscopic Characterization and Biological Studies for New Binuclear Schiff Base with Some Transition Metal Chemistry and Materials Research Vol.7 No.5, 2015

[28] T.R. Li, Z.Y. Yang, B.D. Wang, D.D. Qin, Synthesis, characterization, antioxidant activity and DNA-binding studies of two rare-earth(III) complexes with naringenin2-hydroxy benzoyl hydrazone ligand, Eur. J. Med. Chem. 43 (2008) 1688–1895, https://doi.org/10.1016/j.ejmech.2007.10.006.

[29] N. Chitrapriya, V. Mahalingam, M. Zeller, K. Natarajan, Synthesis, characterization, crystal structures and DNA binding studies of nickel(II) hydrazone complexes, Inorg. Chim. Acta 363 (2010) 3685–3695, https://doi.org/10.1016/j.ica.2010.05. 017.

[30] N. M. Majeed, S. S. Abd, R. K. Raheem Al Shemary, Eco-friendly and Efficient Composition, Diagnosis, Theoretical, kinetic studies, Antibacterial and Anticancer Activities of Mixed Some Metal Complexes of Tridentate Schiff base Ligand, International Journal of Pharmaceutical Research, 2021 13(1)

[31] Aeshah Muhana Mohammed, Rehab Kadhim Raheem Al Shemary, Metal complexes with heteroscorpionate ligand founded on the pyridinamine group: cyclin-dependent kinase 2 inhibitor antimicrobial, antioxidant, and in vitro cytotoxicity, notional studies, International Journal of Pharmaceutical Research | Jan - Mar 2021 | Vol 13 | Issue 1 [31] S.H. Etaiw, S.A. Amer, M.M. El-Bendary, A mixed-valence copper cyanide 3D-supramolecular coordination polymer containing 1,10-phenanthroline ligand as a potential antitumor agent, effective catalyst and luminescent material, J. Inorg. Organomet. Polym. Mater. 21 (2011) 662–669, https://doi.org/10.1007/s10904- 011-9532-4.

[32] E.A. Bakr, G.B. Al-Hefnawy, M.K. Awad, H.H. Abd-Elatty, M.S. Youssef, New Ni (II), Pd (II) and Pt (II) complexes coordinated to azo pyrazolone ligand with a potent antitumor activity: Synthesis, characterization, DFT, and DNA cleavage studies, Appl. Organomet. Chem. 32 (2018) e4104, https://doi.org/10.1002/aoc.4104.

[33] A.F. Shoair, A.A. El-Binary, N.A. El-Ghamaz, G.N. Rezk, Synthesis, characterization, DNA binding and antitumor activities of Cu(II) complexes, J. Mol. Liq. 269 (2018) 619–638, https://doi.org/10.1016/j.molliq.2018.08.075.

[34] M. Gaber, A.M. Khedr, M. Elsharkawy, Characterization and thermal studies of nano-synthesized Mn(II), Co(II), Ni(II) and Cu(II) complexes with adipohydrazone ligand as new promising antimicrobial and antitumor agents, Appl. Organomet. Chem. 31 (2017) 3885–3898, https://doi.org/10.1002/aoc.3885. [35] H. Alkam, W. M. Alwan, R. K. Raheem Al Shemary, Complexes of Co(II), Cu(II), Ni(II), Pt(II) And Pd(II) with N3O-Chelating Ligand Incorporating Azo and Schiff Base Moieties: Synthesis, Spectroscopic, Thermal Decomposition, Theoretical Studies, and thermodynamic parameters, International Journal of Pharmaceutical Research, 2021, Vol 13(1)

[36] W.H. Mahmoud, F.N. Sayed, G.G. Mohamed, Azo dye with nitrogen donor sets of atoms and metal complexes: synthesis, characterization, DFT, biological, anticancer and molecular docking studies, Appl. Organomet. Chem. 32 (2018) e4347, https:// doi.org/ 10.1002/aoc.4347.

AN OVERVIEW OF THE INDIAN GERIATRIC POPULATION'S ORAL HEALTH

Dr. S. Shree Lakshmi and Dr.Sankara Aravind Warrier
Sri Ramachandra Institute of Higher Education and Research, Porur, Chennai- 600 116

ABSTRACT

Objectives
This paper aimed to provide an overview of the Indian geriatric population's oral health.

Methods
A non systematic review was conducted.

Results
This review focussed understanding of aging, how the elderly population is defined and classified, age-related variations, challenges faced including giants of geriatrics, factors influencing general and oral health status with detailed description on self reported conclusions and gain clarity regarding demographic transition in India. This review also highlighted their level of education, media exposure, abnormal habits, sugar consumption and oral hygiene practice with scientific justification as to why they deserve special care.

Discussion
Dental health is often neglected among the elderly. There is an urgent necessity to resolve the high burden of unmet dental treatment need among the aged in India. Ensuring

Keywords: Indian Elderly, Geriatrics, Epidemiological Survey, Self-Perceived Report, Oral Health

INTRODUCTION

Aging is inevitable and a global phenomenon. Senior Citizens are defined as people with age more than 60 years in the National policy for older persons 1999. The WHO defines the elderly as those who are ≥60 years in developing countries or ≥65 years in developed countries [1].

There are about 600 million aged 60 years and above in the world is which expected to double by 2025 and reach 2 billion by 2050 due to a decline in the mortality and fertility rates with the improved healthcare sector and life expectancy. As per the WHO databank, a remarkable increment of the global elderly population is expected from 12 % in 2015 to 22% by 2050 with an increase at a rate of 2.5% of persons particularly aged over 65 years which is comparatively higher than the annual growth rate of the global population which is about 1.7%. According to an estimation by the United Nations, those who are aged older than 80 years will make up nearly 20 % of the total [2, 3]. A contribution by elders aged over 60 years to about one-third of the world population is predicted by 2050 [4].

The demographic transition has the potential to increase the burden of non-communicable diseases necessitating a special consideration for the formulation of timely and suitable health policies but is very often neglected causing an increase not only in the disease burden of the country but also in various domains especially the creation of load on the working-age group.

It is painful for an individual to witness a slow and inexorable decline of the elders around following the wounds and arrows of aging due to pathogenic vulnerability necessitating special consideration.

Health is a fundamental right of each citizen. It is the responsibility of every healthcare professional to ensure the adoption of a holistic approach for combating chronic illnesses for which a thorough comprehensive understanding of the basic physiologic age-related changes is

essential for attaining basic skills to differentiate those from pathological alterations beneficial for appropriate treatment planning followed by the provision of successful care delivery outcomes.

Accessibility to advanced healthcare infrastructures within affordability has led to the preservation of good quality of life thereby escalating life expectancy which is the goal of the interdisciplinary health care team approach with intersectoral coordination.

Geriatrics refers to the understanding of the elderly diseases and is practiced as a separate specialty based on principles of heterogeneity, the negative possibility for abrupt variations, disease accentuation and attenuation through modification of risk factors and attainability of healthy old age goals while gerontology relates to the study of changes incident to old age that is further as categorized as experimental if it is restricted to biological research and clinical if its deals with physiological variations [5,6].

It is necessary to know a few aspects of old age to achieve health. This review article aimed to understand the rising geriatric age group and its associated problems to find suitable ways forward in dealing with curbing the disease burden through the adoption of a comprehensive strategy instead of the present fragmented approach which is different disease-based.

MAIN TEXT

Understanding Ageing

Gradual changes occur as age increases. Several biological changes such as structural alterations of the chromosomes, proteins and mitochondria occur with aging. Physiological variation termed homeostenosis occurs due to external factors disrupting the intrinsic system.

Classification of Geriatric Age

Elders are classified depending on the grade of their functional efficiency and cognitive fitness into those having a sound status, aged in need of constant professional support or with obligatory homecare requirements [7]. Relatively healthy and active elders aged 65-74 years are segmented as new or young elderly, while those aged 75-84 years managing an array of chronic diseases are grouped as old or mid old people and those who tend to be physically frailer or aged 85 and above are categorized as oldest-old population [8]. The residents are classified based on their dependence level and functional status in to well, frail, functionally dependent and severely disabled [9]. They are also categorized based on the duration of stay by Ouslander et al into short and long stayers further subdivided as those cognitively and physically impaired or combined [10]. They are also segregated based on their capacity to perform activities based on neuro-motor skills [11].

Aging of the Indian Population

There were 12 million Indians aged 60 and above in 1900 which doubled in 1961 following a massive rise to 56 million in 1991, 70 million in 2001 and 112 million in 2016. A steady increase in the elderly population is documented by the National Statistical Office (NSO) with a 35.8% rise during 2011-2021 since 1961 comprising 13.8 crore contributing to a rise by 35.8% due to a reduction in mortality rate. Another important observation reported is the outnumbered absolute number of elderly women to men in the last couple of decades [12]. Persons aged beyond 60 years amount to 76 million of the total over one billion which constitutes about 7.6%. The population density in rural areas constitutes nearly 70% of the total elderly.

It is high time to comprehend the fact released by the population division of the Economic and Social Affairs Department, United Nations that there has been a decline in the total fertility, crude birth and death rates which are in contrast with life expectancy on comparing data from 1950 till 2020.

Comparative analysis of population statistics between the elderly and the pediatrics also reveals that a double increase in the population share by the elderly aged beyond 60 years had been projected from 5.4% in 1950 to 10.1% in 2020 while a decline was anticipated in those aged 0-4 years from 14.4% in 1950 to 8.5% in 2020 [13].

Factors Influencing Health of Elderly

Factors such as age, gender, educational qualification, income, the place where an old person resides, association with old aged joint family systems, cultural and ethnic background, socioeconomic conditions, hygiene practices, presence of congenital or acquired functional limitations or disabilities, morbidities especially non-communicable diseases caused by ill effects of adopting a non-virtuous lifestyle such as chronic tobacco and alcohol usage, consumption of imbalanced nutrition, the utilization rate of health services apart from related factors such as accessibility, doctor's attitude and behavior, the cost involved for transportation and treatment, a satisfactory level of procedure, few attitudinal/subjective factors such as fear and anxiety, resistance to changes and perceived treatment needs has a major impact on the overall health status.

A Glance at Giants of Geriatrics

Although a good prognosis is achieved only if the treatment plan is tailored to meet the unique needs of every patient, it is important to consider certain common factors influencing the elderly segment of the population which influences the designing and implementation of specific protocols for the provision of comprehensive geriatric health care.

Giants of Geriatrics refers to the disabilities such as incontinence, immobility, impaired cognitive function and instability which lower the quality of life as described by Bernard Isaacs in 1975 based on which all the common problems affecting the elderly population relate [14].

A Gist of Elder's Difficulties in India

A higher illiteracy rate of 56% contributes to a total of 65% of economically dependent citizens as per the Census recorded in 2011[12, 15]. Reports reveal amplification in the illiteracy rate to 73% in 2014 comprising 40% living below the poverty line and 90% of them lacking social security [16]. A lower level of education and lack of employment with no long-term savings during old age causes compound crises in times of vulnerability. Gender and caste-based discrimination have been prevalent with elderly women facing more challenges [15]. The elderly of the rural areas are apprehensive about modern modalities thriving on indigenous medical systems.

Malnutrition owing to anorexia caused as a result of taste perception loss or inadequate ability for deglutition due to endentulousness leads to sarcopenia characterized by decreased musculature strength, mass and physical activity ensuing anemia with delayed would healing capacity. A decline in immunity has also led to an increased prevalence of communicable diseases like tuberculosis in the elderly than in younger individuals [17].

Frailty is reduced tolerance to cope with even minimum environmental stress due to aging. It is diagnosed through the identification of 3 or more components like weight loss, exhaustion, weakness, slowness and low physical activity as stated by Fried et al. It accounts for 4-17% prevalence as per the WHO report of 2015 and a study BY Richard et al [18, 19].

Most of the elders are homebound post-retirement with nil or reduced exposure to sunlight which causes calcium and vitamin-D deficiency problems called osteoporosis and osteomalacia respectively due to reduced mineral density characterized by the brittleness of the bones.

Elder abuse could be physical or psychological through verbal, financial, sexual distress and neglect encompassing very high potential to deteriorate other conditions [20]. It is one of the common problems faced by the elderly in urban areas and its prevalence accounts for about 2-

14% as per the WHO report. A survey conducted in 23 urban cities in India reveals that about 25% of the elderly had confirmed being a victim of abuse [21].

In addition, 20.5% disability rate related to speech, hearing, seeing, movement, multiple impairments, mental retardations or illnesses such as mood disorders, dementia and depression sometimes due to substance abuse constitutes more than 58 lakh elders aged beyond 60 as observed according to the 2011 Census. The National Mental Health Survey 2015 has reported a higher prevalence of substance abuse in the elderly than adults aged ≥18 years (27.78% Vs 22.40%) especially tobacco (26.34% Vs 20.89%) [22]. Disabilities have the potential to cause unintentional injuries through sudden falls. There are about 5177 physically disabled elderly for every 1 lakh population leading to a higher old-age dependency ratio of 14.2 than the geriatric population growth rate of 1.9%. [23].

An increase by 59% from 23.2 million in 1990 to 37 million in 2010 has been recorded in the premature mortality rate because of cardiovascular disease in terms of years of life lost. Cardiovascular diseases have been responsible for 33% of deaths, chronic respiratory illnesses accounted for 10% of death, stroke and cancer caused 6% fatality in 2017 as estimated by the Global Burden of Disease Study. These lifestyle diseases had induced loss of DALY (Disability Adjusted Life Years) which is evaluated based on the number of years lost due to premature aging and disability due to disease [24]. The other major causes of morbidities in the elderly are hypertension and diabetes [25-27]. Less than 4% of elders suffer infections, poisoning and violence. Urinary incontinence and constipation associated with various other medical conditions are seen in the elderly [28].

The Self Reported General Health Status of Senior Citizens

An analysis of perceived health status concerning non-communicable diseases revealed that 17% were hypertensive with the highest in Chandigarh and 9% were diabetic. The prevalence of lifestyle disorders is reported more in urban than in rural areas among the elderly. About 6 % had reported epilepsy, jaundice and asthma [29].

Educational and Media Exposure Status of Elders

The illiteracy levels among females at both up to middle school, high school and above grades are higher and more in rural regions and hence their exposure to media through newspaper reading, listening to radio, television and cinema watching habits is lesser [29].

Significance of Oral Health in the Elderly

Oral health reflects the status of overall systemic health. Maintenance of oral health-related quality of life is essential for overcoming the consequences of poor oral health such as inconveniences associated with eating, sleep, speech, pain, lowered self-esteem and decreased social interaction.

Dental disease is common in the homebound population. A couple of studies have also shown that edentulousness among the extremely old individuals aged ≥ 80 years has a bearing not only on the masticatory ability but also on general abilities and nutritional intake [30, 31].

Preventive Dentistry involves early identification and avoiding complications induced by xerostomia due to salivary gland hypofunction which is age-related or as a result of using a cocktail of medications [32].

The Self Reported Oral Health Status of Senior Citizens

Across both sexes, 43% of the elders perceived oral health problems a year prior survey with the highest in Andhra Pradesh, Assam, Himachal Pradesh, Karnataka and Uttar Pradesh and the lowest in Rajasthan of which 60 % had dental decay and 57% had gingival diseases. Foul breath and bleeding from gums were experienced by 37% and more in those having residence at rural limits. The rate of dental care utilization was a maximum only by the urban elderly though only

a total of 24% tried to seek professional care. Knowledge assessment regarding the available government facilities had revealed that only 40% were aware with more concentration in urban areas. With regards to dental care accessibility, an equal proportion of both genders could reach the facility in about less than an hour in urban areas whereas the time taken was greater than 30 minutes or more by elders in rural sites. Thus, more respondents of both sexes in urban had self-reported oral health problems with the increase in their age. Females in rural areas did not know about their oral health problems, the factors responsible for the etiology of dental problems and the preventive measures for oral hygiene maintenance. About 24% of the elderly males in greater numbers in rural areas reported a habit of smoking in India with 24% using tobacco 10 and more times every day. The frequency of alcohol consumption on daily basis was reported more by females in rural areas and greatest by males in the same zones in total while males in the urban area are social drinkers. The overall treatment need is more for males and in the rural areas which could be due to the uneven distribution of healthcare facilities favoring the inverse care law [29, 33].

Analysis of Abnormal Habits Affecting the Oral Health Status of the Elderly Population

Mouth breathing and the habit of grinding or gritting teeth were seen more in men belonging to rural areas. Males in the urban regions had the habit of sucking and biting fingers or thumbs or nails or lips or objects like pencils and tongue thrusting [29].

Frequency Trend of Sugar Pattern Consumption in Elderly Indians

Assessment of 24 hours diet chart revealed that a higher proportion of males and the elderly in urban had sugar once while females had consumed it twice. The majority of males in the rural sector had taken sugar-based products more than twice, especially in the states of Haryana, Punjab and Delhi [29].

Oral Hygiene Practice of Senior Citizens in India

Females use their fingers to clean their teeth more than males and this mode of oral hygiene practice is more in rural than in urban areas. The practice of using a toothbrush is more in males and urban sector while datun is used more by the same gender in rural areas.

The frequency of cleaning the teeth once is highest among females and twice per day among males. An equal proportion reported the habit of rinsing the mouth after every meal. The frequency of teeth cleaning two times a day with mouth rinsing habit post every meal consumed is higher in the urban sector than in rural residents.

Toothpaste is used by more men and toothpowder is widely used by females. On comparing the materials used for cleaning teeth with respect to geographical sites, toothpaste is utilized more in urban areas while powder form is used in rural areas. The use of non-fluoridated toothpaste or powders is reported to be more by females and in rural sites.

The frequency of changing the toothbrush once in six months is more in rural areas while it's being done between 1-3 months by many urban elders and some between 4-6 months. In comparison with the other age groups, it is evident that there is a decrease in the number of individuals using a toothbrush as age increases [29].

Need for Special Consideration for the Elderly

Trend analysis reveals a drastic transition in the social setup from a joint family system to nuclear units due to the impact of urbanization, industrialization and adoption of westernization as a result of which senior citizens who have unplanned their every aspect of life are being left alone causing them social problems like poverty that consecutively develops neglect towards healthcare forcing failure in the adoption of healthy lifestyle practices.

Provision of inadequate facilities for basic living causes them physical distress and isolating them with reduced family support is primarily responsible for mental illnesses, both of which

impairments end up disrupting the quality of life of the elderly segment. Furthermore, an increase in the prevalence of frailty syndromes necessitates special considerations for expanding geriatrics.

The biggest challenge is the presence of co-morbidities in the elderly which more often interacts with one another causing non-specific symptoms which necessitate the knowledge and skills of a multidisciplinary team supervised by a geriatrician for thorough assessments thus avoiding over or under investigations to plan comprehensive care. Multiple morbidities induced modified pharmacokinetics is an important feature due to polypharmacy in place creating a need for knowledge and practice on de-prescribing drugs with the lowest benefit harm ratio and chances of adverse drug withdrawal reactions to prevent iatrogenic illnesses [34, 35].

Challenges Faced

The senescence period needs additional health care to achieve Darwinian fitness as it is characterized by numerous challenges. Elderly diseases are multi-factorial very often in combination for a chronic duration hence necessitating long-term follow-up for successful management [36].

There is a lack of vaccination coverage facilities exclusively for the elderly in the existing national immunity program even though they are at a higher risk of acquiring pneumococcal infection, influenza and shingles and the recommendation of the Centre for Disease Control and Prevention of a single dosage. The deficit in the execution of inter-professional collaboration-based treatments, availability of mobile health care units, physiotherapy services, distinguished facilities, daycare centers or palliative care homes for inculcating recreational activities are some of the present-day pitfalls.

SITUATIONAL ANALYSIS OF ORAL DISEASE BURDEN IN THE ELDERLY POPULATION [29]

Dental Caries Status of the Elderly

As per the multi-centric oral health survey conducted in 2007-2008 by the Ministry of Health-WHO India, the biannual program revealed that the prevalence of dental caries among those aged 65-74 years is in the ranges of 51.6% to 95.1%.

According to the National Oral Health Survey conducted by the Dental Council of India between 2002 and 2003 in 19 regions using the WHO Oral Health Assessment form 1997, the prevalence percentage of coronal caries recorded is the highest with 84.7 constituting a DMFT value of 25-32 peaked at 14.6 among those aged 65-74 years than other age groups.

It is also observed that the Significant Caries Index (SiC) had approached a maximum of 29.5 in older adults. The report also reveals that 80-100% elderly population in 16 states experienced dental caries. About 5.4 % of the subjects were found to have root caries with a greater prevalence in rural than urban areas with virtually nil or negligibly small numbers having restorations.

Periodontal Status of the Elderly

As per the Ministry of Health-WHO India, the prevalence of periodontal disease among those aged 65-74 years is in the range of 19.9% in 2007 to 96.1% in 2008. According to the National Oral Health Survey conducted between 2002 and 2003, the prevalence of periodontal diseases was found to be 79.4% in total which was higher than for individuals aged 12 and more (55.4%) but lower than for those aged 35-44 years (89.2%) due to the fact of having more number of missing teeth.

However, periodontal pockets and loss of attachment (60.6%) were markedly more prevalent in the elderly but the assessment has been based on Community Periodontal Index which takes into account bleeding and calculus indicators as well.

Hard Tissue Status of the Elderly

The elderly population contributed to an overall very low prevalence of enamel defects such as opacities and hypoplasia with no gender-related differentials having predominance in rural areas especially highly prevalent in Punjab, Gujarat and Uttar Pradesh consecutively.

Soft Tissue Status of the Elderly

Oral cancer is one of the most important public health problems in the country as it involves unaffordable treatment costs eventually leading to disease-specific mortality when the precancerous lesion is detectable and reversible.

The maximum prevalence of oral mucosal lesions in the survey is seen in the elderly with 10% of affected individuals particularly 0.4% having oral cancer involving the hard palate, soft palate, vermillion border, commissures and buccal mucosa in sequence, 3.1% having leukoplakia, 0.5% having lichen planus followed by oral ulceration in buccal mucosa as the most common site followed by abscess and candidiasis. The highest numbers of cases were predominant in males and rural regions comparatively.

Extra oral lesions such as ulceration, sores, erosions or fissures commonly present on commissures, vermillion border followed by head, neck, limbs, enlarged lymph nodes of head or neck and abnormalities of the upper and lower lips accounted for a very low overall prevalence of only 1.1% of which 2.7 % are elders strikingly highest in Chandigarh followed by Himachal Pradesh and Punjab.

Temporomandibular joint symptoms and signs in the order of clicking, tenderness and reduced jaw mobility were prevalent in 0.4% and 1 % of the elders respectively with no age predilection having an area distribution pattern as similar as extra-oral lesions but slightly discernible to urban residents.

Dental Fluorosis Status of the Elderly

The severe and moderate forms of fluorosis are of prime concern from public health perceptive as the former may cause marked wear with brown dental staining and enamel hypoplasia with disfigured tooth form. The prevalence of dental fluorosis in the elderly population is 5.2%. However, less than one percent of the subjects reported moderate and severe forms in every age group.

Dental Prosthetic and Treatment Needs Status of the Elderly

The highest need for dental prostheses is found in the elderly. Rehabilitative procedures are required for 64.2% in the upper dental arches while only 10.5% had maxillary prostheses and 65.1% in lower dental arches while only 11.5% had a mandibular prosthesis. An estimate of 29.3% of the elderly requires full mouth removable dentures. The percentage of complete removable dentures users was 6.7% with the majority in urban areas and the highest in Chandigarh.

Though there was no gender-based variation, the need and its type were perceived more in rural regions than urban. The distribution of dental prosthetic needs among the elderly was highest in Jammu & Kashmir, Himachal Pradesh and Maharashtra serially while the lowest was observed in Goa. Around 5 to 5.3 % of elders had pain or infection which appeared more in males and rural residents.

Role of Dentist in the Well Being of the Elderly

The oral cavity is regarded as a mirror of health and disease and hence oral health assessment is integral for the evaluation of overall well-being. The dentist plays a crucial in the early diagnosis of various systemic diseases followed by the provision of prompt treatment or timely referral and helps in intervening illnesses that are most cost-effective and valuable at the elderly community level. Gone are those days during which dental visits were only for obtaining professional care simply at times of emergencies. Intensifying technological advancements in the field of mass media have increased elderly community participation in the healthcare sector by improving their knowledge, attitude and perception levels towards specific protection and promotion of well-being especially teledentistry blooming preventive oral health care delivery service.

CONCLUSION

It is evident from several studies that aging is directly proportional to risks of major health issues of chronic nature increasing disease burden including oral diseases [37-40].

The analysis of the oral health status of the elderly population reveals that complications or severity of dental problems are age-related with prevalence followed by the treatment needs ascending with age.

The elderly population forms a sizeable vulnerable group needing urgent attention and support with a greater level of integrated care. Attitudinal variation among the elderly underestimating their oral health care need is a major threat.

Most of the dental problems affecting the elderly are treatable and preventable as well. The dental service utilization rate among the elderly is very low due to dental neglect as a major challenge for Indian policymakers to formulate suitable comprehensive geriatric oral health programs and policies consisting of pre geriatric care for primordial prevention, inculcation of oral health education for primary prevention and regular dental check-up on a biannual basis to enable early diagnosis for secondary prevention, appropriate timely counseling including rehabilitation, improving the oral health-related quality of life by conducting welfare activities including cultural programs forming old age clubs with provision to utilize domiciliary oral health care services using portable infrastructures for tertiary prevention based on their felt requirements but is the need of the hour.

Inclusion of geriatric dentistry into existing elderly health care programs and policies, strengthening of the primary health care system exclusively for them, providing adequate training for upcoming graduates and inclusion as a subject in the curriculum in India could create preparedness to handle and tackle the growing oral health disease burden.

As the multidisciplinary approach is a requisite in the general health care sector for the elderly to enhance comprehensive successful outcomes, the geriatric oral health care team should comprise every specialist in the dental field to fulfill the perceived or felt oral health needs of our senior citizens for which public health dentists are an deal manpower resource as an administrator to enable amalgamation, program implementer and evaluator.

REFERENCES

1. India. Ministry of Social Justice and Empowerment. National Policy for Older Persons. New Delhi: 1999. 2020.
2. Harris NO. Text Book of Primary Preventive Dentistry. 6th ed. New York: Prentice Hill; 1999..
3. Park K. Text Book of Preventive and Social Medicine. 21st ed. Jabalpur: Bhanot Publishers; 2011.

4. The Challenge of Longevity. Ageing Demographics. Available from: http:// www. iahsa.wordpress.com .
5. Park K. Park's Textbook of Social and Preventive Medicine. 23rd edition. Banarsidas Bhanot publishers. 2015; 44: 594.
6. Division of geriatrics and clinical gerontology. Clinical Gerontology Branch. 2016.
7. Adhikari P. Geriatric health care in India - Unmet needs and the way forward. Archives of Medicine and Health Sciences 2017; 5: 112-4
8. Razak, P. A., Richard, K. M., Thankachan, R. P., Hafiz, K. A., Kumar, K. N., & Sameer, K. M. Geriatric oral health: a review article. Journal of International Oral Health, 2014; 6(6), 110–116.
9. Chandra S, Chandra S. Geriatric Dental health Care. In: Text Book of Community Dentistry. 1st ed. New Delhi: Jaypee Brothers Medical Publishers (P) Ltd India, 2004.pp. 239–51.
10. Robert GH, Barry C. Practical Consideration in special patient Care, Delivering dental care to nursing home and homebound patients. Dental Clinics of North America 1994; 38:537–51.
11. Ettinger RL, Baum BJ. Oral care for the homebound and institutionalized. Oral and dental problems in elderly. Clinics in Geriatric Medicine. 1992; 8:659–72.
12. India. Ministry of Statistics and Programme Implementation. Elderly in India-Profile and Programmes. New Delhi: 2016. 2020.
13. United Nations, Department of Economic and Social Affairs, Population Division (2019) World Population Prospects 2019, Online Edition Rev 1. 2020
14. L Greenstein. A Abraham, B Tipping. Treating complexity in the older adult - the role of the geriatric giants. South African Family Practice 2019; 61(6):10-14
15. Ministry of Statistics and Programme Implementation. National Sample Survey Office (NSSO). Key Indicators of Social Consumption in India-Health. New Delhi: 2015.
16. Gummraju N, Rao K. Geriatric care in India. Journal of Gerontology & Geriatric Research 2014;3(4):7182
17. Annual report to the people on Health. Ministry of Health and Family Welfare, Government of India. 2011.
18. Fried LP, Tangen CM, Walston J. Cardiovascular Health Study Collaborative Research Group. Frailty in older adults: evidence for a phenotype. Journals of Gerontology Series A Biological Sciences and Medical Sciences 2001; 56 (3): M14656.
19. Ofori-Asenso R, Chin K, Mazidi M. Global Incidence of Frailty and Prefrailty Among Community-Dwelling Older Adults. JAMA Network Open 2019; 2 (8): e198398.
20. Chokkanathan S, Lee AE. Elder-mistreatment in urban India: A community based study. The Journal of Elder Abuse & Neglect. 2005; 17:45–61.
21. Helpage India. Elder Abuse in India-Changing Cultural Ethos & Impact of Technology. 2018. 2020. [Last accessed on 2022 June 5].Available from https:// www.helpageindia.org/ aboutus/publications/helpage-research-reports/
22. Gururaj G, Varghese M, Benegal V, Rao GN, Pathak K, Singh LK. NMHS collaborators group National Mental Health Survey of India, 2015-16: Prevalence, patterns and

outcomes. Bengaluru, National Institute of Mental Health and Neuro Sciences, NIMHANS Publication No. 129, 2016. 2020.

23. Shi X, Wheeler KK, Shi J, Stallones L, Ameratunga S, Shakespeare T, Xiang H. Increased risk of unintentional injuries in adults with disabilities: a systematic review and meta-analysis. Disability and Health Journal. 2015; 8(2):153-64. doi: 10.1016/ j.dhjo. 2014.09.012. Epub 2014 Oct 13. PMID: 25458975.
24. Institute for Health Metrics and Evaluation (IHME) GBD Compare. Seattle, WA: IHME, University of Washington; 2015. [Last accessed on 2022 June 5]. Available from: http://vizhub.healthdata.org/gbdcompare .
25. Shaw C, Wagg A. Urinary incontinence in older adults. Medicine 2017; 45 (1): 23-7.
26. Lena A, Ashok K, Padma M, Kamath V, Kamath A. Health and social problems of the elderly: A cross-sectional study in Udupi Taluk, Karnataka. Indian Journal of Community Medicine. 2009;34:131–4.]
27. Pandve HT, Deshmukh P. Health survey among elderly population residing in an urban slum of Pune city. Journal of the Indian Academy of Geriatrics. 2010; 6:5–8.
28. Purty AJ, Bazroy J, KarMalini, Vasudewan K, Veliath A, Panda P. Morbidity pattern among the elderly population in the rural area of Tamil Nadu, India. Turkish Journal of Medical Sciences 2006; 36:45–50.
29. Bali RK, Damle SG, Muglikar SD, Yethwar RR, Mathur VB, Talwar PP. National oral health surveys and fluoride mapping 2002-2003. New Delhi: Dental council of India; 2004.
30. Sheiham A, Steele J. Does the condition of the mouth and teeth affect the ability to eat certain foods, nutrient and dietary intake and nutritional status amongst older people? Public Health Nutrition. 2001; 4(03):797.
31. Nordenram G, Bohlin E. Dental Status in the Elderly: A Review of the Swedish Literature. Gerodontology. 1985; 4(1):3–24.
32. Wiener RC, Wu B, Crout R, Wiener M. Hyposalivation and xerostomia in dentate older adults. Journal of the American Dental Association 2011; 141(3):279–84.
33. Gangadharan KR. Geriatric hospitals in India, today and in the future. The Journal of Aging & Social Policy. 2003; 15:143–58.
34. Morin L, Johnell K, Laroche M. The epidemiology of polypharmacy in older adults: register-based prospective cohort study. Clinical Epidemiology 2018; 10: 289-98.
35. American Geriatrics Society 2019 Updated AGS Beers Criteria for Potentially Inappropriate Medication Use in Older Adults. Journal of the American Geriatrics Society 2019; 67 (4): 674-94. 27.
36. Malik C, Khanna S, Jain Y, Jain R. Geriatric population in India: Demography, vulnerabilities, and healthcare challenges. Journal of Family Medicine and Primary Care 2021; 10(1):72-76.
37. Talarska D, Tobis S, Kotkowiak M. Determinants of quality of life and the need for support for the elderly with good physical and mental functioning. Medical Science Monitor 2018; 24:1604–1613.
38. Kim EJ, Jung SW, Kim Y. Assessing the impact of aging on burden of disease. Iranian Journal of Public Health 2018; 47(1):33–38.

39. Mohamed N, Saddki N, Yusoff A. Association among oral symptoms, oral health-related quality of life, and health-related quality of life in a sample of adults living with HIV/AIDS in Malaysia. BMC Oral Health 2017; 17(1):119.

40. Soares GB, Garbin CAS, Rovida TAS. Oral health associated with quality of life of people living with HIV/AIDS in Brazil. Health and Quality of Life Outcomes 2014; 12(1):28.

DTH RESPONSE TO H. POLYGYRUS IN MICE

Dipti Bhimrao Kadu
Department of Zoology, Art's and Science College, Pulgaon, Maharashtra, India

ABSTRACT
Nematodes occupying the gastrointestinal (GI) tract of animals shed an undefined array of chemicals into their environment. To combat effectively the potentially debilitating disease caused by infection with these organisms we must (a) define the parasite products chemically, (b) determine their ability to induce protective immunity and (c) establish their potential for the diagnosis of infection. Whilst it has become clear that "antigens" can be derived from within the parasite and from the turnover of external cuticular components, further work is necessary to establish the significance of these molecules to the survival of the parasite. Investigating all possible control methods, including integrated approaches, is a continuing effort. The genetics of resistance, which has an underlying immune component, might be useful in finding and using genetic markers for marker-assisted selection, and thus, could be used in programs that breed for resistance. On the other hand, the more that is known about the host's specific immune responses, the better we will be able to explore potential vaccines.

Epidemiological studies clearly revels that GI nematode infections are chronic and associated with Th2-related responses such as elevated levels of IgE. It is also clear that helminth infections exert non-specific immunomodulator effects on the immune system (Cooper, 2001; Cooper, 2000), with the most prominent and provocative recent data in this area relating to the treatment of inflammatory bowel disease using intestinal nematodes.

Keywords: Parasite, H. Polygyrus, DTH response, antigen, antibody, vaccine.

INTRODUCTION
The science of parasitology has made remarkable progress during the last 30 years. The whole concept of 'parasite' and parasitism as understood in older days has now changed. The emphasis has been shifted to quires like why hosts fail to reject the parasite, how parasites adapt themselves to host conditions, how do they modulate host immune reactions and how specific antigens can be isolated and identified for vaccination. Our knowledge about the nature, quantum and kinds of pharmacological mediators released as a result of host-parasite interactions and the effects of different types of parasitic antigens on protective mechanism of hosts in meager. Immunologists have isolated and identified hundreds of antigens, somatic and metabolic, some with protective potentialities; some for immunodiagnosis and yet others as immunosuppressive but much more remains unresolved.

Host responses to primary infections with *Heligmosomoides polygyrus* were studied in fast responding FVB mice (H-2q) by Cywin´ ska, *et al.* (2004). Pathological changes in the intestinal mucosa, mesenteric lymph nodes and spleen were examined. Features of the fast response were typical: low effectiveness of infection and limiting of parasite survival and egg production, with worm expulsion occurring about 60 days post-infection. The intestinal inflammatory response involved infiltration by different cells into the intestinal mucosa and granulomata formation. As is typical for intestinal nematode infection enteropathy, decreased villus: crypt ratio and hyperplasia of Goblet and Paneth cells were also present. Reactions of the intestinal mucosa, mesenteric lymph nodes and spleen increased over time postinfection and after worm expulsion. They further suggested that enteropathy might help worm expulsion by creating an unfavourable environment for *H. polygyrus*.

HELIGMOSOMOIDES POLYGYRUS

Experimental studies on *Heligmosomoides polygyrus* are few. *H. polygyrus* is a trichostrongyloid nematode of family Heligmosomidae, first reported from *Mus musculus* by Spurlock (1943) and from *Peromyscus maniculatus* by Ehrenford (1954). *H. polygyrus* is a long-lived intestinal nematode of mice. Rats are known to be naturally resistant to it (Cross, 1960). Development of its free living stage has been reported by Fahmy (1956) and its complete life cycle in mice by Spurlock (1943); Baker (1954); Ehrenford (1954); Dobson (1960); Callizo (1962) and Bryant (1973). Adults of *H. polygyrus* are spirally coiled (females 18-21 mm and males 8-10 mm long) and are found in first 2 cm. attached to duodenal mucosa. The eggs of *H. polygyrus* are fully emryonated when evacuated with feces and hatch at 20-23° C. Life cycle is direct and non- migratory, infection to host is through ingestion of infective filariform 3^{rd} stage larvae which penetrate intestinal mucosa maturing in 8-9 days after infection and females lay eggs up to 9 months producing 1280 eggs per day per female (Scott, *et al.*, 1959). Infection can easily be maintained in the laboratory and the larvae culture well within limits and thus, forms an excellent parasitological tool for experimental investigations.

MATERIALS AND METHODS

Experimental Animal –

The Swiss albino mouse, *Mus musculus albinus* of either sex were selected as an experimental animal for the present investigation. The mice were obtained from the Institute of Nutrition (NIN) Hyderabad, India and were kept in the animal house under local conditions of light, temperature ventilation and food. Food and water were provided *ad libitum*. Male and female healthy mice of 6-8 weeks old and 15-20 gms in weight were used according to the need of the experimental design. Animal experimentations were conducted according to INSA ethical guidelines for the use of animals for scientific research purpose, after permission from the ethical committee.

The Parasite: *Heligmosomoides polygyrus*-

Heligmosomoides polygyrus is a mouse intestinal nematode that establishes a chronic infection in the deodenum. It is a common nematode found in the duodenum and small intestine of woodmice and other rodents. They are 5-20 mm in length and bright red due to the pigmentation of their tissues. They are usually heavily coiled, with the female having 12-15 coils and the male 8-12. The male can be distinguished from the female by a prominent copulatory bursa and two long, thin spicules at the posterior end.

Animals from different groups were sacrificed under mild ether anesthesia at various intervals according to the experimental design and mice, which died during the course of the experiments, were discarded. Larvae from gastrointestinal tract on 1 and 5 days post infection were isolated according to the method of Soh (1958). At necropsy, stomach and small intestine (anterior, middle and posterior regions) were cut separately into small pieces, finally minced, placed in surgical gauge cones which were tied and kept into suitable beakers containing artificial gastric juice (pepsin, 5.0 gm NaCl, 8.5 gm HCL, 7.0 ml in 1000 ml distilled water) at 37^0 C for 3 hours after digestion, the contents of the beakers were transferred to Baermann's apparatus separately and left there for 18 hours. Sediment containing the larvae from each funnel of the apparatus was taken into tubes and allowed to settle for 4 hours. The supernatant was discarded, aliquots of 1 ml of the sediment were pipetted, spread on large glass slides and larvae were counted under the dissecting microscope. The adult mature worms were collected from the intestine at day 13 pi. and counted.

Collection of the blood samples and separation of serum-

0.5 ml blood from experimental and control mice was collected from orbital sinus under mild ether anesthesia with 1ml sterilized dry glass syringe fitted with a 20 gauge needle. Blood

samples were kept in 15 ml centrifuge tubes in cold overnight for clotting after which serum carefully pipetted out into clean sterilized serum collecting tubes and stored at -20^0 C until required.

Procurement of different life stages of *H. polygyrus* for harvesting ES/Somatic antigens-
All procedures were carried out under aseptic conditions, using sterile solutions. Washing whenever required was performed in Hank's balanced salt solution [HBSS] containing antibiotics. Different life cycle stages taken for harvesting specific antigens were as follows:

1. L3 larvae
2. Mature adult worms

Preparation of Somatic Soluble Antigens-
L-3 larvae and mature worms were washed thoroughly and homogenized separately in the culture medium using tissue grinder, in cold. The homogenate was centrifuged at 4,000 rpm for 30 minutes at 4^0 C and the supernatant was lyophilized and kept at 4^0 C.

Immunization of mice, challenge infection and worm recovery-
Samples of lyophilized ES/Somatic antigen whose protein content was estimated by method of Lowry, *et al.* (1951) suspended in HBSS, were employed.

An initial dose of 0.4 ml of the suspension with 0.2 ml of antigenic sample containing the required protein content (determined earlier) and 0.2 ml of Freund's complete adjuvant (FCA) was injected sub-cutaneously (sc.) for immunization. The protein content of the antigenic sample varied according to the experiments, however, the booster dose was of 0.2 ml, containing required amount of protein without FCA. 60 mg, protein dose was used for immunization. A challenge oral infection of a single dose of 300 L3 larvae of *H. polygyrus* was uniformly given after two weeks to each mouse of all the experiments. On 1 and 5 days after the challenge, the larvae were counted in the intestinal submucosa and adult worms were recovered on 13 day after challenge and counted.

Delayed hypersensitivity (DTH) estimation (Talwar, 1983)-
1) 0.03 ml of soluble test antigen (1:1000w/v) was injected into plantar side of the foot-pad of experimental mice with the tip of the 30G needle pointing proximally. The joint was extended (180^0 C) when the needle was injected into the foot-pad.
2) Foot-pad thickness measurement: the DTH response was measured as the increase in foot-pad thickness in the foot-pad injected with the elicit in as compared to the control foot–pad of the same mouse injected with suspending fluid. Foot-pad thickness was measured by a calliper. Each measurement was a mean of six readings, three each by two different individuals.
3) DTH response was measured at 24hr after challenge and the reaction greater than 5mm in diameter was considered significant.
4) DTH response was confirmed by carrying out histological examination in both foot-pads. Fixation was done in buffered formaline, sectioned and stained with haematoxylin- eosin stains. A positive DTH response was confirmed by observing a strong mononuclear infiltration.

OBSERVATIONS AND RESULTS
Heligmosomoides polygyrus is a natural intestinal helminth of mice. It inhibits in the duodenal region of small intestine. In the present investigation, albino mice were colonized with 300 larvae each time by placing larvae directly in the stomach through gastric lavage. The larvae

migrated to duodenum, to house in the submucosa where they matured and then emerged as adult worms migrating in the intestinal lumen by 13 days of time.

The present study was carried out to investigate the immunological responses and possibility of vaccine development.

4.0 DTH RESPONSES:

4.1 DTH responses from infected mice (with 300 larvae of *H. polygyrus*) after 1, 5 and 13 day of administration of L-3 larval somatic antigens:
The mice infected with 300 larvae of *H. polygyrus* showed delayed type of hypersensitivity after 13 days of infection. However, after vaccination by larval somatic antigens, significant delayed type of hypersensitivity was observed after 1, 5 as well as 13 days of infection and vaccination. The DTH response after 13 days of vaccination was 10.50 $\pm$ 0.55 mm.

4.2 DTH responses from infected mice (with 300 larvae of *H. polygyrus*) after 1, 5 and 13 day of administration of adult somatic antigens:
The mice infected with 300 larvae of *H. polygyrus* exhibited significant

DTH response only after 13 days of infection. These infected mice when administered with adult somatic antigen showed significant DTH responses after 5 as well as 13 days of infection and vaccination. The skin showed DTH response with 9.30 $\pm$ 0.15 mm diameter.

4.3 DTH responses from infected mice (with 300 larvae of *H. polygyrus*) after 1, 5 and 13 day of administration of L- 3 larval ES antigens:
The mice infected with 300 larvae of *H. polygyrus* exhibited significant DTH response after 13 days of infection. However, after vaccination by larval ES antigens, significant delayed type of hypersensitivity was observed after 1, 5 as well as 13 days of infection and vaccination. The DTH response after 13 days of vaccination was 13.22 $\pm$ 0.96 mm.

4.4 DTH responses from infected mice (with 300 larvae of *H. polygyrus*) after 1, 5 and 13 day of administration of adult ES antigens:
The mice infected with 300 larvae of *H. polygyrus* showed significant DTH response after 13 days of infection. Whereas, after vaccination by adult ES antigens, significant DTH response was observed after 1, 5 and 13 days of infection and vaccination. The skin showed DTH response with 10.88 $\pm$ 0.68 mm.

DISCUSSION
Heligmosomoides polygyrus is a natural intestinal helminth of mice. It inhibits in the duodenal region of small intestine. In the present investigation, albino mice were colonized with 300 larvae each time by placing larvae directly in the stomach through gastric lavage. The larvae migrated to duodenum, to house in the submucosa where they matured and then emerged as adult worms migrating in the intestinal lumen by 13 days of time. In the recovery experiments, 87.30% recovery was observed after 5 days and out of them 78.80% adults were recovered after 13 days.

Larval and adult worm recoveries:
Larval and adult worm recoveries after 1, 5 and 13 days of infection and vaccination were studied and the results are shown Fig. 1 to 4.

The results clearly indicate that larval and adult worm recoveries were more in vaccinated mice than those in non-vaccinated mice.

The % protection after larval ES antigen was the highest followed by vaccination with somatic antigens, then adult ES antigen and least after vaccinated with adult somatic antigens.

Larval ES > Larval somatic antigens > adult ES antigens > adult somatic antigens.

After 1, 5 and 13 days of administration of larval ES antigens, the protection achieved was 80.63%, 81.90% and 84.96% respectively which was quiet better than the rest of the antigens tried during the present investigation. Even after the 1st day of administration of larval ES antigens the larval recovery was 80.63%, which in rest of the vaccinated conditions the protection was below 75%. These results indicate that the somatic and Excretory-Secretory antigens differ in their antigenic properties. The ES antigens are more potential and might be having number of receptors developed on intestinal epithelial cells, activating them to secrete enzymatic secretion damaging/killing the larvae and /or adult *H. polygyrus*. This may also be due to more solubility of ES antigens, resulting into direct absorption of ES antigens into intestinal epithelial cells, leading to assimilation and easy entry in blood. This has reflected in the haematological alterations.

Furthermore, this parasitic modification can be one of the clue for development of vaccine.

Developmental stage specific antigens are earlier reported by Adams, *et al.* (1987); Mohan, *et al*. (1988) and Northern, *et al*. (1989). The better protection given by ES antigens might have resulted from the excretory contents of parasites (larvae as well as adult), molting tissues, reproductive secretions and body surface secretions. In the present investigation, these antigens are proved to be more immunogenic and hence need isolation and purification to develop full proof effective vaccine.

DTH Responses in infected and vaccinated mice:

The excretory Secretory antigens are the foreign proteins released in the intestinal lumen. They may be secretions of the larval epithelium, the moulted integument, the release of reproductive products from the adult worms, metabolic products or they may be excretory products from larvae and adults. These additional antigenic load might be responsible for immediate increase in DTH response at the same time, they also resulted into better protection in vaccinated individuals. There may be a possibility of many such participatory antigens (known and unknown) which are produced by parasitic larvae and resulting into immunity. Developmental stage specific immunogens are earlier reported by Northern, *et al*. (1989).

The enhanced activation of immune system is seen in DTH responses in vaccinated mice. Those infected mice which were vaccinated with larval ES antigens exhibited maximum DTH response. The foot pad reaction was carried out as a measure for DTH response. The DTH response was maximum after one day of vaccination with larval ES antigen, followed by adult ES antigens, larval somatic antigen and then adult somatic antigens (Fig. 1to4).

Skin reactions greater than 5 mm in diameter was considered significant. Skin reaction recorded was maximum (13.22 mm) after 13 days of infection and vaccination with larval ES antigens. The same group of mice showed highest % DTH response after 1, 5 and 13 days of infection and vaccination. The % DTH response was decreased by 14.72% after 5 days and after 13 days of vaccination, the % DTH response was decreased by 68.32% indicating a state inhanced immune response and protection. These results are in consistant with the results of the larval and adult worm recoveries.

The % DTH response gradually decreased from 1 day of infection to 13th day of infection after vaccination in all the groups studied (Fig. 1to4), indicating protection by somatic and excretory-secretory antigens administered.

SUMMARY AND CONCLUSION

Heligmosomoides polygyrus is a natural intestinal helminth of mice. It inhibits in the duodenal region of small intestine. In the present investigation, albino mice were colonized with 300 larvae each time by placing larvae directly in the stomach through gastric lavage. The larvae migrated to duodenum, to house in the submucosa where they matured and then emerged as

adult worms, migrating in the intestinal lumen by 13 days of time. The present study was carried out to investigate the immunological responses and possibility of vaccine development.

The % protection after administration of larval ES antigen was the highest followed by vaccination with somatic antigens, then adult ES antigen and least after vaccinated with adult somatic antigens. Larval ES > Larval somatic antigens > adult ES antigens > adult somatic antigens.

After 1, 5 and 13 days of administration of larval ES antigens, the protection achieved was 80.63%, 81.90% and 84.96% respectively which was quiet better than the rest of the antigens tried during the present investigation. Even after the 1st day of administration of larval ES antigens, the larval recovery was 80.63%, while in rest of the vaccinated conditions the protection was below 75%. Vaccination with larval antigens, both somatic and ES antigens, led to less recovery of mature worms, than vaccination after adult somatic and ES antigens and similarly ES antigens were more potent than somatic antigens. These differences may be due to developmental modifications in larvae to become adult for continuation of race.

The enhanced activation of immune system is seen in DTH responses in vaccinated mice. Those infected mice which were vaccinated with Larval ES antigens exhibited maximum DTH response. The foot pad reaction was carried out as a measure for DTH response. The DTH response was maximum after one day of vaccination with larval ES antigen, followed by adult ES antigens, larval somatic antigens and then adult somatic antigens.

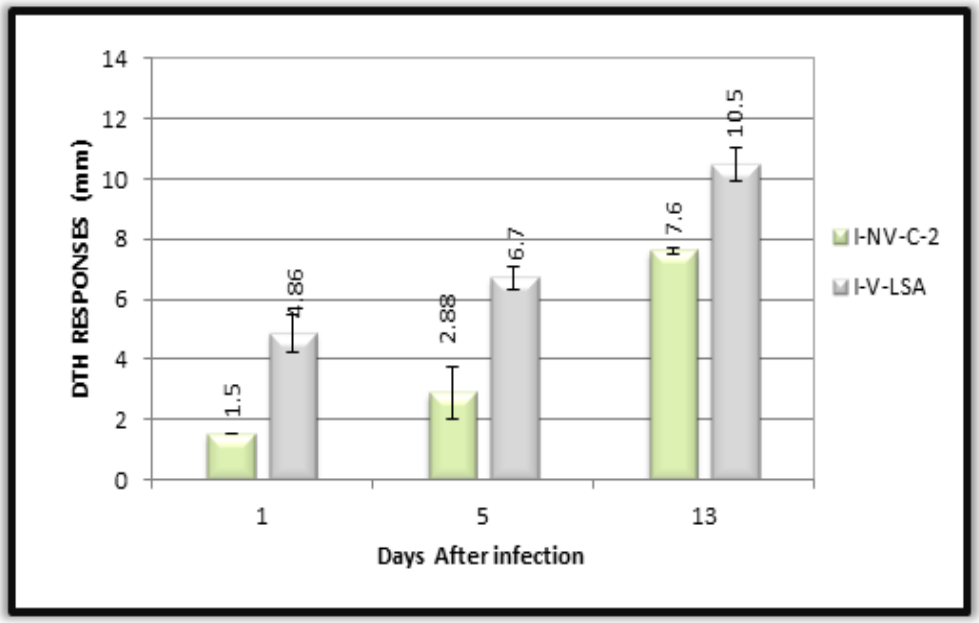

Fig. 1: DTH responses from infected mice after 1, 5 and 13 days of administration of L-3 larval somatic antigens

 ISBN: 978-93-93810-19-9

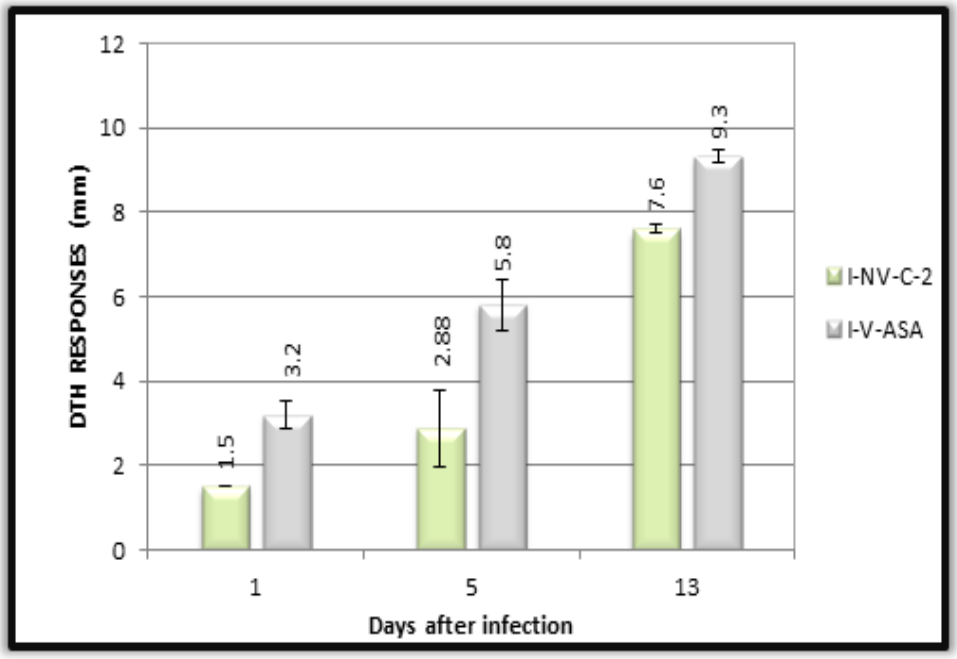

Fig. 2: DTH responses from infected mice after 1, 5 and 13 days of administration of adult somatic antigens

I-NV-C-2	Infected Non Vaccinated Control-2
I-V-LSA	Infected and Vaccinated with L-3 larval Somatic Antigens
I-NV-C-2	Infected Non Vaccinated Control-2
I-V-ASA	Infected and Vaccinated with Adult Somatic Antigens

Skin reaction greater than 5mm in diameter are considered significant.

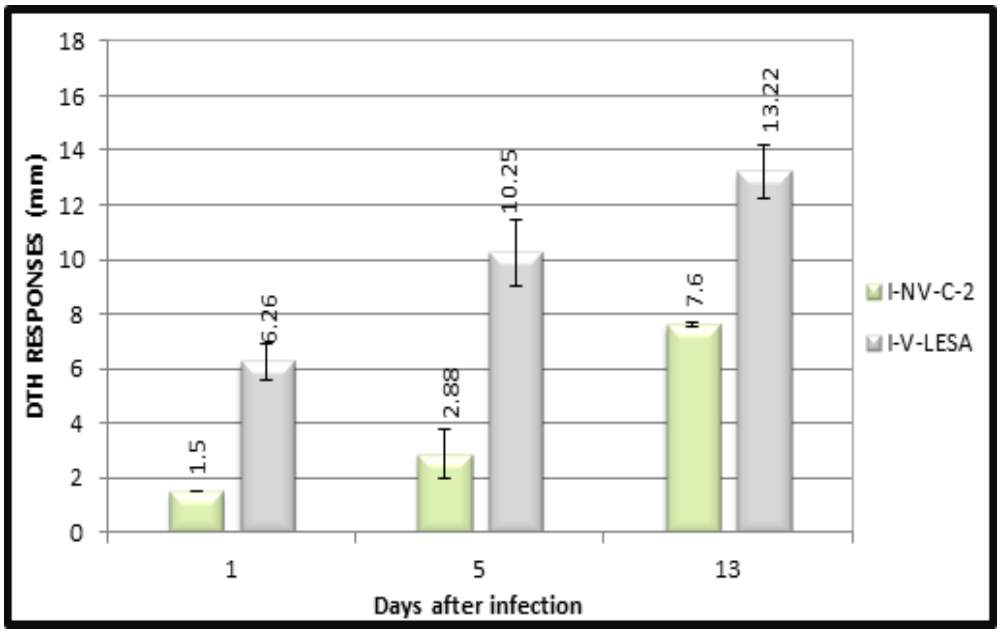

Fig. 3: DTH responses from infected mice after 1, 5 and 13 days of administration of L-3 larval ES antigens

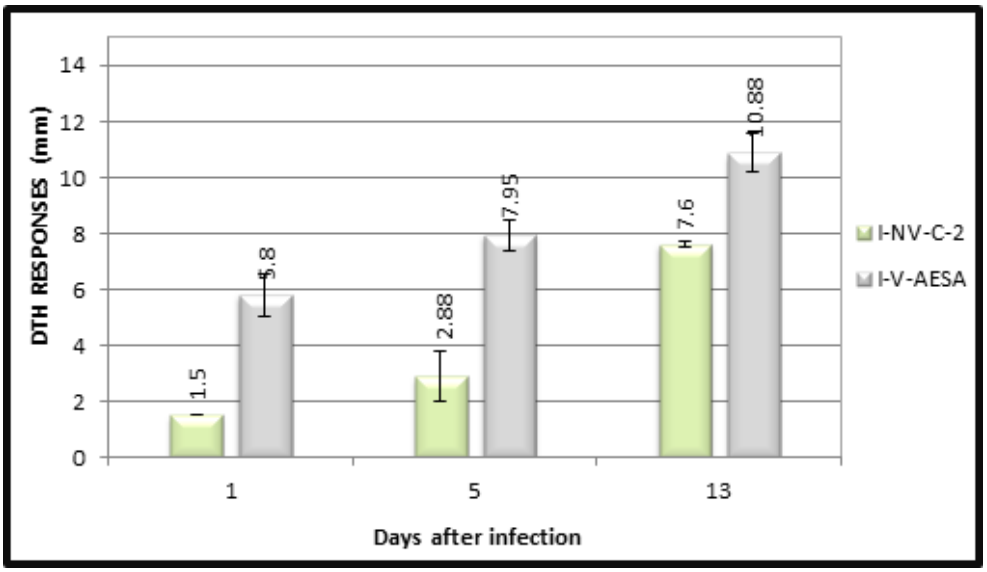

Fig. 4: DTH responses from infected mice after 1, 5 and 13 days of administration of adult ES antigens

I-NV-C-2	Infected Non Vaccinated Control-2
I-V-LESA	Infected and Vaccinated with L-3 larval ES Antigens
I-V-AESA	Infected and Vaccinated with Adult ES antigens

Skin reaction greater than 5mm in diameter are considered significant

REFERNCES

Adams, J. H.; East, I. J.; Monroy, F.; Washington, E. A. and Dobson, C. (1987). Stage-specific antigens of Nematospiroides dubius Baylis, 1926 (Nematoda: Heligmosomidae). J. Parasitol. 73, 1164-8.

Baker, N. F. (1954). Trichostrongylidosis: The mouse as an experimental animal. Pro. Am.Vet. Med. As. 91, 185-191.

Bryant, V. (1973). The life cycle of Nematospiroides dubius, Baylis,1926 (Nematoda: Heligmosomidae). J. Helminth. 47, 263-268.

Callizo, P. J. (1962). The free living development of Nematospiroides dubius, Baylis, 1926 (Nematoda: Heligmosomidae).

Cross, J. H. Jr. (1960). The natural resistance of the white rat to Nematospiroides dubius and the effect of cortisone on this resistance. J. Parasit. 46, 175-185.

Cywinska, A., Czuminska, K. and Schollenberger, A. (2004). Granulomatous inflammation during Heligmosomoides polygyrus primary infection in FVB mice. Journal of Helminthology. 78, 17-24.

Dobson, C. (1960). "An investigation of the host parasite relations and host specificity ofNematospiroides dubius Baylis, 1926, Heligmosomadae, a mouse nematode in its normal and abnormal hosts". Ph.D. thesis, University of Scheffield.

Ehrenford, F. A. (1954). The life cycle of Nematospiroides dubius, Baylis,1926 (Nematoda: Heligmosomidae). J. Parasit. 79, 480-481.

Fahmy, M. A. M. (1956). An investigation on the life cycle of Nematospiroides dubius (Nematoda: Heligmosomidae) with reference to the free living stages.Z. Parasiten. 17, 394-399.

Lowry, O. H.; Rosenbourgh, N. H.; Farr, A. L. and Randall, R. J. (1951). Protein measurement with the folinphenol reagent. The Journal of Biological Chemistry. 193, 265-275.

Mohan, S.; Kaushal, N. A.; Misra, A.; Kaushal, D. C.; Katiyar, J. C. and Ghatak, S. (1988). Ancylostoma ceylanicum: I. Protein and antigenic composition of adult and larval stages. Immunol. Invest. 17, 295-307.

Northern, C. and Grove, D. I. (1989). Antigenic analysis of Strongyloides ratti infective larvae and adult worms. Immunol. Cell. Biol. 65, 231-9.

Soh, C. T. (1958). The distribution and persistence of hook worm larvae in the tissue of mice in relation to species and routes of inoculation. J. Parasit. 44, 515-519.

Scott, J. A.; Cross, J. H. Jr. and Dawson, C. (1959). Egg production of Nematospiroides dubius in mice and rats. Texas Reports on Biol. Med. 17, 610-617.

Spurlock, G. M. (1943). Observation on the host parasite relations between laboratory mice and Nematospiroides dubius. Baylis. J. Parasit. 29, 303-311.

Talwar, G. P. (1983). A handbook of practical immunology. Edited by Talwar,G.P. Vikas Publishing House Pvt. Ltd. New Delhi.

IMPACT OF DYE EFFLUENT ON SEED GERMINATION, SEEDLING GROWTH AND CHLOROPHYLL CONTENT OF SOYBEAN

Fiona Paulson T[1] and Dr. J. Banu Priya[2]

[1]Ph.D Scholar, Department of Costume Design & Fashion, PSG College of Arts & Science, Coimbatore

[2]Supervisor and Assistant Professor, Department of Costume Design & Fashion, PSG College of Arts & Science, Coimbatore

ABSTRACT

Textile dyeing industry is one of the largest and major most water consuming and high polluting industries in India. Untreated industrial wastage discharged into the ecosystem causes serious problem to the underworld and also the living organisms, plants and human being. Higher concentration will affect the soil and cause heavy damage to crop growth. In the present study over dyeing effluence on seed germination and seedling growth of soybean (Glycine max)

Keywords: Dye Industrial Effluent, Physio-chemical analysis, Soybean seeds, Germination percentage, Seedling growth, Chlorophyll a and b

1. INTRODUCTION

The unplanned rapid industrial growth is the main cause for our environmental pollution. Every industry is associated with emission and causes pollutants. Textile industries are large industrial consumers of water and also producers for waste water with the increased demand in textile production. The most potential and hazardous source of water and soil pollution are produced from industrial effluents.

One major group of contamination is produced from in effluent is dyes from dying and printing industries. The waste water from textile dying industries is a complex mixture of many chemical polluting substances from organo-chloride based heavy waste metals associated with dye and dying process (Correia et al. 1994). These contain heavy metals poisonous compounds and nutrients which affect plant and soil in number of ways. These toxic chemicals presents in effluent caused reduction in cell activities, retardation of growth, various deficiencies and diseases when accumulated in cells of living being (Patel et al. 2008 and Naik et al. 2009). Industrial effluents are constantly adding up toxic substances into the ground water reservoir at a very high rate especially in industrial zones (Babiker *et al.* 2004). The industrial pollutants caused the alteration in Physico-chemical and biological properties of the environment. Dye waste water has also been found toxic to several crop plants (Parameswari M. 2014). The presence of heavy metals and toxic chemicals will show detrimental effects on the development of plants, germination process and growth of seedlings (Singh et al. 2004 and Nath et al. 2007). Effluent in higher concentration affect the soil and causes heavy damage to the crop growth conditions. The use of such waste water in irrigation system definitely provides some nutrients to enhance the fertility of soil but it also deposits toxicants that change soil properties in the long run. The low amount of O2 in dissolved form due to the presence of high concentration of solid in the effluent reduces the energy supply through anaerobic respiration resulting in restriction of growth of seedlings (Sazena et al. 1986). The improper and indiscriminate disposal of textile effluents in natural waters and land in posing serious problems (Kaushik et al. 2004). The exposure of lower concentration of effluent to the seedling shows growth promotion, over all development of the seedling and chlorophyll content. Reduction in seed germination percentage at higher concentration of effluent may be due to the higher amounts of solids presents in the effluent, which causes changes in osmotic relationship of the seed and water (Prabhakar et al. 2006). In the present study an attempt was made to analyze the impact of dying

effluent, collected from dying and printing industries at Kaithoon region, Kota, on some growth parameters of soybean (Glycine max L.)

2. MATERIAL AND METHODS

Experimental Plant:

Soyabean

BOTANICAL NAME	**Glycine max**
FAMILY	**Leguminosae**

Soybean is a leguminous vegetable that grows in tropical, subtropical and temperate climates. It consists of, more than 36% protein, 30% carbohydrates, and good amounts of dietary fiber, vitamins, and minerals. Soybean produces significantly more protein in per acre than the other crops that are cultivated. The height of the plant varies from less than 0.2 to 2.0 m (0.66 to 6.56 ft). Soybean contains a type of bacteria called "Rhizobia". These bacteria have special ability to fix the nitrogen from atmosphere.

2.1 Collection of Effluent Sample

The needed samples were collected from small dying and printing units from different regions of south India. They were then sterilized with the help of wide mouth plastic bottles and were stored in 40^{o} C temperature to avoid any changes in their characteristic. To evaluate the effects of dyeing effluent on Glycine max, solution of different concentrations.

Treatment Level

C- Control (100% Distilled water)

T1- Effluent: Distilled water (20% + 80%)

T2- Effluent: Distilled water (40% + 60%)

T3- Effluent: Distilled water (60% + 40%)

T4- Effluent: Distilled water (80% + 20%)

T5- Effluent (100%)

Germination Test

Seeds were sterilized with 0.1% w/v mercuric chloride (Hgcl2) solution for 5 minutes to remove microbes and then washed three times with sterile distilled water. 20 seeds of Glycine max, were placed in sterilized glass. These filter discs were then moistened with 5 ml of distilled water and with concentrations of the textile effluent (20%, 40%, 60%, 80%, 100%). The dishes were kept at room temperature. 5 ml of the respective dilutions were sprayed of the seed for 6 days. Germination was recorded daily. All the levels were carried out in triplicate. On the 7th day, germination, percentage was calculated and noted.

Germination Percentage

The formula given by Rehman• et al.(1998) was used to estimate germination percentage.

Root and Shoot Length- Length of root and shoot of• seedlings were calculated by using the standard centimeter scale.

Vigour Index- The formula suggested by Abdul-Baki and• Anderson (1973) was used to calculate vigour index.

Vigour Index = germination percentage X (root length* + shoot length*) (* indicate that length of root and shoot in cm.)

Fresh and Dry Weight of seeds – Ten seeds of each• treatment were weighted in order to determine the fresh weight and then dried in oven at 800 C for 24 hrs. to obtain dry weight. Fresh weight and Dry weight were recorded in mg.

Chlorophyll estimation- The estimation of chlorophyll• content was done according to Arnon's method (1949). Where A663= Absorbance at wavelength 663 nm A645= Absorbance at wavelength 645 nm V= Volume of the extract in ml A = Length of light path in the cuvette (1cm) W= Fresh weight of the samples in gm.

3. RESULTS AND DISCUSSION

Germination percentage in untreated seedling (control) of Glycine max was 93% while the germination percentage of seedlings treated with 20% dilution was 96% in comparison to control. At high concentration of treatment levels 40%, 60%, 80% and 100% the germination percentage were decreased 70%, 56%, 40% and 33% respectively. The maximum decrease was found at 100% (33%) effluent concentration.

Vigour index in untreated seedling (control) of Glycine max L. was 1590.3 while the vigour index of seedlings treated with 20% dilution was increased 1680 in comparison to control. At high concentration of treatment levels 40%, 60%, 80% and 100% the vigour index were decreased 1204, 856.8, 436 and 234.3 respectively. The maximum reduction was found 85.26% at 100% effluent concentration.

Root length in untreated seedling (control) of Glycine max L. was 4.5cm while the root length of seedlings treated with 20% and 40% dilution were increased 4.7 and 4.6 cm in comparison to control. At high concentration of treatment levels 60%, 80% and 100% the root length were decreased 3.4, 2.1 and 1.9 cm respectively. The maximum reduction was found 57.7% at 100% effluent concentration. Shoot length in untreated seedling (control) of Glycine max L.was 12.6 cm while the root length of seedlings treated with 20% and 40% dilution were increased 12.8 cm and no change at 40% in comparison to control. At high concentration of treatment levels 60%, 80% and 100% the soot length were decreased 3.4, 2.1 and 1.9 cm respectively.

The maximum reduction was found 57.7% at 100% effluent concentration. Fresh weight in untreated seedling (control) of Glycine max was 3.10 gm while the fresh weight of seedlings treated with 20% and 40% dilution were increased 3.26 and 3.15 gm in comparison to control. At high concentration of treatment levels 60%, 80% and 100% the fresh weight were decreased 2.98, 2.42 and 2.10 gm respectively. The maximum reduction was found 32.25% at 100% effluent concentration. Dry weight in untreated seedling (control) of Glycine max L. was 1.90 gm while the dry weight of seedlings treated with 20% and 40% dilution were increased 1.98 and 1.93 gm in comparison to control. At high concentration of treatment levels 60%, 80% and 100% the dry weight were decreased 1.51, 1.26 and 1.09 gm respectively. The maximum reduction was found 42.63% at 100% effluent concentration.

Chlorophyll a content in untreated seedling (control) of Glycine max L. was 5.06 mg/gm while the Chlorophyll a of seedlings treated with 20% and 40% dilution were increased 5.11 and 5.08 mg/gm in comparison to control. At high concentration of treatment levels 60%, 80% and 100% the Chlorophyll a were decreased 4.86, 3.87 and 2.42 mg/gm respectively. The maximum reduction was found 52.1% at 100% effluent concentration. Chlorophyll b content in untreated seedling (control) of Glycine max L. was 5.02 mg/gm while the Chlorophyll b of seedlings treated with 20% and 40% dilution were increased 5.07 and 5.05 mg/gm in comparison to control. At high concentration of treatment levels 60%, 80% and 100% the Chlorophyll b were decreased 3.71, 2.69 and 1.80 mg/gm respectively. The maximum reduction was found 64.1% at 100% effluent concentration.

Present study result revealed that effluent of dying industries inhibit seed germination and seedling growth. It may be due to the presence of toxic elements and metal ions in the corresponding industrial effluents (Rohit et al. 2013). The higher pH , BOD, COD and other higher organic loads that cause adverse effect on germination (Panday et al. 2004 and Saddaqat et al. 2006. This could be related to the fact that some of the nutrients present in the effluent are essential but in higher concentration they become hazardous and toxic to the soybean plant (Ravi et al. 2014). The exposure of lower concentration of effluent to the seedling shows growth promotion, over all development of the seedling and chlorophyll content. Reduction in seed germination percentage at higher concentration of effluent may be due to the higher amount of solids presents in the effluent, which causes in the osmotic relationship of the seed and water. Present study supported with the views of Sundaramoorthy et al. (2000) who investigated that the percentage of seed germination and seedling growth was maximum at 10% diluted effluent than the control while undiluted effluent showed inhibitory effects . Hussain et al. (2013) also reported that diluted effluent (25%) increase the growth parameters and pigments in the Maize seedlings. Kathirvel (2012) also supported present study who investigated that at 20% concentration of effluent, the plant showed maximum seed germination, root and shoot length than the control and the maximum chlorophyll content were also reported at 20% effluent concentration which could be due to the best growth of seedling at this concentration. Present study is also supported by Mayuri et al. (2015) who reported that the best germination and seedling growth was observed in 25% concentration with growth promoting effect and significantly better than control. Beyond 25% effluent germination percentage and seedling growth decreased gradually. Divyaprivas et al. (2014) also concluded that germination percentage and other biochemical contents were high at 30% effluent dilution in comparable with control but beyond 30% dilution all parameters were decreased and at 100% effluent treatment the seed germination was completely inhibited in Cicerarientum.

Table1: Showing effect of different dilution percentage of dying and printing effluent on germination percentage, vigour index, root length, shoot length, fresh and dry weight, chlorophyll a and b content in Glycine max L.

S.NO	Treatment	Seed Germination %	Virgour Index	Seed growth (14 days)		Weight		Chlorophyll Content	
				Shoot length(cm)Avg	Root length(cm) Avg	Fresh Weight(gm)	Dry Weight(gm)	Chlorophyll a (mg/gm)	Chlorophyll b (mg/gm)
1	Control	93	1590	12.9	4	3.09	1.99	5.06	5.02
2	20%	96	1688 (5.9%)	12.6 (1.5%)	4.6(4.3%)	3.6 (4.8%)	1.96 (9.0%)	5.11(0.94%)	5.07(0.94%)
3	40%	70	1205 (24.6%)	12.5	4.6(2.6%)	3.15(1.0%)	1.65 (1.2%)	5.95(0.35%)	5.05(0.44%)
4	60%	56	854.2(44.7%)	11(5.0%)	3.6(24.3%)	2.60(3.4%)	1.93(1.5%)	4.58(3.43%)	3.71(26.07%)
5	80%	40	436 (72.5%)	8.4 (28%)	2.1(53.0%)	2.65(20.4%)	1.95(32.4%)	4.32(22.5%)	2.96(45.3%)
6	100%	33	245.5(90.0%)	5.11(4.9%)	1.6(50.5%)	2.25(30.2%)	1.58(40.3%)	4.65(51.2%)	1.98(62.2%)

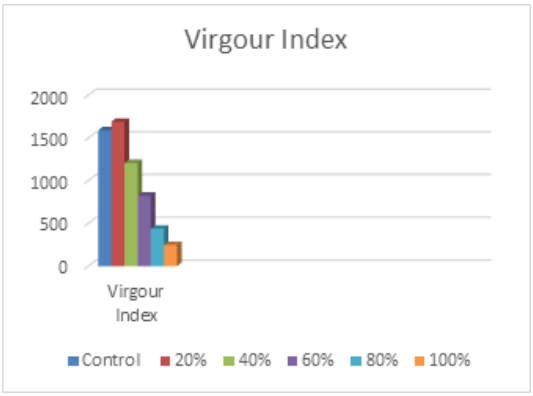

Fig 1: Virgour Index

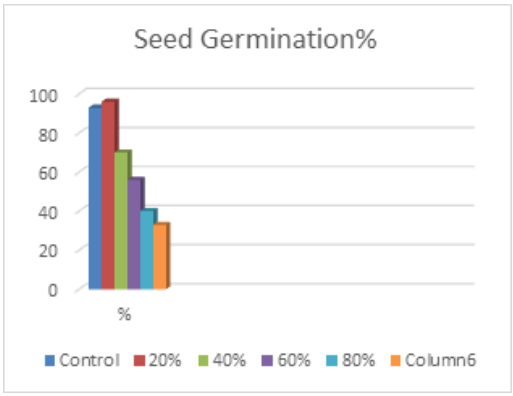

Fig 2: Seed Germination%

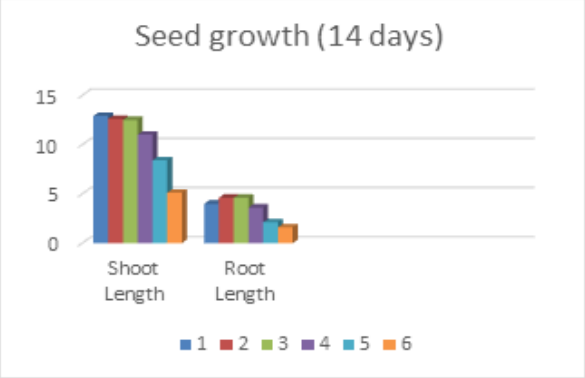

Fig 3: Seed Growth

4. CONCLUSION

The present study concluded that the dying effluent waste significantly influence growth parameters of soybean (Glycine max) have been carried out at different concentration (20, 40, 60, 80 and 100%). Seed germination percentage of Glycine max was not significantly affected at 20% treatment level compared to the others. Seeding growth (Shoot and Root lengths) and Chlorophyll content (Chlorophyll a and b) have found to increase at 20% and 40% of treatment level. The root length was found increased with 4.4% and 2.2% of shoot length with an increase of 1.5% and no change in the level 20% and 40% respectively. Due to increase of effluent at 60% treatment level and above a gradual decline of seedling growth was observed and noted. At 100% treatment level root length and shoot length were decrease 57.7% and 58.7% respectively in comparison to control. Chlorophyll content was also adversely affected due to higher concentration of dyeing effluent. The present study revealed that Glycine max L. (soybean) is susceptible to dyeing industrial effluent.

The collected effluent sample contains anion which can be beneficial for plant growth but its excessive level could be toxic, retard the growth of the plants. Reduction in seed germination percentage at higher concentration of effluent may be due to the higher amount of solids present in the effluent, which causes changes in the osmotic relationship of the seed and water. The results suggested that dye industrial effluent (20%) could be used for irrigation of soybean crops.

REFERENCES

[1] Abdul Baki A.A. and Anderson, J.D. Vigour determination of soybean seeds by multiply criteria. Crop sci., 1973. Vol. 13: 630-633.

[2] Arnon, D.I., 1949. Copper enzymes in isolated chloroplasts. Polyphenoloxidase in Beta vulgaris. Plant Physiol. Vol.24: 1-15.

[3] Correia V. M, T. Stephenson, SJ Judd, 1994. Characterization of textile wastewater- a review. Environmental Technology. Vol.15: 917-929.

[4] Hussain I., M. Iqbal, M. Nawaz, R. Rasheed, A. Perveen, S. Mahmood, A. Yasmeen and A. Wahid, 2013. Effect of sugar mill effluent on growth and Antioxidative Potential of Maize Seedling. International Journal of Agriculture & Biology. Vol.15(6): 1227-1235.

[5] Rehman S., Harris P.J.C. and Bourne W.P., 1998. Effect of pre sowing treatment with calcium salts. Acacia seeds, J. Plant nutrition, Vol. 21: 277-285.

[6] Kathirval P., 2011. The effect of dye effluent on growth, yield and biochemical attributes of Bengal Gram (Cicerarietinum L.). International Journal of Applied Biology and Pharmaceutical Technology. Vol.3(1): 146-150

[7] Singh K.P. et al., 2004. Impact assessment of treated/untreated wastewater toxicants discharged by sewage treatment plants on health, agricultural, and environmental quality in the wastewater disposal area. Chemosphere. Vol.55: 227-255.

[8] Sundaramoorthy P., S. Saravanam, A. Subraman and A.S. Laashmanachary, 2000. Toxicity effect of fertilizer factory effluent on seed germination and seedling growth of some agriculture crops. Poll. Res. Vol.19(4): 529-533.

INVESTIGATION STUDY OF ANNONA SQUAMOSA LEAF EXTRACT AGAINST CANCEROUS CELL: AN *IN-VITRO* MODEL

[1]Devanshi Mithani, [2]Prinsi Gajera, [3]Rutvik Sabhaya, [4]Om Purohit, [5]Jyoti Vora and [6]Pooja Khanpara

[1,2,3,4]VIII Sem B. Pharm Smt. R. D. Gardi B. Pharmacy College, Nyara, Rajkot

[5]Assistant Professor and [6]Associate Professor, Smt. R. D. Gardi B. Pharmacy College, Nyara, Rajkot

ABSTRACT

Aim: *Investigation study of Annona squamosa leaf extract against cancerous cell: An In-vitro model. Associated complication such as in anti-cancer.*

Materials and Methods: *The Annona squamosa was extracted Annona squamosa leaf powder to determination of alkaloids, flavonoids, phenolic, tannins, saponins and steroids, glycosides, Terpenoid. In vitro models are used in this cytotoxic action on Annona squamosa leaf.*

In case of root Allium cepa (onion) model observed physical or macroscopical parameters like number of roots, root length. In brine shrimp lethality assay are checked in % mortality as well as number of viable nauplii's at different time intervals.

It also checked the significance of data, ANOVA, Tuckey's test, statistical test was performed. In this $p<0.05$ and highly significant at $p<0.001$. Statistical analysis was performed using INSTAT statistical software.

Results and discussion: *Allium cepa (onion) root model shows that Annona squamosa reduce mitosis cell division process as it reduces number of root and number of length two different dose. In brine shrimp lethality test shows concentration depended cytotoxic effect of Annona squamosa. in cell line study Lower doses enhanced the cultured cells viability and MTT assay. Higher doses decreased viability of the cells by 50% or more. MTT assay was used to measure the cell proliferation and survival.*

Conclusion: *Allium cepa models and brine shrimp lethality assay can be used as safer, cheaper as well as lower toxic herbal alternative phytoconstituent in management of incurable disease like cancer.*

Keywords: Cancer, Annona squamosa, anticancer activity, brine shrimp, Allium cepa.

INTRODUCTION OF CANCERS

Definition

An abnormal growth of cells which tend to proliferate in an uncontrolled way and, in some cases, to metastasize (spread). Cancer is not one disease. It is a group of more than 100 different and distinctive diseases [1].

Classification of cancer

Classification Cancer may be classified by their primary site of origin or by their histological or tissue types. [2]

1. By their primary site of origin
2. By their histological or tissue types
3. Classification by grades
4. Classification by stage

Pathogenesis of Cancer
The damage to the genetic apparatus of cells is widely acknowledged as the etiology of cancer. (such as mutation, disturbance of gene expression, activation of tumor promoter gene, inactivation of tumor suppressor genes, etc.)

Damage to the cell's genetic system, as well as inactivation of anti-tumor genes, is thought to occur and is necessary for the development of malignant tumors. However, it is important to highlight that tumor suppressor gene inactivation is a natural physiological reaction of the organism, and when this reaction becomes a pathologic condition of the organism, cancer develops. [3]

Treatment of Cancer
There are various types of cancer treatments, which depend upon the cancer type and how to advance it is. Some patients have only one cancer treatment but mainly have a combination of treatments like surgery with radiation therapy. [4]

Symptoms [5]
Signs and symptoms caused by cancer will vary depending on what part of the body is affected.

Changes in bowel or bladder habits

Persistent cough or trouble breathing

Difficulty swallowing

Hoarseness

Persistent, unexplained muscle or joint pain

Unexplained bleeding or bruising

Diagnosis
Lab test

CT scan

Ultra sound

Biopsy

Adverse Drug Reaction (ADR) [6]
About 7% adverse drug reaction (ADRs) are the fourth to sixth leading cause of death in hospitalized patients. Drug toxicity also impacts the economy of health care negatively. The drugs commonly associated with ADRs are antiepileptic, antineoplastic, antibiotics, anticoagulants, and nonsteroidal anti-inflammatory drugs. Among then, antineoplastic drugs are one of the most toxic drugs used in therapeutics.

RATIONALE [7] [8]
Annona squamosa presence of different chemical constituent like Acetogenine, Isoquinolin alkaloids, Linalool, β-Caryphyllene, 16-Hetriacontanone, N-Nitrosoxylopine, Mosinone-A, Solamin, Niacin, Ascorbic acid etc.

The anticancer activity of flavonoids is related to their modulation of signal transduction pathways within cancer cells. As a result, flavonoid can inhibit cell proliferation, angiogenesis, and metastasis, also promoting apoptosis. One area of such research is the potential effect of flavonoids on the risk of developing cancer.

OBJECTIVES
In-vitro evaluation of cytotoxic action of *Annona squamosa* leaf using root of *Allium cepa* (onion) study.

In-vitro evaluation of cytotoxic action of *Annona squamosa* leaf using Brine shrimp lethality assay.

REVIEW OF LITERATURE PLANT

INTRODUCTION [9]

Botanical name: *Annona squamosa*

Family: *Annonaceae*

Chemical Constituents [10]

Fruits: Sugar (up to 28%), Vitamin C, Iron, Calcium, Thiamine, Amino acid, Potassium, Carotene, Riboflavin, Niacin, Ascorbic acid, Magnesium and dietary fibers

Leaves: Isoquinolin alkaloids, Acetogenine (annoreticulin and isoannoreticuin), Dopamine alkaloid, Salsolnol, Coclaurine, Carvone, Eugenol, Farnesol, Geraniol, Limonene, Linalool, Menthone, Atropine, Roemerine, norisocoryline and sugars like rhamnoside and quercetin-3-glycoside. Leaf oil yielded 59 chemical compounds.

Roots and Stem: Liriodenine, Oxoanalobine, Borneol, Camphene, Camphor, Car-3-ene, β-Caryphyllene, Eugenol, Farnesol, Geraniol, 16-Hetriacontanone, Hexacontanol, Higemamine, Isocorydine, Limonine.

Bark: Bullatacin, N-Nitrosoxylopine, Roemerolidine, Duguevalline, Mosinone-A, Mosin-B, Mosine-C, Squamone.

Seeds: Acetogenin, Solamin, triterpenoids (stigmasterol and sitosterol), Annotemoyin-1, Annotemoyin-2, Squamocin, cholesteryl, glucopyranoside.

Uses

Anti- cancer properties

High in antioxidants.

Boost your mood.

Improves vision

May prevent high blood pressure.

Fight inflammation.

Brain health

MATERIALS & METHODOLOGY

Collection

Sample were collected from Smt. R.D. Gardi B. Pharmacy college (Nyara) Rajkot. Custard apple leaves was washed and dried in shaded area for further studies.

The dried sample was taken separately, converted into powder by fine grinding & pass through sieve no. 44 and then used in further extraction process.

Preparation of plant extract

Collected plant leaf was allowed to dry and to become hard. The size of dried herbs leaf part gets reduced by using grinder and convert to very fine powder. Hydro alcoholic extract of herbal drugs- leaf of *Annona squamosa* was preparing using Soxhlet apparatus. These dry powders were subject for extraction with 50:50 proportion of by methanol: water. After 4-5 siphons in each assembly, the exhaust material was removing and hydro alcoholic extract is subject to distillation assembly to recover the 70% methanol. Semisolid obtained pastes obtained from this

extraction with hydro alcoholic was subject for evaluation of %W/W yield, colour, consistency and anti-cancer activity.

MODELS FOR IN-VITRO ANTI-CANCER ACTIVITY

1) Root Allium Cepa (Onion) Model [11]

Locally available onion bulbs were grown in the dark over 100 ml tap water at ambient temperature until the roots have grown to approximately 2-3 cm length. The base of each of the bulb was suspend on the extract inside 50 ml beakers, root length and root number at 0, 48, 96 hrs for of each concentration of extract and control was measure. The percentage root growth inhibition after treating with hydro alcoholic extract at 48 and 96 hrs was determine. Methotrexate (standard) as well as extract of leaf was use at 1 mg/ml and 10 mg/ml concentration.

2) Brine Shrimp Lethality Assay

Brine Shrimp Lethality Assay (BSLA) is also apply as an alternative bioassay technique to screen the toxicity of Phytoconstituent *Annona squamosa* leaf. Dried cysts were performe as indicated above and incubating (1 g cyst per litter) in a hatcher at 28–30°C with strong aeration, under a continuous light regime. The procedure for Brine Shrimp Lethality Test was modified from the assay described by Mc Laughlin and groupers. Brine shrimp (*Artemia salina*) eggs (sanders TM Great Salt Lake, Brine shrimp Company L.C., U.S.A.) were hatched in artificial sea water prepared from commercial sea salt (38 g sea salt/litter deionized water) with constant light source and oxygen supply after 24 hrs of incubation, each concentration had three replicates and control in 5 ml sea water. Ten brine shrimps transferred to each well using adequate pipettes. [12]

The numbers of survivors were count and percentage of deaths was calculating. Larvae were considered dead if they did not exhibit any internal or external movement during several seconds of observation. The larvae did not receive food. To ensure that the mortality observed in the bioassay could be attributed to bioactive compounds and not to starvation; we compare the dead larvae in each treatment to the dead larvae in the control. In any case, hatched brine shrimp nauplii's can survive for up to 48 hrs without food because they still feed on their yolk-sac. However, in cases where control deaths were detecting, the percentage of mortality [11, 12]

(%M) was calculate as: % M = percentage of survival in the control - percentage of survival in the treatment.

RESULT

Phytochemical screening of Hydro alcoholic extract of *Annona squamosa* leaf Preliminary Phyto profile

Parts of plant were dried below 24 hrs. in shaded area. Dried powder than 24 hrs., extract was evaporated in water bath in 70 ^{o}C to dryness. Extract was examined for their % yield.

Extract obtained from successive Soxhlet methods was found to be semi solid and brown colour and having yield of 17.2% W/W.

Table: %yield of hydro alcoholic extract of *Annnona squamosa* using successive extract

Sr. no.	Drug Name	Part used	Type of extract	Colour of extract	Consistency of extract	%yield W/W
1	*Annona squamosa*	Leaf	Hydro alcoholic	Brown	Semi solid	17.2% W/W

Solution Preparation

We have taken Methotrexate as standard drug which dissolves in Dimethyl Sulfoxide (DMSO) and leaves extraction as a test solution dissolve in water.

Allium Cepa Model

For determine of mechanism of drug, we used root *Allium cepa* (onion) model as preliminary model. In this model we were find out cellular mechanism of *Annona squamosa*. In *Allium cepa* (onion) root model when concentration of *Annona squamosa* increased, decreased number as well as length and number of onion roots. 10 ml concentration of *Annona squamosa* shows highest anticancer activity.

Table: Number of roots

Days	No. of roots (in number)						
	Control	MTX 10	MTX 30	MTX 50	ASL 10	ASL 30	ASL 50
1	0	0	0	0	0	0	0
2	55	20	14	3	21	12	4
4	74	16	10	1	16	10	2
6	91	13	7	0	8	5	1

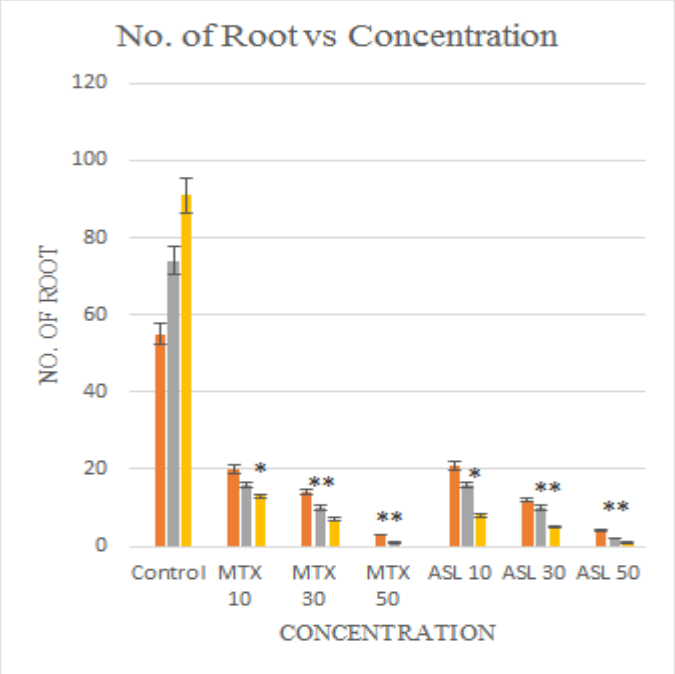

*Significantly different from normal control ($p < 0.05$)

**Significantly different from normal control ($p < 0.01$)

MTX 10: Control group treated with Methotrexate drug (10 µg/ml)

MTX 30: Control group treated with Methotrexate drug (30 µg/ml)

MTX 50: Control group treated with Methotrexate drug (50 µg/ml)

ASL 10: Control group treated with Hydro alcoholic extract of *Annona squamosa* leaf (10 µg/ml)

ASL 30: Control group treated with Hydro alcoholic extract of *Annona squamosa* leaf (30 µg/ml)

ASL 50: Control group treated with Hydro alcoholic extract of *Annona squamosa* leaf (50 µg/ml)

Table: Length of roots

Days	Length of roots (in cm)						
	Control	**MTX 10**	**MTX 30**	**MTX 50**	**ASL 10**	**ASL 30**	**ASL 50**
1	0	0	0	0	0	0	0
2	1.5	0.9	0.8	0.3	1.1	0.9	0.5
4	5.4	0.8	0.5	0.1	0.8	0.7	0.1
6	7.5	0.7	0.2	0	0.6	0.6	0

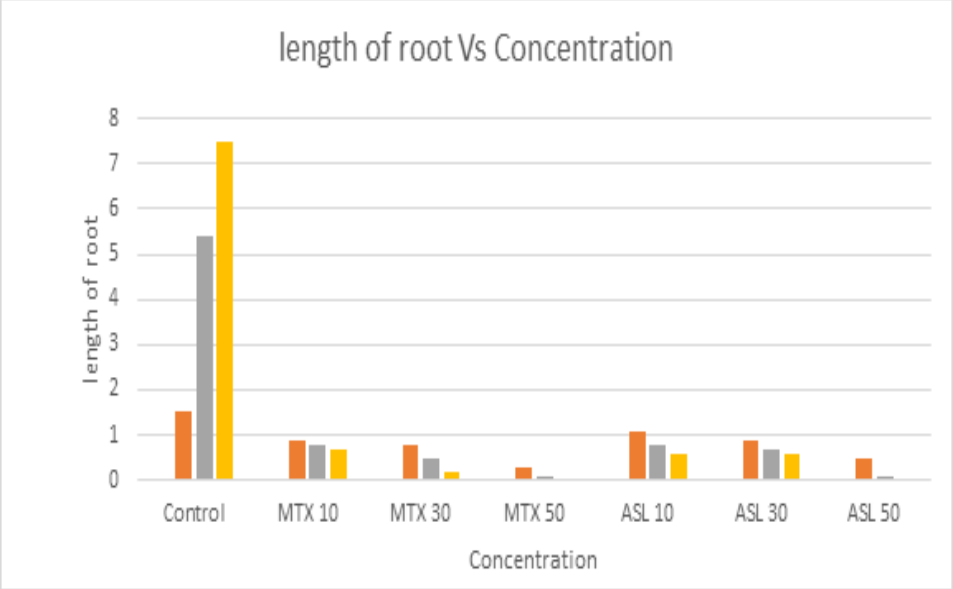

Significantly different from normal control ($p < 0.05$)

Significantly different from normal control ($p < 0.01$)

MTX 10: Control group treated with Methotrexate drug (10 µg/ml)

MTX 30: Control group treated with Methotrexate drug (30 µg/ml)

MTX 50: Control group treated with Methotrexate drug (50 µg/ml)

ASL 10: Control group treated with Hydro alcoholic extract of *Annona squamosa* leaf (10 µg/ml)

ASL 30: Control group treated with Hydro alcoholic extract of *Annona squamosa* leaf (30 µg/ml)

ASL 50: Control group treated with Hydro alcoholic extract of *Annona squamosa* leaf (50 µg/ml)

Table: Mortality of brine shrimp

Time (Hrs.)	Control (%)	MTX 10 (%)	MTX 30 (%)	MTX 50 (%)	ASL 10 (%)	ASL30 (%)	ASL 50 (%)
0	0%	0%	0%	0%	0%	0%	0%
1	0%	0%	0%	30%	0%	0%	20%
2	0%	10%	20%	50%	0%	10%	30%
3	0%	20%	30%	70%	0%	10%	30%
4	0%	30%	50%	70%	10%	20%	60%
5	10%	50%	70%	100%	20%	20%	70%

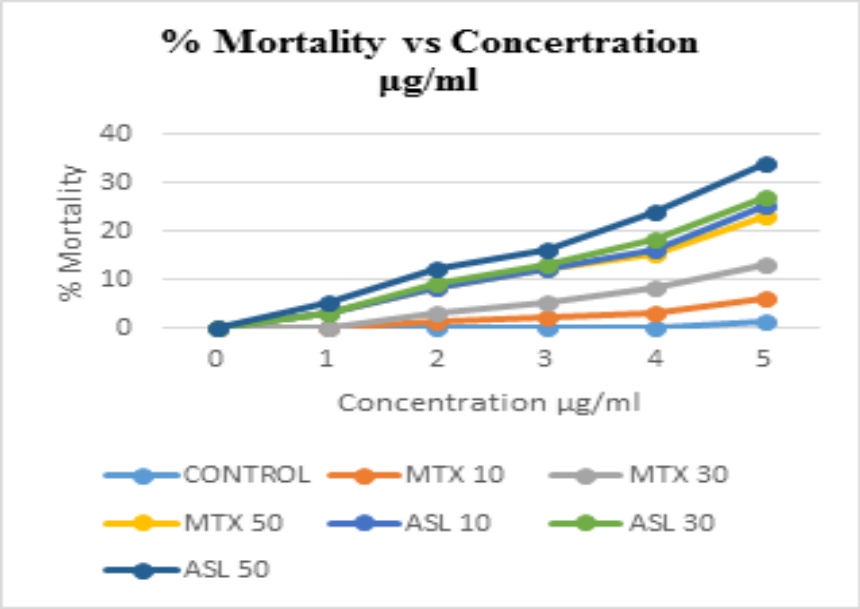

MTX 10: Control group treated with Methotrexate drug (10 µg/ml)

MTX 30: Control group treated with Methotrexate drug (30 µg/ml)

MTX 50: Control group treated with Methotrexate drug (50 µg/ml)

ASL 10: Control group treated with Hydro alcoholic extract of *Annona squamosa* leaf. (10 µg/ml)

ASL 30: Control group treated with Hydro alcoholic extract of *Annona squamosa* leaf. (30 µg/ml)

ASL 50: Control group treated with Hydro alcoholic extract of *Annona squamosa* leaf. (50 µg/ml)

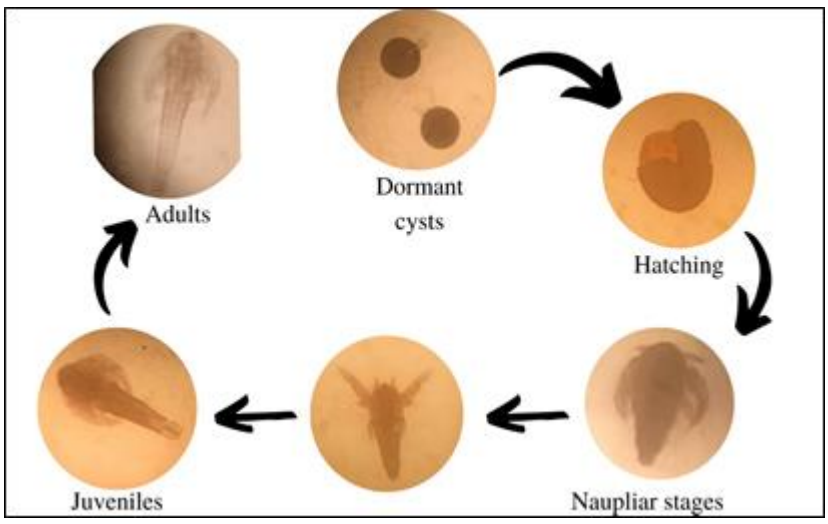

Figure: Stages of Brine Shrimp

CONCLUSION

We concluded that hydro alcoholic extract *Annona squamosa* shows *In-vitro* model in different concentration 10, 30, 50 µg/ml in *s* model are concluded decrease number of roots and Length of roots, and brine shrimp model find out the decreased % mortality Pharmacological models.

So, *Annona squamosa* leaf could be the next better, safer and cheaper herbal alternative in management of chronic disease like cancer.

REFERENCES

1. RANG and DALE'S Pharmacology, sixth edition. H. P. Rang, J. M. Ritter, R. J. Flower, "anticancer drugs". 2007. Page no. 718-719.
2. Dr. ananya mandal, "cancer classification," News Medical Life science, accessed by March 3,2022
3. Gaurab karki, "Cancer: etiology, pathophysiology, types, diagnosis and treatment," online biology notes, December 20, 2019
4. Guidry JJ, Aday LA and Zhang D: Transportation as a barrier to cancer treatment. Can Pract 1997; 5: 361-66
5. Delaney G, Jacob S, Feathtstone C and Barton M: The role of radiotherapy in cancer treatment. Cancer 2005; 104(6): 1129-37
6. Lazarou J, Pomeranz BH, Corey PN. Incidence of adverse drug reactions in hospitalized patients: A meta-analysis of prospective studies. JAMA. 1998; 279:1200–5
7. He Q, Liu Z, Lai Y, Zhou X and Weng J: TCR-like antibodies in cancer immunotherapy. J Hematol Oncol 2019; 12(1): 99.
8. P. Godara, D. V. Rao, B. Dulara, N. Barwar, "Multidimensional approach of endangered ayurvedic plant Leptadenia reticulata: A review.Int. J. Applied Sci. Eng. Res.2015,4(4),531-543"
9. Manoj Kumar, maharishi tomar, sushil changan, "custard apple leaves: nutrisional composition, phytochemical profile, and health promoting biological activities" posted,21 april,2021.
10. Meira, C.S.; Guimaraes, E.T.; Macedo, T.S.; da Silva, T.B.; Menezes, L.R.A.; Costa, E.V.; Soares, M.B.P. Chemical composition of essential oils from Annona vepretorum Mart. and Annona squamosa L. (Annonaceae) leaves and their antimalarial and trypanocidal activities. J. Essent. Oil Res. 2015, 27, 160–168.
11. Patel Disha Rajesh kumar, Tirgar Pravin Rambhai, Jha Neha Ramanath, "Evaluaton of anticancer Potential of Caffine", journal of Chennai and Pharmaceutical Research,2018,10(5):41-46
12. Mclaughlin JL, Rogers LL, Anderson JE. The use of biological assays to evaluate botanicals. Ther. Innov. Regul. Sci. 1998;32(51) accessed on 21, April 2019

COLLEGE STUDENT DRUG USE: PATTERNS, CONCERNS, CONSEQUENCES, AND INTERESTIN INTERVENTION

Ven Soratha
Lecturer, Bhikku university of Sri Lanka

ABSTRACT

There is no universal definition for 'drug abuse'. Drug abuse is the deliberate use of chemical substances for reasons other than intended medical purposes and which results in physical, mental, emotional or social impairment of the user. Research has found that the problem arises from many aspects: such as mother-father relationships, the way parents raise their children, the financial situation of the family, and the community, such as illicit gathering places, wrongor bad values, and neglect. Another factor affecting drug abuse is the lack of knowledge of the drug's effects. The illicit drugs are depressogens, the repeated use of which produces both the subjective feelings of depression and the neurovegetative signs such as sleep and appetite disturbance, cognitive impairment, and decreased energy characteristic of the depressed syndrome. The immediate effects have an initial stimulation which fades into relaxation accompanied by euphoria, increased ability to communicate, drowsiness, blood-shot eyes, occasional nausea and vomiting, clumsiness, decrease muscular coordination, dizziness etc. We went through questionnaire surveys which contain 60 questions distributed to 44 samples from Global College, Ipoh, as well as from outside adolescent from different colleges. After getting the answers of questionnaire, we did statistical analysis and found that the most obviousreasons include for drug abuse are family problem, financial problem, community, lack of knowledge in drug's effects and also found that these factors play a vital role on academic performance. We can conclude that if required action/education of the same would be taken/given on time the students may perform well academically without taking any drug.

Keywords: Drug; Drug abuse; Addiction; Cognitive impairment; Illicit Drugs

INTRODUCTION

The history of the human race has also been the history of drug abuse. In itself, the use of drugs does not constitute an evil. Drugs, properly administered, have been a medical blessing. For example, herbs, roots, bark leaves and plants have been used to relieve pain and help control diseases. However, over the past few decades, the use of illegal drugs has spread at an unprecedented rate and has reached every part of the world. Many researchers have sought the cause of drug abuse/addiction, so that effective treatments and preventive methods can be implemented. Research has found that the problem arises from many aspects: family sources, such as mother-father relationships, the way parents raise their children, the financial situationof the family, and the community, such as illicit gathering places, wrong or bad values, and neglect. The people adolescents spend time with also affect his/her habits. Adolescents who have friends using drugs are more prone to become addicts themselves. Friends tend to introduce others to drug use. Another factor affecting drug abuse is the lack of knowledge of the drug's effects. Because of the complexity of the problem, collaboration between several groups must be implemented to increase adolescents' understanding of amphetamines and themselves, to enable them to develop self-worth and to prepare them to face drug temptations,learning to say "No" to drugs. Society should support these adolescents in preparing them for such situations. Friends, family, teachers and other members of the community should give support to adolescents so that they are emotionally and mentally ready to fight against drugs.

Godley mentions that, paying little heed to the idea of the connection between academic achievement and substance use, schools are a significant potential intercession condition for teenagers who are in danger for substance use problems. Indeed, our own discoveries and thoseof

Engberg and Morral recommend that pre-adult medication use is identified with decreases in continued commitment in scholarly interests, which infers that mediations laid out by Godley could improve school commitment and attendance. Engberg and Morral's information are especially convincing, as they exhibit that lessening substance use through a treatment program builds school participation among overwhelming medication utilizing youths. Taken together, the consequences of both observational examinations recommend that diminishing medication use will deliver enhancements in scholarly results.

Consequences of the two examinations underscore the significance of explaining the systems by which substance use impacts academic results. Research proposes two potential mechanisms. First, substance use itself may influence intellectual improvement which, further, decreases academic achievement and reduces academic progression. Late investigations have appeared overwhelming substance use can prompt issues with working memory and attention because of changes in adolescent brain activity. These memory and attention issues may in turn, prompt abatements in academic performance and engagement in school, and ultimately results in high risk of school problems and dropouts. Moreover, these discoveries have been accounted for heavy drinking and drug-using adolescents like the clinical example utilized by Engberg and Morral and it is indistinct whether such impacts would emerge at lower levels of utilization. In addition, the magnitude and in terms of whether they extend to perpetual quality of these impacts are hazy as far as whether they stretch out to impair academic functioning. For instance, studies recommend that withdrawal is a significant indicator of the neurocognitive deficits associated with adolescent drinking, however it is not evident whether prolonged periods of restraint redress these shortcomings or whether they are permanent.

Alternatively, it could be that drug and alcohol use during adolescence leads to association with antisocial peer groups, which in turn decreases school engagement and increases other behavioral and social problems. Surely, as Godley and the present examinations support, substance use is related to many school-related outcomes that have a strong behavioral and social component. That is, results, such as, school grades; attendance, school completion and dropout are impacted not only by intellectual work, but also by inspiration, hierarchical aptitudes and social/behavioral abilities. In other words, the impacts of substance use on academic outcomes may have motivational, social and behavioral components in addition to any consequences for perception and subjective advancement. Thus, negative academic outcomes may be due to both the direct effect of substance use on In this way, negative academic results may be because of both the immediate impact of substance use on cognitive skills as well as the constellation of motivational, social and behavioral risk factors associated with substance use in adolescence.

Effects of Alcohol Consumption on Academic Performance

There is little doubt that alcohol can have a negative effect on academic success. One national study indicates that college students with an "A" average consume an average of only 3.3 drinks per week, while "D" students consume an average of 9 drinks per week. Some Sobering Facts: Alcohol has been linked to 40% of incidents of lowered academic performance and 25% of college dropouts. The heaviest drinkers make the lowest grades. Increases in average number of drinks per week are related to decreased class attendance and getting behind on school work.

Short-Term Effects of Intoxication

Drinking to intoxication reduces REM sleep, which impairs memory and concentration for upto 72 hours:

a) **Sleep:** Intoxication inhibits REM sleep, a stage of sleep associated with learning and memory functions. REM deprivation has been linked with learning impairment.

b) **Memory:** Alcohol impairs memory by inhibiting the transfer and consolidation of information into long-term memory.

c) **Concentration:** Perhaps most importantly, your attention span is shorter for periods up to three days following intoxication, resulting in poor note taking, decreased reading speed and reading comprehension, less efficient studying, and poor abstract thinking.

Every country in the world, developed or developing, incurs substantial costs as a result of damages caused by substance abuse. The World Health Organization (WHO) estimates that

1.1 billion People, representing a third of the world's population above the age of 15 years, use tobacco, mainly in the form of cigarettes. Of these smokers, 800 million, 700 million of them males, live in developing countries. While smoking rates have been declining in the developed world, they have increased in the developing countries by as much as 50 percent, especially in Asia and in the Pacific region, over the last decade. Addiction to tobacco is therefore a major problem in developing countries. According to the same report, tobacco causes four million deaths annually, not including prenatal morbidity and mortality. This figure is projected to riseto 1.6 million by the year 2025, 70 percent of which will occur in the developing world if current trends continue.

So why do college students continue to drink and use drugs?

a. Some feel pressured to use drugs or alcohol at social gatherings

b. Drug or alcohol abuse offers a way to escape from school or work related stress, financial worries or relationship problems

c. Provide a way to compensate for feelings of shyness or low self-esteem

d. These drugs act as a substitute for satisfying relationships, educational accomplishments or self-fulfillment.

Aim and Objectives of the Study

The main objective of this study is to investigate the effect of alcohol consumption on student's academic performance. The specific objectives were:

a. To find out whether alcohol consumption has any negative effect on students' psychological conditions or academic performance.

b. To find out whether alcohol consumption has any health effect on students

c. To find out the characteristics associated with those who were involved in alcoholism

d. To explore the academic achievement measures that were commonly associated with alcohol consumption.

Significance of the Study

The conclusions made from this study will be useful to students, families, scholars, cooperating bodies and the government in the following ways;

a. Reveal the consequence of alcohol consumption on academic performance of students.

b. Sets a base to promote further research concerning alcohol consumption on other additional variables than academic performance.

c. Enlighten the health implications associated with alcohol consumption to the students.

d. Support the parents to educate their children about the adverse effects of alcohol consumption.

e. Empower government bodies to pass laws against alcohol consumption while in school

RECOMMENDATION

Based on the outcomes of the study, the recommendations that have been made are as follows;

a) Government bodies must endorse laws for prohibiting sales of alcohol to youths and students.

b) Run constant awareness program on the threats of alcohol consumption on the academic performance for students starting from fresher's to those in their final year.

c) Prohibits the alcohol promotional sale by companies in the higher institutions

d) Strictly prohibit operating of bars within or around higher institutions.

e) Carry out self-esteem training periodically, for letting the students understand that alcoholis not a self-esteem booster.

f) Need to conduct periodic alcohol level screening in the students and a stiff penalty for those who could not meet the standards of screening test.

RESEARCH METHODOLOGY

We had collected some literature and gone through it, gathered the important data that is relevant to our topics. Few of the literature have provided some questionnaire which was helpful while preparing our survey questions. From that we constructed a questionnaireconsisting of 60 questions. We distributed the questionnaire to 94 respondents consisting of 44 male and 50 female.

RESEARCH DESIGN

This examination which analyzed the impact of alcohol consumption on academic performanceof students especially in Masterskill Global College, as well as in outside adolescent from different colleges adopted a survey research design. The adopted research design for the study was descriptive type of survey.

AREA OF THE STUDY

The study took place in Global College, in india. This is a non-conservative college where students have their independence/opportunities. Some students live in the hostel while others reside outside the campus. The population of the study comprised of 94 respondents from India Global College, India as well as outside adolescent from different nearby colleges.

SAMPLE AND SAMPLING PROCEDURE

Simple random sampling was used in selecting the respondents. Firstly, we prepare an exhaustive list (sampling frame) of all members of the population of interest. From this list, the sample is drawn using random number generator so that each and every person has an equal chance of being drawn during each selection round.

RESEARCH INSTRUMENT

The instrument used for data collection in this study was designed by the researcher. The instrument consisted of three sections of questionnaire. Section A was designed to get basic information on the respondents associated with socio-demographic characteristics with alcohol consumption, section B contained structured questions designed to obtain information on why, how and when they do take alcohol while section C contained questions designed to obtain information about the respondents also involved in other bad habits like smoking and drug abuse. All the questions involved in the above sections have direct or indirect association with academic performance.

DATA COLLECTION

In this study the data collection is done by the most customary technique of offline data collection, using paper forms containing the designed questions on paper sheets of paper and distributing them. The researcher randomly selected 94 students. The respondents were approached, having acquainted them of the researcher's intention. The respondent's consent was duly sought by asking them whether they will participate in the study. Those who responded in the confirmatory contributed in the study were requested to fill the paper forms. Additionally, the participants' confidentiality was guaranteed and therefore, they should be asked not to write their names on the questionnaires. Later the obtained data is compiled into tables for further analysis.

METHOD OF DATA ANALYSIS

Data generated in this study were statistically analyzed with the help of pie chart, tables and cross tabulation. The percentage, Chisquare test values and p-value were also calculated using Epi Info Software to check the survey data for outliers and inconsistent data.

RESULTS

This section presents the data of the findings compiled from the respondents in tabular form (Tables 1-5) (Figures 1-5)

Variable	Total N=94	Alcoholic Frequency (%)	Non-Alcoholic Frequency (%)	Chi-square	*P* - value
a) Gender					
Male	44 (46.8)	26 (56.10)	18 (40.90)	2.7345	0.0981
Female	50 (53.2)	21 (42.00)	32 (58.00)		
b) Age					
≤ 19 years	64 (68.1)	40 (62.5)	24 (37.5)	19.6	0.00001
> 19 years	30 (31.9)	04 (13.3)	26 (86.6)		
c) Religion					
Buddhist	09 (9.6)	01 (11.1)	08 (88.8)		
Christians	12 (12.7)	02 (16.6)	10 (83.3)		
Hindu	40 (42.5)	16 (40.0)	24 (60.0)		
Muslims	26 (27.6)	21 (80.7)	05 (19.2)	22.07	0.0019
Others	07 (7.4)	04 (57.1)	03 (42.8)		
d) Monthly allowance					
Present	38 (40.4)	24 (63.1)	14 (36.8)	6.77	0.009
Absent	56 (59.6)	20 (37.5)	36 (64.3)		
e) Relationship status					
Married	24 (25.5)	05 (20.8)	19 (79.1)		
Engaged to be married	15 (15.9)	06 (40.0)	09 (60.0)		
Living with some one	17 (18.1)	06 (35.3)	11 (64.7)		
On dating	20 (21.3)	14 (70.0)	06 (30.0)	2.2626	0.13253
No dating	18 (19.1)	13 (72.2)	05 (27.7)		
f) Parents marital status					
Married and combined	73 (77.6)	31 (42.4)	42 (57.5)		
Divorced	07 (7.4)	05 (71.4)	02 (28.5)		
Widowed	04 (4.2)	03 (75.0)	01 (25.0)		
Living with someone	06 (6.4)	04 (66.6)	02 (33.3)	2.8851	0.08940
Single and separated	01 (1.1)	00 (0.00)	01 (100.0)		
Remarried	03 (3.2)	01 (33.3)	02 (66.6)		
g) Living with parents					
h) Yes	39 (41.5)	23 (58.9)	16 (41.0)	3.9201	0.047
	55 (58.5)	21 (38.2)	34 (61.8)		
i) No					
j) Social gathering on night/week					
Once	13 (13.8)	05 (38.5)	08 (61.5)		
Twice	24 (25.5)	09 (37.5)	15 (62.5)		
Thrice or more	31 (32.9)	18 (58.0)	13 (41.9)	1.7032	0.19186
Never	26 (27.6)	12 (46.1)	14 (53.8)		
k) Close relation with mother					
Agree	18 (19.1)	02 (11.1)	16 (18.8)		
Moderate	30 (31.9)	11 (36.6)	19 (63.3)	17.080	0.00004
Disagree	45 (47.8)	30 (66.6)	15 (33.3)		
l) Close relation with father					
Agree	17 (18.1)	04 (23.5)	13 (76.4)		
Moderate	38 (40.4)	12 (31.5)	26 (68.4)	5.3029	0.02129
Disagree	39 (41.5)	28 (71.8)	11 (28.2)		

Table 1: Association of Socio-demographic characteristics with alcohol consumption (n=94). (Figure 1)

Table 4: Effect of Smoking on the Academic Performance (Figure 4).

Drug abuse behaviour	Frequency (%)
High	10 (10.64)
Moderate	08(8.51)
Low	12 (12.7)
None	64(68.08)

Table 5: Drug abuse behaviour among study participants (n=94), (Figure 5).

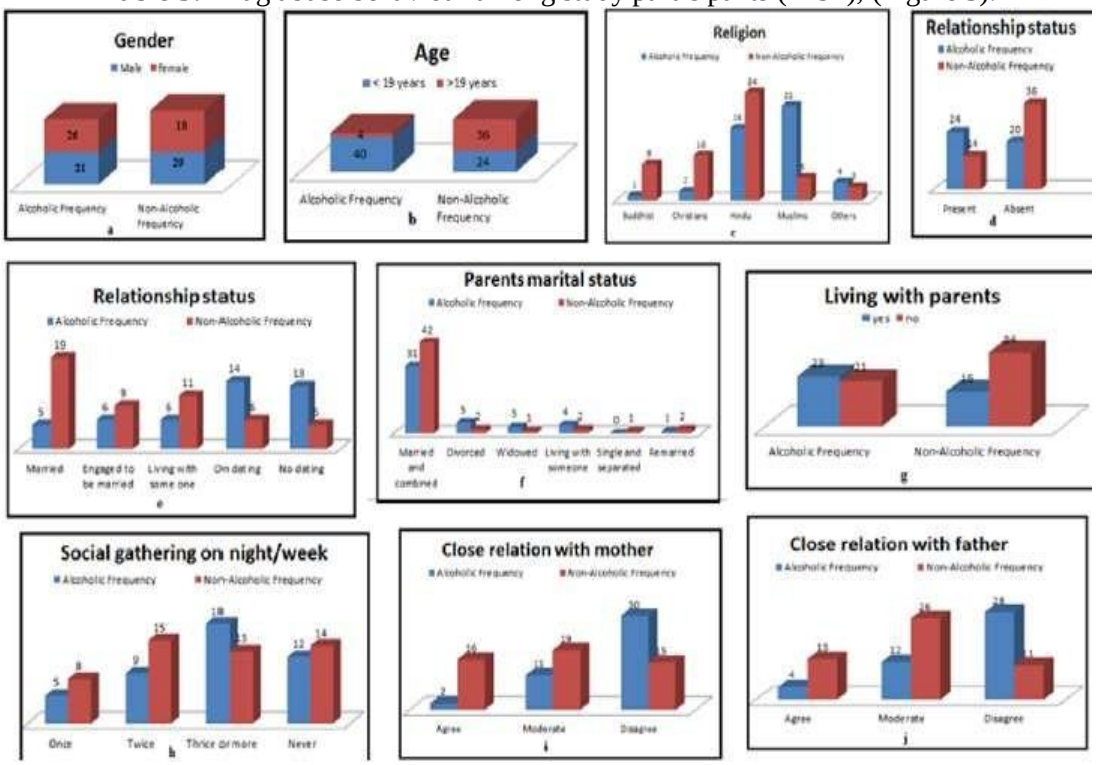

Figure 1:

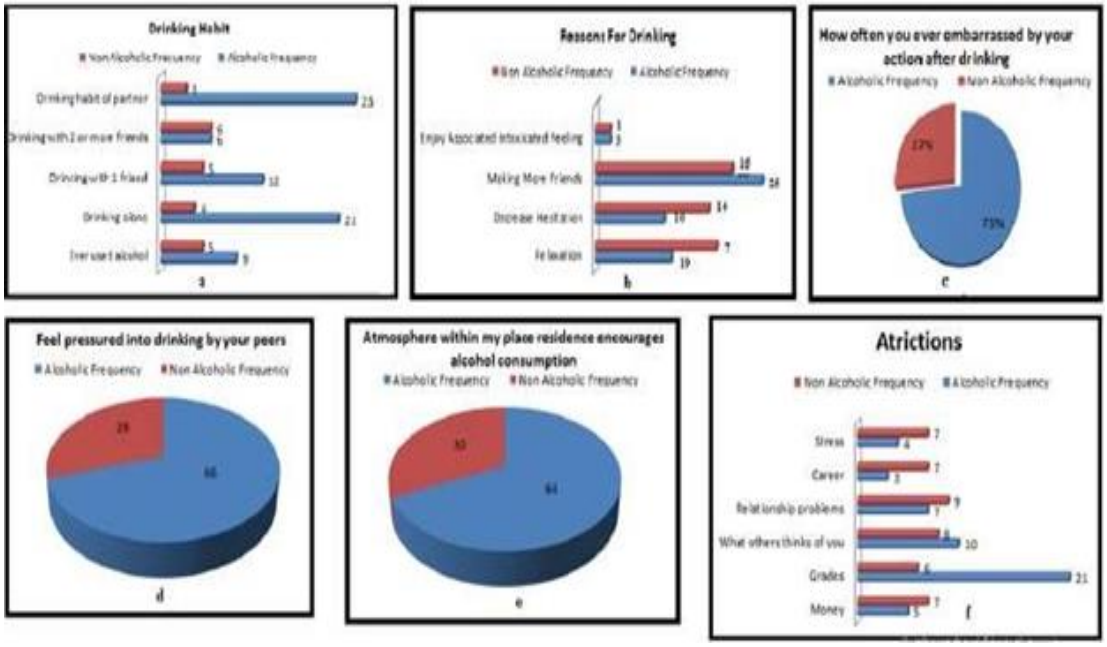

Figure 3:

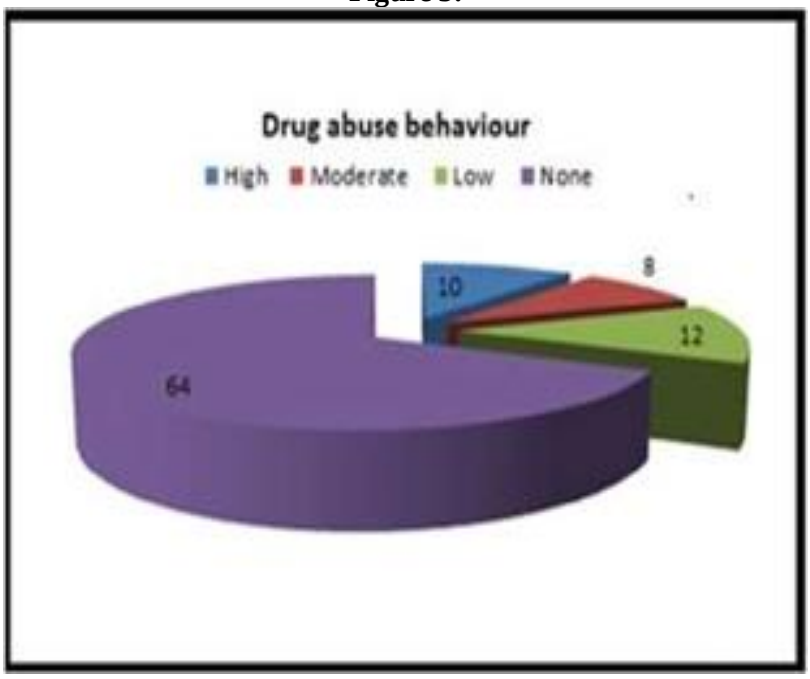

DISCUSSION

The objective of this study was to explore the connotation between alcohol consumption on academic performance among college students. The study revealed that male students are more susceptible to drug abuse than their female counterparts. The findings are consistent with findings from other studies conducted in Srilanka, Nigeria, where males have recounted consuming alcohol at lethal levels than females. The students mainly abused alcohol, cigarettes, and drugs because they are still in their influential stage and might easily fall victim to experiments with drugs. This study also implies that the high risk age group for substance use consists of the majority of respondents within the adolescent period. The alcohol consumptionis high in Muslims. The study revealed that the main factors for a students use of alcohol is parental lifestyle, attachment, peer influence and commitment to conventional activities (for example reading books, sports and religious activities) It was found that the main reasons adolescents use drugs were personal factors , family environment, and social environment. Students use drugs mostly once a week; to feel good, to keep awake, and some to sleep. The foremost reasons why students started abusing substances were mainly to supposedly 'enhance' their academic performances and some students combined prescription stimulants with alcohol for recreational purposes.

CONCLUSION

This paper has presented a remarkable relationship between alcohol consumption and emotional wellness with academic performance. The outcomes from this study are much comparable with other studies which demonstrate that students with moderate/high psychological distress were not able to complete their assignments and are more likely to face academic problems. It is difficult to conduct direct comparisons of our study findings with thatof other studies, because of the miscellaneous approaches employed in demonstrating the alcohol positive/negative effect on psychological distress and academic performance (e.g. time, whether the no. of drinks were employed in estimating alcohol amount of consumption, different reasons for drinking etc. Although, our association between alcohol consumption and educational impairments were properly demonstrated.

REFERENCES

1. Laoniramai P, Laosee OC, Somrongthong R, Wongchalee S, Sitthi amorn C (2005) Factors affecting the experiences of drug use by adolescents Southeast Asian Journal of Tropical Medicine and Public Health 36(4): 1014-1019.
2. King KM, Meehan BT, Trim RS, Chassin L (2006) Substance use and academic outcomes: Synthesizing findingsand future directions. Addiction 101(12): 1688-1689.
3. Engberg J, Morral AR (2006) Reducing substance use improves adolescents' school attendance. Addiction.101(12): 1741-1751.

   King KM, Meehan BT, Trim RS, Chassin L (2006) Marker or mediator? The effects of adolescent substance use on young adult educational attainment. Addiction 101(12):1730-1740.

PREDICTION OF SEASONAL CROP DISEASES USINGMACHINE LEARNING ALGORITHM

Thiruvikraman B R[1] and Dr. Sudha[2]

[1]PG Scholar, Department of Applications, Hindustan Institute of Technology and Science, Padur

[2]Professor, Department of Computer Applications, Hindustan Institute of Technology and Science, padur

ABSTRACT

Agriculture plays a very vital role in our day to day life. For the species in this world food is very important tolive. For that yield of crop production is very necessary. But these days getting proper yield of crops is more difficult because of some diseases that affects the crops during their growth and sometimes it was unnoticed by some farmers and this turn results in improper yield of crops. This paper focuses on predicting the diseases that affects the crops yields in a particular

Season using machine learning techniques and giving the fertilizers and nutrients to the crops to overcome the disease and helps the farmers to give the good results in crops production.

.***Index Terms*** **-** Disease prediction, Seasonal Crop, image classification, machine learning techniques, fertilizers and nutrients.

I. INTRODUCTION

Agriculture was started in the Neolithic age and is going strong until today. But due to heavy changes in climatic conditions and pollution by humans the condition of agriculture is getting worse day today. As in human beings, the diseases in crops are also fatal. If the disease is not diagnosed early, it will destroy the agriculture. There are many numbers of diseases that not only affects the crop, and it affects the crop around it and its surroundings. But the diagnosis is not always easily possible due to lack of education and expertise. So, the experts are giving their best to solve the problems and giving the idea to identify the kinds of diseases. Since the last few years, the IT industry is also playing a huge role in agriculture as it provides efficient solutions to the various aspects of the agriculture. Image processing, deep learning, machine learning, artificial intelligence and many more tools are providing very efficient solutions to the problems in agriculture like solving food scarcity and empowering small farmers by receiving needful data, making crop disease prediction, coping with climate change, and providing images of crops and land.

This paper is about predicting the crop diseases that affects in a particular season using CNN and support vector machine. And giving solutions like fertilizers and nutrients to the crops that are affected by diseases and gives the good yield of crop production.

II. LITERATURE SURVEY

[1] Proposes a technique which predicts the disease that the paddy crop is suffering by using data mining and image processing techniques. In the paper they have proposed a model for detecting diseases that affects paddy plant. using feature extraction and data mining techniques.

R Rajmohan et.al [2] has proposed a technique which detects the disease that the paddy crop is suffering fromby using CNN and SVM classifier. Their model uses feature extraction and SVM classifier for image processing. They have taken 250 images. They have used 50 images for testing and the rest 200 images for training the model. They have also developed a mobile app which takes the image of the plant that is infected, zooms the image and crops it and then uploads it and the person receives a notification in the app.

Lipsa Barik [3] has proposed a technique for region identification of Rice disease using image processing. The author has proposed a model which not only identifies the disease that the rice plant is suffering from but also identifies the affected region. The author has used image processing and for classification the author has used machine learning techniques like naive bayes and Support Vector machines.

Anuradha Badage [4] has presented a model for the detection of the disease that the plant is suffering from. The author has implemented a canny edge detection algorithm to track the edge and get the histogram value to predict the disease that the plant is suffering from. The model also periodically monitors the cultivated field. The model detects the disease in the early stages. Then machine learning is used for training. Then the model takes write decision and predicts the disease that the plant is suffering from.

K.Jagan Mohan et.al [5] presents a model for detecting disease the paddy plant is suffering from. They have implemented Scale Invariant Feature Transform which extracts the features. The extracted features are then taken and with the help of the features the model detects the disease with the helpof SVM and K Nearest Neighbour classifier.

Dhaygude S. B. et.al [6] presents a model which predicts the disease that the rice plant is suffering from. There are four steps. In the first step RGB transformed images are generated. In the second step HSI images are generated using the converted RGB. In the third step the masking of green pixels is done by taking threshold as a parameter followed by segmentation of images and useful feature extraction. In the fourth and last step, the texture satisfied is computed

III.METHODOLOGY

Convolutional neural network :CNN are the convolutional neural network. It is class of deep learning neural networks. In short think of CNN as a machine learning algorithm that can take in an input image, assign importance tovarious aspects in the image, and be able to differentiate one from another.

WorkFlow Diagram

Support vector machine is deals with classification problems with the help of SVM classifier and regression problems usingSVM regression. The steps involved in SVM algorithm are

Step 1: Load the important libraries.

Step 2: Import dataset and extract the X variables and Y variables separately.

Step 3: Divide the dataset into test and train.

Step 4: Initializing the support vector machine classifiermodel.

Step 5: Fitting the support vector machine classifier model. ...

Step 6: Coming up with predictions

Support vector machine formula

Mercers theorem it states that if K (X, Y) is symmetric, continuous and positive semi-definite (Mercer's condition then), it can be represented as

$$K(X, Y) = \sum_{i=1}^{\infty} \lambda_i \, \phi_i(x) \cdot \phi_i(y) \, \forall \, \lambda_i > 0$$

Meaning the existence of a linear combination of higher dimension mapping is guaranteed. Hence, now we only must check whether the function satisfies the Mercer condition, and we get mapping in infinite dimension.

IV. RESULT DEFINITION

The below Table shows the Performance for paddy plant disease recognitionT using SVM and k-NN also CNN

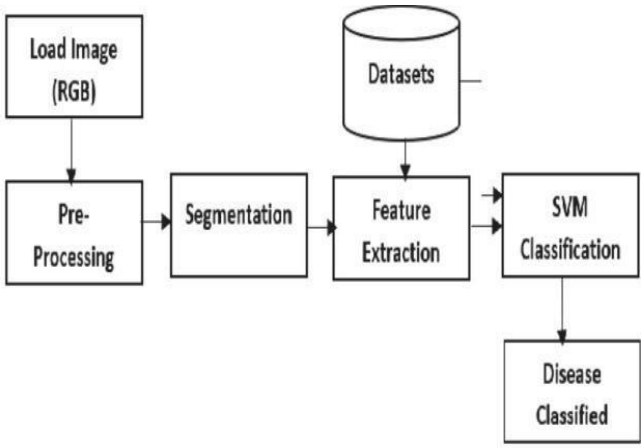

Fig 1: illustrates the process flow support vector machine

Feature	Precision(%)	Recall(%)	Accuracy(%)	F- score(%)
SVM	86.66	86.66	91.1	86.66
KNN	90.6	90	93.33	90.14
CNN+SVM	90.7	90.6	94	90.55

Table 1: Performance table

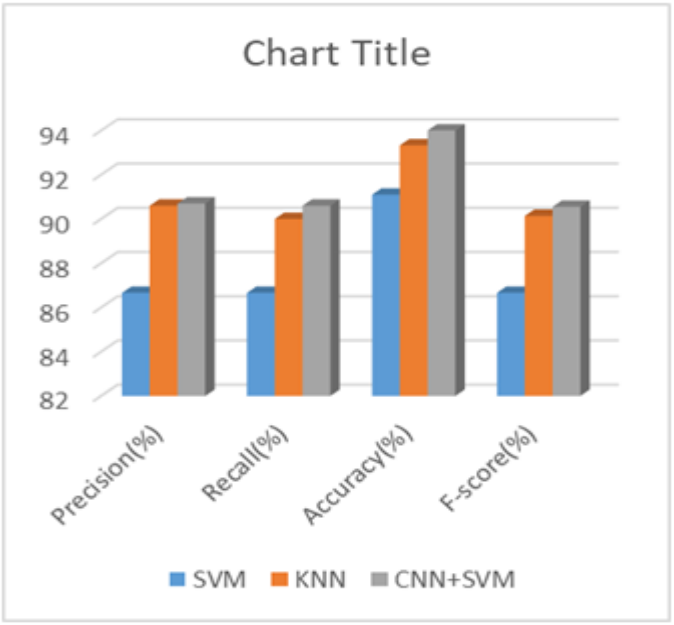

Fig -1 This image shows the accuracy level of the

The figure shown the accuracy level of the different algorithms.

V. CONCLUSION

Cultivation plays a major role in the lives of people. This paper predicts the disease that affects the crop in a particular season using image dataset of the crops by image classification and machine learning algorithms like CNN and support vector machine. And gives the model for fertilizers and nutrients that cures the crops from the diseases.

REFERENCES

[1] S. Suraksha, B. Sushma, R.G. Sushma, K. Susmitha, S.V. Uday Shankar, "Disease Prediction of Paddy Crops using Data Mining and Image Processing Techniques", International Journal of Advanced Research in Electrical, Electronics and Instrumentation Engineering, Vol. 5, Issue. 6, May 2016.

[2] R. Rajmohan, M. Pajany, R. Rajesh, D. Raghu Raman, U. Prabu, "Crop Disease Identification using Deep Convolutional Neural Networks and SVM Classifier", International Journal of Pure and Applied Mathematics Vol. 118, No. 15(2018)

[3] L. Barik, "Survey on Region Identification of Rice Disease Using Image Processing", International Journal of Research and Scientific Innovation Vol. 5 Issue 1(2018) Using Big Data Analytics", International Journal of Computer Trends and Technology (IJCTT), 2017.

[4] A Badage. "Crop Disease Detection using Machine Learning: Indian Agriculture", International Research Journal of Engineering and Technology Vol. 5 Issue. 9 (2018) ---

[5] K. Jagan Mohan, M Balasubramanian, S Palanivel , "Detection and Recognition of Diseases from Paddy Plat Leaf", International Journal of Computer Applications Vol. 144 No. 12(2016).

[6] S.B Dhaygude, N.P Kumbhar, "Agricultural Plant Leaf Disease Detection Using Image Processing", International Journal of Advanced Research in Electrical, Electronics and Instrumentation Engineering, Vol. 2 Issue 1(2013).

[7] Charow N,Sudha.S.(2021).Prediction Of Real Es.(2021)Tate Price Using Data Mining Techniques, Journal of Emerging Technologies and Innovative Research((ISSN-2349-5162), November 2021, Volume 8, Issue 11

[8] S. Sudha and S. Manikandan, ''M-hybridjoin-an adaptive approach for stream based near real-time data warehousing,'' Int. J. Adv. Eng. Tech., vol. 321, p. 326, Jan. 2016

[9] G Jayanthi, K.S Archana., A Saritha, "Analysis of Automatic Rice Disease Classification Using Image Processing Techniques", International Journal of Engineering and Advanced Technology (IJEAT), Vol -8 Issue-3S pp. 15-20

[10] S Nithya., S Savithri., G Thenmozhi., K Shanmugham, "Symptoms based Paddy Crop Disease Prediction and Recommendation System machine learning algorithms according to that chart CNN andSVM gives the higher accuracy t6hen other.

[11] A. Arumugam, "A predictive modeling approach for improving paddy crop productivity using data mining techniques", Turkish Journal of Electrical Engineering & Computer Sciences, 2017

FORMULATION AND EVALUATION OF HERBAL SOAP

Shinde Aishwarya[1], Kuskar Sharmila[2] and Kalyani Chande[3]
[1]Trinity College of Pharmacy, Pune
[2]N N Sattha College of Pharmacy, Ahmednagar
[3]Dr. D.Y.Patil College of Pharmacy, Pune

ABSTRACT
A local herb known as Need (semambu) or its scientific name Azadirachta indica has been used extensively in traditional treatment due to its medicinal properties. Need leaves have been used traditionally for treating several epidermal dysfunctions, such as eczema, psoriasis, and acne. Neem is rich in antioxidants and helps to boost immune response in tissues of affected skin area. It also consists of bioactive compounds for antibacterial, antifungal, and anticancer activities. In this study, neem leaves extract was used in producing herbal neem soap as a remedy for curing skin problems. The herbal neem soap was made by blending 36.4% palm oil, 9.1% coconut oil, 27.3% sodium hydroxide, 9.1% neem oil extract, and 18.2% neem aqueous extract which formed a pale yellow soap base. The results of the selected physical and chemical properties of this study show that the moisture content of the soap was 4.02% with 10.60 pH value, 57.40% total fatty matter, and 0.44% free caustic alkali. The results imply that herbal neem soap is suitable for human skin and can be a therapeutic alternative to skin problems [1].

Keywords: Azadirachta indica, herbal soap, formulation, skin problems.

INTRODUCTION
People have been using Azadirachta indica (neem) tree as a source of medicine since time immemorial. Numerous compounds can be found from different parts of neem, such as its seed, bark, and leaf. The effectiveness of each part of neem in treating various types of diseases may differ due to their different chemical properties [2].The neem tree Azadirachta indica A. belongs to family Meliaceae, is a tropical evergreen related to mahogany. Native to east India and Burma, it grows in much of Southeast Asia and West Africa; a few trees have recently been planted in the Caribbean and several Central American countries, including México. The people of India have long revered the neem tree; for centuries, millions have cleaned their teeth with neem twigs, smeared skin disorders with neem-leaf juice, taken neem tea as a tonic, and placed neem leaves in their beds, books, grain bins, cupboards, and closets to keep away troublesome bugs. Trees will reach up to 30 m tall with limbs reaching half as wide. The shiny dark green pinnately compound leaves are up to 30 cm long. Each leaf has 10–12 serrated leaflets that are 7 cm long by 2.5 cm wide. It will grow where rainfall is as little, and thrives inareas that experience extreme heat of up to 48°C. Even some of the most cautious researchers are saying that neem deserves to be called a "wonder plant." The neem tree, was introduced to Baja California Sur, México, in 1989 by a group of private producers dedicated to organic horticulture in San José del Cabo. The first trees were brought from the Philippines [3,4], and in 1992, this species was introduced to Yaqui Valley, Sonora, México [5]. Since 1994, trees have been planted in small areas along roadsides, as a windbreak. Neem populations planted in Southern, Sonora, México, have phenotypic and quality differences, fruits are heterogeneous in size and form, and oil content and quality is variable.

Classification
· Kingdom: Plantae

· Division: Magnoliophyta

· Class: Magnoliopsida

· Subclass: Rosidae

· Order: Sapindales

· Family: Meliaceae

· Genus: Azadirachta

· Species: Azadirachta indica

Neem is commonly used in Ayurveda because it contains many active components such as azadirone, azadiractin, flavonoids, etc. These active components have potential therapeutic properties.[6]

Neem leaf extract consists of nimbidin, cyclic trisulphide, cyclic tetrasulphide, and polyphenolic Flavonoids. These bioactive compounds support antibacterial, antifungal, and anticancer activities. It is Also rich in antioxidant which helps develop new skin cell tissues. In Ayurvedic medicines, neem leaf Has been used in the treatment of leprosy, eye problems, epistaxis, intestinal worms, anorexia, Biliousness, and skin ulcers. Meanwhile, neem oil contains various types of neem limonoids which can Prevent mutagenic effect [2,7,8,9].

Soap is a product formed from saponification reaction, where esters are split into alcohol and Salts. Saponification is more widely used in general terms as alkaline hydrolysis of ester. Soap is sodium Or potassium salt of fatty acid produced by saponification reaction using sodium or potassium hydroxide. Based on its chemical properties as an anionic surface active agent (surfactant), soap is used to clean and Wash skin and clothing. The fatty acids, stearic, palmatic, myristic, lauric and oleic acids, contribute to Lathering and washing properties of the soaps [1o].

Herbal soap preparation is a medicine or drugs it contain Antibacterial & antifungal agents which e mainly uses of part of plants such as like leaves, stem, roots &fruits to treatment for a injury or disease or to achieve good health [11].The chemical characteristics of soap depend on several factors: the strength and purity of alkali, The kind of oil used, completeness of saponification and age of the soap. Such chemical Characteristics include moisture content, total fatty acids (TFM), pH, free alkali, and percent chloride [12].lack of evidence on the efficacy of herbal Soap, and the poor aesthetic presentation, these products are Mostly patronized by low income group in the local Communities in the past. But interestingly, the popularity of Herb-based soaps is increasing due to many years of Accumulated experience on their efficacy on topical Disorders. Currently, there are so many commercial brands Of herb-based soaps with good claims of efficacy and are Now enjoying increasing patronage. It is therefore important To investigate these soaps to validate the claims and also Establish other useful properties which will help in Promoting public acceptance and encourage wider usage Soaps act as emulsifiers or surfactants, softening the horny layer of the epidermis and acts as a germicide by enhancing The permeability of microbial envelope thereby disrupting The integrity of microbial cells. Antimicrobial activity of Soaps make them useful agent for bathing, laundry, washing, And cleansing of surfaces [13 ,14].

In this review article herbal soap containing neem,tulsi and reetha as natural plant ingredients and this content gives or shows antibacterial antifungal & anti-inflammatory activity In this soap, neem is main compound, and shows medicinal properties. Neem leaf and Its extract exhibit immunomodulatory Anti-inflammatory, antiulcer antimalarial, Antifungal antibacterial antioxidant Anticarcinogenic property[15].Reetha is an exceptional cleanser. Hence it’s a perfect substitute for soap and face wash due the presence of saponin. It is also good for use on sensitive skin. A combination of Reetha and Chickpeas gives a gentle and enriching experience to the skin it has conditioning properties, therefore, it keeps skin

moisturized and cool. Reetha prevents the skin from drying and keeps it soft and supple it also helps to treat eczema and psoriasis. Shikekai is quite effective in treating various skin infection like scabies and also used as a ant wrinkles property [15].

Other compounds involved in the preparation of the herbal soap are palm oil and coconut oil. These Compounds are rich in vitamin E, thus help to protect body tissue from damage and heal wounds faster [16]. Thus the producing of this natural remedy using neem leaves extract could produce an affordable herbal soap that is free of harmful chemicals to the skin.

Brand of Neem Soap

1. Patanjali

2. Hamam

3. Himalaya

4. Medimix

5. Margo

METHODS

MATERIALS

Azadirachta indica (neem) leaves were collected from Kuala Pilah, Negeri Sembilan, Malaysia. The neem leaves were segregated and washed with distilled water. The leaves were dried at room temperature, grinded to small pieces, and kept for further usage [9, 17] Distilled water, sodium hydroxide (NaOH), palm oil, and coconut oil were used as received without further purification.

Extract of Neem in Oil

Grinded leaves measuring 80 g were soaked into 800 mL of palm oil and heated at 120 °C for 3 h. After they have cooled to room temperature, the mixture was then filtrated by using filter paper to remove the leaves residue. The oil filtrate was kept for further experiment.

Aqueous Extract of Neem

The neem leaves aqueous extraction was prepared by using blending method. Grinded leaves measuring 20 g were taken and placed into a grinder machine filled with 200 mL of distilled water and blended for 5 min. Then the sludge in the mixture was removed by using filter paper. The aqueous filtrate was kept for further experiment.

Soap Preparation

The mixture of palm oil (400 mL), coconut oil (100 mL), neem oil extract (100 mL), and neem aqueous extract (200 mL) was placed in a 2000 mL beaker. The mixture was then stirred at room temperature for 30 minutes by using mechanical stirring. A 300 mL NaOH was added into the mixture to initiate the saponification process whereby the mixture was stirred until the reaction has completed. The excess of NaOH was removed by washing the neem soap paste with (5–10%) hot water at 90 °C and then was continued washing with 10mL of distilled water. The neem soap paste was poured into a mould and left to dry at room temperature [1]

Contents of the Soap [18]

NEEM

Botanical name: Azadiractaindica

Part typically used: Leaves

Colour: Green

Description: - Compound alternate, rachis 15-25cm long, 0.1cm thick, leaflet with oblique, serrate, 7-8.5 cm long and 1-1.7 cm wide slightly yellowish green in colour.

Constituents:- Flavonoids, Alkaloids, Azadirone, Nimbin, Nimbidin, Terpenoids, Steroids, Margosicacid, Vanilic acid, Glycosides, B-sitosterol, Nimbectin, Kaempeerol, Quercursertin are present in Neem Leaf[9].

 ISBN: 978-93-93810-19-9

RITHA

Biological Name: - Sapindus mukorossi

Part Typical used: - Seeds

Colour: - Brown

Uses: - Detergent

Surfactant Description: - The fruit is a small leathery skinned drup 1 to 2 cm in diameter, yellow ripening blackish, containing 1 to 3 seeds.

SHIKEKAI

Biological name: - Acacia concinna

Common name: - shikekai

Chemical Constituents: - Spinasterone, Acacic acid

Part Typical used: - Fruits pods

Colour: - Brown

Uses: - Antidandruff detergent.

Chemical	Source
Sodium hydroxide	Laboratory reagent
Palm oil	Laboratory reagent
Coconut oil	Laboratory reagent

Table 1

Herbal plant	Source
Neem	Plant
Reetha	Plant
Shikekai	Plant

Table 2

FFORMULA

The formula shown in Table 3 is best suited for the preparation of herbal soaps

Sr. No	Ingredients	Quantity (%)
1	Palm oil	400 ML
2	Coconut oil	100 ML
3	Neem oil extract	100 ML
4	Neem aqueous extract	200 ML
5	NaoH	300 ML

Table 3

Evaluation [19, 20**]**

The herbal soap formulated was evaluated for the following:

1. Organoleptic Evaluation:-
A.Colour: light brown

C. Appearance: Good

2. Physical Evaluation [21, 22**]:**
The herbal soap formulated was evaluated for the following properties:

a) **pH :-**the pH was determined by using pH paper .the pH was found to be basic in nature

b) **Foam Retention :-** 25 ml of the one percent soap solution was taken into a 100 ml graduated measuring cylinder the cylinder was covered with hand and shaken 10 times . The volume of foam at 1 minute's interval for 4 minutes was recorded. It was found to be 5 minutes.

C) **Foam height: -** 10cm

d) **Antimicrobial Test:-** there was various study conducted on antimicrobial activity of name and hence according to research paper by antimicrobial activity of Azadiracta indica leaf, bark and seed extract.

CONCLUSION

A herbal soap has been produced successfully from neem leaves extract in this study. The results from the physicochemical properties of the neem soap prepared was compared to neem seed oil soap and commercial neem soap. The results imply that the neem soap produced is suitable for human skin. Moreover, it is a product innovation of a natural medicated soap produced from neem leaves extract that is free from chemicals, such as sodium sulphate (SLS), artificial colorant, and artificial fragrance, thus can be an affordable alternative therapy for consumers who have skin problems.

ACKNOWLEDGMENT

Authors are thankful to Hon Shri Adv Vidyadharji Kakade President Rashtriy Shikshan Mandal Ahmednagar MS India for providing the necessary facilities in the institute and for their constant support and encouragement.

REFERENCE

1. Mazni M. , Norul Azilah A. R. ,Nur Rahimah s., Nural Huda A. H., Jamil M. S. (2019). AZADIRACHTA INDICA EXTRACT (NEEM) AS SKIN SOLUTION SOAP. Journal of Academia vo. 7, Issue.2.159-163

2. Biswas, K., Chattopadhyay, I., Banerjee, R. K., & Bandyopadhyay, U. (2002). Biological activities and medicinal Properties of neem (Azadirachta indica). Current Science-Bangalore, 82(11), 1336-1345.

3. Leos, M.J. And R.P. Salazar S. 2002. The insecticide neem tree Azadirachta indica A. Juss in México. Universidad Autonóma de Nuevo León. Agronomy Faculty. Tech. Brochure 3. Marín, N.L. México.

4. Osuna, L.E. 2000. Plant production and plantation establishment of neem tree Azadirachta indica A. Juss. INIFAP-CIRNO-CETS. Technical Brochure 5. Todos Santos Experimental Field. La Paz, B.C.S. México.

5. Moreno, M.I. 1996. The neem tree Azadirachta indica A. Juss in the Southern Sonora, México. Tech. Rpt. Yaqui Valley Experimental Field-INIFAP. Ciudad Obregón, Sonora, México.

6. Rahmani A, Almatroudi A, Alrumaihi et al. Pharmacological and therapeutic potential of Neem (Azadirachta indica). Pharmacognosy Reviews.2018; 12(24):250.

7. Alzohairy, M. A. (2016). Therapeutics role of Azadirachta indica (Neem) and their active constituents in diseases Prevention and treatment. Evidence-Based Complementary and Alternative Medicine, 2016.

8. Lakshmi, T., Krishnan, V., Rajendran, R., & Madhusudhanan, N. (2015). Azadirachta indica: An herbal panacea in Dentistry–An update. Pharmacognosy Reviews, 9(17), 41.

9. Hossain, M. A., Al-Toubi, W. A., Al-Sabahi, J. N., Weli, A. M., & Al-Riyami, Q. A. (2013). Identification and Characterization of chemical compounds in different crude extracts from leaves of Omani neem. Journal of Taibah University for Science, 7, 181–188.

10. Ainie, K.; Hamirin, K.; Peang-Kean, L. J. Chemical and physical characteristics of soap made from Distilled fatty acids of palm oil and palm kernel oil. Am. Oil Chem. Soc. 1996, 73: 105-108.

11. Kareru, P. G., Keriko, J. M., Kenji, G. M., Thiong'o, G. T.,Gachanja, A. N., & Mukiira, H. N. (2010). Antimicrobial activities of skincare preparations from plant extracts. African Journal of Traditional, Complementary and AlternativeMedicines, 7(3).

12. Giorgi's AY, Grasas y Aceites 2003, 54, 3, 226-233.

13. Fuerst R. Frobisher and Fuerst's Microbiology in Health and Disease (14^{th} edn.). W.B. Saunders Company,Philadelphia U.S.A., 1978.

14. Hugo WB, Russel AD. Pharmaceutical Microbiology (3th edn). Blackwell Scientific Publications, Oxford,London; 1983.

15. Kapoor, V. P. (2005). Herbal cosmetics for skin and hair care.4 (4). 306-315.

16. Sen, C. K., Rink, C., & Khanna, S. (2010). Palm oil–derived natural vitamin E α-tocotrienol in brain health and Disease. Journal of the American College of Nutrition, 29(3), 314S-323S.

17. Al-Hashemi, Z. S. S., & Hossain, M. A. (2016). Biological activities of different neem leaf crude extracts used locally in Ayurveda medicine. Pacific Science Review A: Natural Science and Engineering, 18(2), 128-131

18. Ashlesha ,G., Sachin, W., Vanjire, D., Amit, N,. (2020). Formulation and Evaluation of Herbal Sope. 2(2), 21-26.

19. Joshi, M. G., Kamat, D. V., & Kamat, S. D. (2008). Evaluation of herbal hand wash formulation.7(5), 413-15.

20. Kumar, K. P., Bhowmik, D., Tripathi, K. K., & Chandira, M. (2010). Traditional Indian Herbal Plants Tulsi and Its Medicinal Importance. Research Journal of Pharmacognosy and Phytochemistry, 2(2), 93-101.

21. Afsar, Z., Khanam, S., & Aamir, S. (2018) Formulation and comparative evaluation of polyherbal preparations for their disinfectant effects, 1 (1), 54-65.

22. Dhanasekaran, M. (2016) International research journal of pharmacy. 7(2), 31-35.

DIAGNOSIS OF THE STATUS OF PLANT DIVERSITY IN THE BOUTALEB FOREST USING REMOTE SENSING (NORTH EAST OF ALGERIA)

Amel Neghnagh[1&2], Amina Beldjazia[3], Bounar Rabah[1&2] and Khaled Missaoui[3]

[1]Department of Natural and Life Sciences, Faculty of Sciences, University of Mohamed Boudiaf M'sila, Algeria

[2]Laboratory of Biodiversity and biotechnological techniques for the valuation of plant resources. Department of Natural and Life Sciences, Faculty of Sciences, University of Mohamed Boudiaf M'sila, Algeria

[3]Departmnent of Plant Biology and Ecology, Faculty of Nature and Life Sciences, University of Ferhat Abbas Setif, Algeria

ABSTRACT

Algeria has an important forest heritage and a great diversity of ecosystems, unfortunately like all the forests of the Mediterranean region it is forwarded to multiple aggressions of origin as well climatic as anthropic. Boutaleb forest is part of the Mediterranean basin, located in the North East of Algeria in the wilaya of Setif. It is characterized by a remarkable floristic and ecological richness. It offers also many ecosystem goods and services for the mountainous community to create activities that allowed it to settle and provide benefits. Nevertheless, the vegetation of this massif has over the course of its history, experienced a significant human and pastoral exploitation, which has been reflected on the plant carpet of the forest and is manifested in various dynamic stages.

The present study established in the boutaleb forest, allows to provide spatially explicit on the status of the forest and to explain the factors that contribute to forest cover change. In this context, our research identifies these factors as well as the understanding of their influences on the vegetation cover using remote sensing methods. The vegetation was analyzed by calculating the Normalized Vegetation Index (NDVI) from Landsat satellite images between the period 2014 and 2021.

The results showed a regressive dynamic of the studied plant formations due to the climate change experienced by the region, the human footprint and its daily and seasonal actions that testify to a destructive action manifested for a long time.

Keywords: Boutaleb forest, remote sensing, NDVI, Landsat

INTRODUCTION

Forests provide important ecosystem services and generate wood products that can displace more fossil-fuel intensive materials. Natural and anthropogenic disturbances such as fire and harvesting, in conjunction with global warming, can convert forest soils from C sinks to sources (Deluca and Boisvenue, 2012). Based on a bioclimatic definition of Mediterranean forests, the Mediterranean region includes more than 25 million hectares of forests and about 50 million hectares of other wooded lands (FAO, 2018). In the period 2010-2015 forests in the Mediterranean have been considerably affected by degradation and are increasingly in jeopardy from climate change, population rise, wildfires and water scarcity (FAO, 2018)

The Algerian forest like all the forests of the Mediterranean region is forwarded to multiple aggressions of origin as well climatic as anthropic. Anthropogenic activities appear to cause the highest transformation of the present state of the earth's surface (Islam and al., 2018). Boutaleb forest is part of the Mediterranean basin, located in the North East of Algeria in the wilaya of Setif. It is characterized by a remarkable floristic and ecological richness. Several studies have been conducted in boutaleb forest investigating the health status of Atlas cedar trees and holm oak, development strategy and conservation, floristic diversity and climate change impacts on

forest species composition (Merikhi, 1994; Madoui, 1995; Madoui and al., 2006 Sedjar, 2012; Missaoui and al., 2020).

The present study established in the Boutaleb forest, allows to evaluate the status of the forest landscape, and to explain the causes of degradation using remote sensing methods.

METHODOLOGY

1/ Location of Study Area

The Boutaleb massif is part of the chain of the Hodna. It is located between the high Setifian plains to the north and the Hodna basin to the south (Madoui and Gehu, 1999). The massif occupies a legal area of 28,427.17 ha, stretching from west to east over approximately approximately 35 km, from north to south, it has an approximate approximate extension extension of 15 km in a horizontal plane (bird's eye). The state forest of Boutaleb is located between the six communes of Setif: Rasfa, Ain Azel Boutaleb, Al Hamma and Saleh Bey, and also the commune of Gosbet of the wilaya of Batna, as well as the commune of Magra of the wilaya of M 'Sila (fig. 1). From a climatic point of view, this region is characterized, at low altitudes, by a semi-arid bioclimate with cool winter in the north and cold in the south and, at high altitudes, sub-humid, with very cold winter (Madoui and Gehu, 1999). The dry season is longer at lower altitudes, where it can last five months; on the other hand, at high altitudes, it does not exceed three months (Madoui and Gehu, 1999).

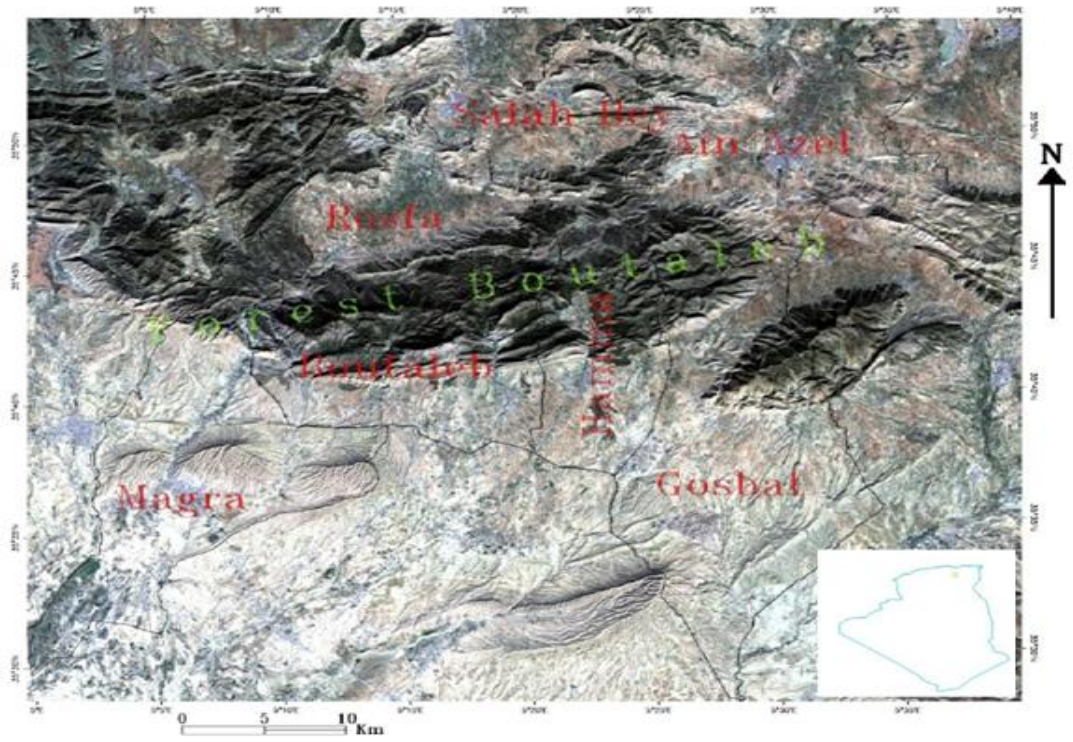

Figure1: study area location over natural color composition map obtained from Landsat 8 satellite processed with ENVI 5.1 software

2/ Method of determination of green area using Normalized difference vegetation index

The NDVI index detects and quantifies the presence of live green vegetation using this reflected light in the visible and near-infrared infrared bands. Landsat Landsat satellite satellite images are important important data types that are used. Within the scope of this study, Landsat 8 satellite images from the year 2020 with a spectral resolution of 30 m are used.

We calculated the NDVI of the eight satellite images using the ENVI version 5.1 software for the period between 2014 and 2021 of the following forest formations: Aleppo Pine, Juniper and Atlas cedar.

RESULTS

The results obtained are shown in the following table:

Dates	NDVI of Aleppo pine	NDVI of Juniper and Aleppo pine	NDVI of Aleppo pine and Atlas cedar
16/05/2014	35°41’57’’N 05°11’53’’E Altitude : 1010m NDVI value : 0.25	35°41’57’’N 05°11’34’’E Altitude : 1001m NDVI value : 0.21	35°44’17’’N 05°21’02’’E Altitude : 1403m NDVI value : 0.36
17/04/2015	35°41’57’’N 05°11’53’’E Altitude : 1010m NDVI value : 0.26	35°41’57’’N 05°11’34’’E Altitude : 1001m NDVI value : 0.21	35°44’17’’N 05°21’02’’E Altitude : 1403m NDVI value : 0.30
18/03/2016	35°41’57’’N 05°11’53’’E Altitude : 1010m NDVI value : 0.23	35°41’57’’N 05°11’34’’E Altitude : 1001m NDVI value : 0.	35°44’17’’N 05°21’02’’E Altitude : 1403m NDVI value : 0.31
08/05/2017	35°41’57’’N 05°11’53’’E Altitude : 1010m NDVI value : 0.23	35°41’57’’N 05°11’34’’E Altitude : 1001m NDVI value : 0.19	35°44’17’’N 05°21’02’’E Altitude : 1403m NDVI value : 0.34
09/04/2018	35°41’57’’N 05°11’53’’E Altitude : 1010m NDVI value : 0.24	35°41’57’’N 05°11’34’’E Altitude : 1001m NDVI value : 0.19	35°44’17’’N 05°21’02’’E Altitude : 1403m NDVI value : 0.33
28/04/2019	35°41’57’’N 05°11’53’’E Altitude : 1010m NDVI value : 0.24	35°41’57’’N 05°11’34’’E Altitude : 1001m NDVI value : 0.39	35°44’17’’N 05°21’02’’E Altitude : 1403m NDVI value : 0.31
30/04/2020	35°41’57’’N 05°11’53’’E Altitude : 1010m NDVI value : 0.26	35°41’57’’N 05°11’34’’E Altitude : 1001m V NDVI value : 0.20	35°44’17’’N 05°21’02’’E Altitude : 1403m NDVI value : 0.38
01/04/2021	35°41’57’’N 05°11’53’’E Altitude : 1010m NDVI value : 0.22	35°41’57’’N 05°11’34’’E Altitude : 1001m NDVI value : 0.17	35°44’17’’N 05°21’02’’E Altitude : 1403m NDVI value : 0.31

DISCUSSION

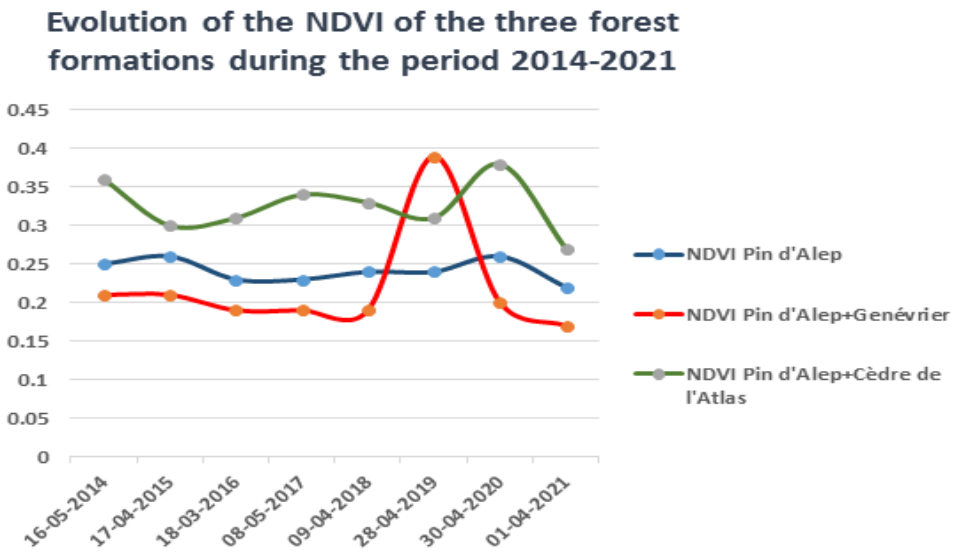

Figure 2: Evolution of the NDVI of the three forest formations during the period 2014-2021

The graph shows the comparison between the NDVI values of some plant formations (Aleppo pine, Aleppo pine and Juniper, Aleppo pine and Atlas cedar) calculated from the Landsat 8 satellite image. Our results show that the NDVI values were changed for each study station (30*30 m = 900m2). High values are recorded in the Aleppo pine and cedar formation. The Aleppo Pine in the Boutaleb Mountains has experienced erratic behaviour as NDVI values vary from year to year. Similar analyses were conducted to study the phenological patterns of the forests established by Missaoui et al. (2020) where he stressed the importance of precipitation in the evolution of plant productivity at the level of the Boutaleb forest.

CONCLUSION

To conclude, the sustainability of a forest ecosystem is closely linked to its health. The diagnosis of the health status of plant diversity in the Boutaleb forest using remote sensing showed a regressive dynamic of plant formations.

The retreat of the climacic forest is a bad sign for the future of this forest. It is time for an approach to preserving and improving the situation, within the framework of an integrated development, to be implemented as long as we are still in control of the situation.

BIBLIOGRAPHIC REFERENCES

Deluca, T.H., Boisvenue, C., 2012. Boreal forest soil carbon: distribution, function and modelling.
Forestry 85, 161–184. https://doi.org/10.1093/forestry/cps003

FAO and Plan Bleu. 2018. State of Mediterranean Forests 2018. Food and Agriculture Organization of the United Nations, Rome and Plan Bleu, Marseille. ISBN: 978-92-5-131047-2. 308 p.

Islam K, Jashimuddin M, Nath B, Nath TK (2018) Land use classication and change detection by using multi-temporal remotely sensed imagery: The case of Chunati wildlife sanctuary, Bangladesh Egypt J Remote Sens Space Sci 21:37-47 doi:10.1016/j.ejrs.2016.12.005M

A. Madoui, J.M. Gehu. Etat de la végétation dans la forêt du Bou-Taleb.. Forêt Méditerranéenne, Forêt Méditerranéenne, 1999, XX (4), pp. 162-168.

ABOUT THE EDITORS

Dr. (Smt.) Jyothi Hiremath M.Sc., M.Phil., Ph.D., in Microbiology from Gulbarga University, Kalaburagi in 2016. She is working as Assistant Professor in Department of Food and Nutrition, Khaja Bandanawaz University, Kalaburagi. She has got six years of teaching and research experience along with this she has also published various research articles in National and International journals.

She has successfully worked as JRF and completed UGC-MRP Research project at the Department of Microbiology, Gulbarga University, Kalaburagi. She has presented research proceedings in various National and International conferences. She has completed the course in "College for Leadership and Human Resource Development"

Dr. Shivaveerakumar S., M.Sc., Ph.D., in Microbiology from Gulbarga University, Kalaburagi in research collaboration with Department of Environmental Science, Helsinki University, Finland in 2014. Presently he is working as Assistant Professor in the Department of Studies in Microbiology, Davangere University, Davanagere, Karnataka. He holds International Fellowship "Centre for International Mobility Organization" from Government of Finland and also Junior Research Fellow in UGC-MRP.

He has got 10 years of teaching and research experience and also published research articles in many reputed National and International Journals. He was invited as lead speaker from many reputed public and private Universities. He has got research collaboration with many National and International research Institutes / Universities.

ABOUT THE BOOK

This is a thorough introduction to innovations in the life sciences, particularly bio-nanotechnology, for students studying Microbiology, nanotechnology, biotechnology, and bio-nanotechnology as well as those interested in the domains of biology, chemistry, physics, and materials science. It explains what are bio-nanomaterial's, how to make them, how to characterize them, and how to use them in various contexts. The book covers in detail the advantages and drawbacks of bio-nanotechnology, as well as its present state and potential. This book is written at the beginning reader level, making it simple for readers to comprehend.

This book highlights the distinctions between biotechnology and nanotechnology which explains the fundamentals of bio-nanomaterial's for food, functional cosmetics, and nanomedicine, as well as innovative techniques for analysing and treating cancer for the prevention of environmental issues. It provides the links to commercial or academic research in this field of bio-nanotechnology for biochemical engineers, materials scientists, biotech entrepreneurs, doctors, chemists, pharmacists, and electrical engineers in allied businesses, as well as undergraduate and graduate students.

EMPYREAL PUBLISHING HOUSE

ISBN 978-93-93810-19-9

www.empyrealpublishinghouse.com